ABSTRACT

RUARK-SEWARD, CASEY LORAINE. A Multi-Pronged Approach to Identify and Characterize Novel RNA Viruses within Soybean Cyst Nematode. (Under the direction of Drs. Eric Davis and Tim Sit).

The study of invertebrate - and particularly nematode - viruses is advancing with the widescale use of transcriptome sequencing. Five single-stranded RNA viruses were previously identified within the economically important soybean cyst nematode (SCN; *Heterodera glycines*). From qRT-PCR, endpoint PCR, and Sanger sequencing, it was determined that these viruses are widespread and replicating within greenhouse and North Carolina field populations of SCN and also present within clover (*H. trifolii*) and beet (*H. schachtii*) cyst nematodes. Additionally, two previously undiscovered viral-like genomes were identified from analyses of the transcriptome data of several inbred SCN populations. Both of these proposed new nematode viruses are negative-sense RNA viruses and have been named SCN nyami-like virus (NLV) and SCN bunya-like virus (BLV). Moreover, we analyzed publicly available transcriptome data of two potato cyst nematode (PCN) species, *Globodera pallida* and *G. rostochiensis* using the same approach. From these data, a third virus was discovered and called PCN picorna-like virus (PLV). PCN PLV is a positive-sense RNA virus, and to the best of our knowledge, is the first virus described within PCN. The presence and replication of the two novel SCN viruses were confirmed experimentally with the exception of PCN PLV due to host quarantine restrictions. Finally, a fluorescence *in situ* hybridization (FISH) protocol was developed to localize viral RNA and host mRNA within whole second-stage juveniles (J2s) of SCN. Three SCN RNA viruses [Socyvirus-1 (SbCNV-1), SCN NLV, and SCN BLV] were colocalized with host glyceraldehyde 3-phosphate dehydrogenase (GAPDH) and found in cells throughout the body of SCN second-stage

juveniles with the exception of the intestinal tract. While much work needs to be done to understand the biological and evolutionary significance of these nematode viruses, the research presented here indicates that viral infections of plant-parasitic nematodes are more widespread than originally believed.

A Multi-Pronged Approach to Identify and Characterize Novel RNA Viruses within Soybean Cyst Nematode

by
Casey Loraine Ruark-Seward

A dissertation submitted to the Graduate Faculty of
North Carolina State University
in partial fulfillment of the
requirements for the degree of
Doctor of Philosophy

Plant Pathology

Raleigh, North Carolina

2018

APPROVED BY:

Eric Davis Committee Co-Chair	Tim Sit Committee Co-Chair
Stephen Koenning	Steven Lommel

Charles Opperman

DEDICATION

To my parents,

Who taught me I could be anything

Except a figure skater.

BIOGRAPHY

Casey grew up in many locations including North Carolina, Virginia, Nebraska, and Alabama. After graduating from a rural Alabama high school, Casey first discovered molecular biology through an internship at HudsonAlpha Institute for Biotechnology. She then went on to earn a B.S. in Cellular, Microbial, and Molecular Biology from Auburn University while gaining research experience via a long-term project studying the physiology of an opportunistic bacterial pathogen of humans. Desiring a more direct and immediate application of her basic research, Casey was led to the field of plant pathology. After working as a Kelman Scholar with Tim Sit and Steve Lommel at NC State, she returned as a Ph.D. student within the Department of Plant Pathology to research nematode viruses. While at NC State she has discovered her passions of translating molecular biology research into useful management tools for agricultural pests and studying complex, endosymbiotic relationships.

ACKNOWLEDGMENTS

Thank you to my committee members for your mentorship. I will always appreciate the encouragement I received weighted with a heavy dose of skepticism, all of which has led me to produce better data. I am grateful for the snacks and sarcasm that Tim Sit provided on a daily basis. Thanks to Rick Davis for always finding time to answer my research questions despite a busy schedule. I would also like to acknowledge the technicians that have helped me along the way, particularly Chunying (Lisa) Li. Thank you to Eva Johannes and Mariusz Zareba in the CMIF for teaching me to use a very fancy and expensive microscope. Appreciations are extended to the departmental office staff for all of the help over the years. I would also like to recognize collaborators from other institutions, particularly Melissa G. Mitchum (University of Missouri). Thanks to the other plant pathology graduate students for your comradery, especially my lab mate Jessica Brown.

I would like to thank the NC Soybean Producers Association for supporting the research within Chapter 2 of this dissertation, and the National Science Foundation Graduate Research Fellowship Program which has provided so much flexibility in my research and studies. From my earlier days, I am grateful to Drs. Bob Zahorchak (HudsonAlpha Institute for Biotechnology) and Sang-Jin Suh (Auburn University) for giving an inexperienced teenager a chance to learn molecular biology.

Of course, thank you to my husband, parents, and brother for the constant support and for not asking too many times, “When will you be finished, again?” A special thanks to my dog for encouraging work-life balance.

TABLE OF CONTENTS

LIST OF TABLES vii

LIST OF FIGURES viii

CHAPTER 1: Literature Review 1

Nematodes 1

Endosymbionts of Nematodes 4

Viruses Infecting Nematodes 12

Literature Cited 20

CHAPTER 2: **Soybean Cyst Nematode Culture Collections and Field Populations from North Carolina and Missouri Reveal High Incidences of Infection by Viruses** 29

Abstract 30

Introduction 30

Materials and Methods 32

Results 38

Discussion 44

Acknowledgements 49

Literature Cited 50

CHAPTER 3: **Novel RNA Viruses within Plant Parasitic Cyst Nematodes** 64

Abstract 65

Introduction 65

Materials and Methods 67

Results 73

Discussion 79

Acknowledgements 82

Literature Cited 83

CHAPTER 4: **Localization of Viral RNA and Host mRNA within Soybean Cyst Nematode via Whole-Mount Fluorescence *in situ* Hybridization** 97

Abstract 98

Introduction 98

Materials and Methods 101

Results 107

Discussion 111

Acknowledgements 116

Literature Cited 117

APPENDICES 130

APPENDIX A: Chapter 2 Supplemental Information 131

APPENDIX B: Chapter 3 Supplemental Information 138

APPENDIX C: Chapter 4 Supplemental Information 142

LIST OF TABLES

CHAPTER 2: Soybean Cyst Nematode Culture Collections and Field Populations from North Carolina and Missouri Reveal High Incidences of Infection by Viruses

Table 2.1 Inbreeding protocol, date of origin and HG type of SCN greenhouse populations used in this study 54

Table 2.2 Primers used for amplifying selected regions of virus RNA-dependent RNA polymerases (RdRPs) from total RNA samples 56

Table 2.3 Number and percent of North Carolina SCN greenhouse and NC field population samples infected with viruses as detected with qRT-PCR 57

Table 2.4 Detection of known SCN viruses in other species of plant-parasitic nematodes via qRT-PCR 58

CHAPTER 3: Novel RNA Viruses within Plant Parasitic Cyst Nematode

Table 3.1 Number of sequence reads and mean read coverage of viral genomes from mined transcriptome data sets 89

Table 3.2 Primers used for this research study and their application 90

Table 3.3 Genbank accession numbers for partial viral genomes 91

Table 3.4 qRT-PCR Ct values and relative titers of soybean cyst nematode (SCN) viruses within SCN research populations 92

Table 3.5 qRT-PCR Ct values and relative titers of cyst nematode viruses within plant parasitic nematode (PPN) 93

CHAPTER 4: Localization of Viral RNA and Host mRNA within Soybean Cyst Nematode via Whole-Mount Fluorescence *in situ* Hybridization

Table 4.1 Fluorescent DNA probes used for fluorescence *in situ* hybridization (FISH) 120

Table 4.2 Primers used to generate strand-specific cDNA templates 121

Table 4.3 Primers used to detect viral sequences and *Heterodera glycines* internal control (GAPDH) via qRT-PCR 122

LIST OF FIGURES

CHAPTER 2: Soybean Cyst Nematode Culture Collections and Field Populations from North Carolina and Missouri Reveal High Incidences of Infection by Viruses

Figure 2.1 Titer and replication of negative-sense RNA viruses within SCN life stages measured with qRT-PCR 59

Figure 2.2 Log_2 average relative abundance ratios of respective viruses in SCN egg samples from populations maintained in research greenhouses 60

Figure 2.3 Log_2 average relative abundance ratios of respective viruses in SCN egg samples from NC and MO infested fields..... 61

Figure 2.4 Log_2 average relative abundance ratios of SCN samples in which virus is detectable via qRT-PCR..... 62

Figure 2.5 Amplification of SCN viruses within *Heterodera trifolii*..... 63

CHAPTER 3: Novel RNA Viruses within Plant Parasitic Cyst Nematode

Figure 3.1 Characterization of soybean cyst nematode (SCN) nyami-like virus (NLV)..... 94

Figure 3.2 Characterization of soybean cyst nematode (SCN) bunya-like virus (BLV)..... 95

Figure 3.3 Characterization of potato cyst nematode (PCN) picorna-like virus (PLV) 96

CHAPTER 4: Localization of Viral RNA and Host mRNA within Soybean Cyst Nematode via Whole-Mount Fluorescence *in situ* Hybridization

Figure 4.1 Comparison of FISH methodologies for fluorescent probe entry..... 123

Figure 4.2 Autofluorescence of SCN eggs and J2s with 565 and 633 nm laser lines..... 124

Figure 4.3 Localization of SCN mRNA..... 125

Figure 4.4 Colocalization of SCN Socyvirus-1 (SbCNV-1) with host GAPDH 126

Figure 4.5 Colocalization of SCN Nyami-like virus (NLV) with host GAPDH 127

Figure 4.6 Colocalization of SCN Bunya-like virus (BLV) with host GAPDH 128

Figure 4.7 Strand-specific amplification of viruses within SCN J2s and eggs 129

CHAPTER 1

Literature Review

NEMATODES

Nematodes are invertebrate, unsegmented roundworms that live in a wide variety of habitats ranging from fresh and salt waters to arid deserts. Moreover, these worms can feed on bacteria, fungi, plants, or animals. Nematodes are usually microscopic and abundant in the environment, and there are a large number of known and undescribed species. The most recognizable nematodes to those unfamiliar with the field of nematology may be animal parasites such as dog heartworms (*Dirofilaria immitis*) and human hookworms (*Ancylostoma duodenale* and *Necator americanus*). The life cycle of a nematode involves six life stages occurring in the following order: egg, first-stage juvenile (J1), J2, J3, J4, and adult. In between developmental stages, there are molts in which the cuticle is shed and reproductive organs further develop. In all plant-parasitic nematodes (PPN), the first molt occurs within the egg and the second-stage juvenile (J2) emerges; this is also most often the infective stage of PPN.

Plant parasitic nematodes are some of the most detrimental pathogens to crop production, and species that attack roots do so by puncturing plant cells with a stylet (hollow, protrusible feeding tube) to acquire nutrients. Stylets are present in all PPN; however, not all nematodes with stylets parasitize plants. Aboveground symptoms of nematode infection are difficult to conclusively distinguish for diagnostic purposes as the plant may appear stunted, wilted, and yellowed as a result of root damage. To accurately determine if nematodes are present, soil samples need to be analyzed and viewing roots can be helpful if symptoms such

as swelling or necrosis are present or if endoparasitic plant nematodes are embedded within the root tissue. In addition to root pathogenic nematodes, there are foliar nematodes, typically belonging to the genus *Aphelenchoides,* which are of primary importance to ornamental production. *Aphelenchoides* can remain on the outside of the plant or invade leaf and stem tissues (Moorman, 2017). These nematodes can readily move in water droplets, and symptoms appear as dark, wet-looking regions as well as chlorosis on the leaves. There are also a few nematode species that are vectored by insects and infect trees such as *Bursaphelenchus xylophilius* (pinewood) and *B. cocophilus* (red ring).

The majority of PPN of economic importance feed on crop plant roots with the highest impacts occurring from root-knot (genus *Meloidogyne*) and cyst (genera *Heterodera* and *Globodera*) nematodes (Jones *et al*., 2013). Root-knot and cyst nematodes are both primarily sedentary, endoparasitic feeders where the nematode completely invades the root, selected host root cells are transformed into a complex feeding site, and the adult female becomes pyriform and immobilized. Root-knot nematodes create specialized feeding sites called giant cells; these are multinucleated cells produced by repeated nuclear division without cytokinesis (Jones and Payne, 1978). Contrastingly, cyst nematodes form multinucleated feeding sites called syncytium; however, syncytia are formed by dissolution of neighboring plant cell walls. Giant cells and syncytial cells are essential for these parasites to survive as they allow the immobile growing nematode to receive rich nutrients from the plant, and these specialized sites are a major reason why root-knot and cyst nematodes are considered the first and second-most important economic nematode pathogens, respectively.

Other feeding habits used to classify nematodes include migratory and ectoparasitic. Migratory nematodes can feed either on the surface of roots (ectoparasitic) or within root

tissue (endoparasitic), and females retain locomotive functions and a vermiform shape. Likewise, sedentary feeders can be either ecto- or endoparasites, and not all nematodes fit within clearly defined groups and will exhibit some combination of feeding habits.

Five of the most destructive species of root-knot nematode include *Meloidogyne arenaria, M. enterolobii, M. hapla, M. incognita,* and *M. javanica.* Typically, *Meloidogyne* spp. have broad host ranges, and there is at least one species (of the approximately 100 described) that can parasitize almost every vascular plant (Jones *et al*., 2013). Because root-knot nematodes can infect so many plants, estimates of economic loss are difficult to find. Studies have shown that *M. incognita* is capable of causing 100% yield loss in tomato microplots (Di Vito *et al*., 1991) and 80% yield loss of potato microplots (Russo *et al*., 2007). As mentioned previously, cyst nematodes are also among the most destructive PPN. Major species of economic importance in this group include soybean cyst (SCN; *Heterodera glycines*), beet cyst (BCN; *Heterodera schachtii*), potato cyst (PCN; *Globodera pallida* and *G. rostochiensis*), and cereal cyst (CCN; *Heterodera avenae* and *H. filipjevi*) nematodes (Jones *et al*., 2013). In particular, the ability of cyst nematodes to survive dormant in the soil makes crop rotation and eradication difficult despite the fact that cyst nematodes usually have a narrow host range. It has been estimated that SCN causes damages amounting to $1.5 billion (US) annually in the United States alone (Chen *et al*., 2001), and this pathogen affects soybean crops worldwide. Furthermore, PCN are thought to cause a 9% reduction to global potato production annually (Turner and Rowe, 2006).

ENDOSYMBIONTS OF NEMATODES

Endosymbionts live within the body of a host organism; bacteria are most often considered, although fungi and viruses are also capable of this relationship. In relation to their host, endosymbionts can be obligate or facultative symbionts. Obligates rely completely on their host and in reciprocation contribute to necessary host functions. These microbes have likely evolved for a long period of time with their host and they typically have reduced genome size, live within specialized host cells (bacteriocytes), and are transmitted vertically (Ratzka *et al*., 2012). Within *Xiphinema* nematode species, the obligate endosymbiont *Verrucomicrobia* colonizes the gut epithelial cells of juveniles and males; however, during the final molt into an adult female the bacteria invade the growing oocytes to be vertically transmitted (Vandekerckhove *et al*., 2002). Contrastingly, facultative endosymbionts are not required for host development, not usually within all individuals of a host population, not contained within specialized bacteriocytes, and can be transmitted vertically or horizontally (Ratzka *et al*., 2012). Fungi can also be endosymbionts, although more rarely, and tend to be facultative and transmitted horizontally (Gibson and Hunter, 2010). Viruses are more recently being explored as potential endosymbionts of invertebrates as next generation sequencing has become more prevalent. DNA viruses of the family *Polydnaviridae* have been shown to be beneficial symbionts of parasitoid wasps (White *et al*., 2013). These viruses are necessary for survival of the wasp as they deliver virulence genes to the host of the parasitoid wasp. These virulence genes both prevent the host immune system from killing wasp offspring and altering development and metabolism to benefit the wasp while killing the host. Interestingly, eight RNA viruses have been found within plant parasitic cyst nematodes; however, the function of these viruses is yet to be determined (Bekal *et al*., 2011;

Bekal *et al*., 2014; Ruark *et al*., 2018). Viral infection of nematodes will be discussed later in more detail within the subsection of the chapter "Viruses infecting nematodes" and is the topic of this dissertation.

Endosymbionts are found within invertebrates including insects and nematodes but, to date, appear to be less common in the latter group (Palomares-Ruis *et al*., 2016). In insects, endosymbionts have been attributed to nutritional upgrading, manipulation of reproduction, heat tolerance, or protection against pathogens (Gibson and Hunter, 2010; Ratzka *et al*., 2012). Most animals are not capable of synthesizing ten essential amino acids and must consume them from their food source; this is true for both insects and nematodes. Insects belonging to the Order Hemiptera possess various endosymbionts for nutritional supplementation as their liquid diets of either plant sap or blood are imbalanced food sources (Brown, 2014). Plant phloem is devoid of essential amino acids, but phloem-feeding insects have circumvented this problem by acquiring endosymbionts that synthesize these compounds for them (Hansen and Moran, 2011). One of the best-studied examples is the pea aphid and its endosymbiont *Buchnera*. *Buchnera* resides in bacteriocytes within the haemocoel and are vertically transmitted through populations (Wilson *et al*., 2010). This relationship benefits both organisms as the aphid supplies its nonessential amino acids to *Buchnera*, and the bacterium supplies the aphid with essential amino acids.

Wolbachia pipientis is a bacterium found in over 60% of insect species and is the most prevalent known endosymbiont of arthropods (Brown *et al*., 2016). In most insects, *Wolbachia* acts as a reproductive parasite influencing factors such as feminization or killing of males, parthenogenesis induction, or cytoplasmic incompatibility (Gavotte *et al*., 2006). More recently, *Wolbachia* has been shown to confer resistance against RNA viruses, affect

locomotion, and increase insect egg production when fed diets with supplemental iron (Kent and Bordenstein, 2011). However, *Wolbachia* strains were recently discovered in sap-feeding insects and nematodes that act as nutritional mutualists and do not directly affect host reproduction. Previous reports claimed that this bacterium existed only in filarial nematodes (Foster *et al*., 2005; Taylor *et al*., 2012); however, *Wolbachia* has also recently been found in species of plant parasitic nematodes (PPN) (Brown *et al*., 2016).

The functionality of *Wolbachia* endosymbionts in nematodes has been studied in the most detail within *Brugia malayi* which is responsible for human lymphatic filariasis (elephantiasis). Through comparative genomic analysis of *B. malayi* and *Wolbachia*, complementary metabolic functions were discovered (Taylor *et al*., 2012; Voronin *et al*., 2016). *Wolbachia* provides *B. malayi* with flavin adenine dinucleotide (FAD), riboflavin, and heme as the nematode lacks genes for these compounds. Likewise, the nematode host provides *Wolbachia* with materials it cannot synthesize such as biotin, Co-A, ubiquinone, and folate. Furthermore, *Wolbachia* lacks two enzymes required to complete glycolysis (6-phosphofructokinase and pyruvate kinase). Thus, without the aid of *B. malayi* the bacterium cannot convert glucose into pyruvate. Antibiotic treatment of nematodes increased the amount of available glucose as *Wolbachia* did not deplete the nematode host's supply. However, the endosymbiotic bacterium is essential and the nematode will slowly die without its presence.

Interestingly, *Wolbachia* was discovered in PPN species *Radopholus similis* (burrowing nematode) and *Pratylenchus penetrans* (lesion nematode) (Brown *et al*., 2016). Bacterial cells were visualized throughout nematode tissue, but areas of the intestine and ovaries were most densely packed. Brown *et al*. (2016) concluded that PPN are actually the earliest hosts

for *Wolbachia,* and bacterial isolates from PPN are more closely related to isolates of sap-feeding insects rather than filarial nematodes. Although the function is not yet clear, the authors have preliminary evidence that *Wolbachia* may contribute to iron metabolism and heme synthesis in plant parasitic nematodes. This functionality is supported by the fact that both heme and iron are limited in plant roots. The authors suggest that *Wolbachia* assisting with heme/iron acquisition may have enabled PPN to transition to a root-endoparasitic lifestyle. Thus far, other attributes of filarial *Wolbachia* (i.e. riboflavin and FAD synthesis) were not found in *Wolbachia* of PPN; however, the *Wolbachia* genome is still in draft form.

To add further complexity to the issue, *Wolbachia* can be infected by a bacteriophage. The most common phage, named WO, infects 89% of *Wolbachia* that are reproductive parasites of insects (Kent and Bordenstein, 2011). Thus far, *Wolbachia* of nematodes (filarial and PPN) do not appear to be infected by phage. In the reproductive parasites, WO phage are thought to interact with insect host cells. The WO genome has sequence similarity to virulence-associated genes, but its exact function has yet to be determined. However, it has been hypothesized that WO enables *Wolbachia* to enter host cells and scavenge nutrients. Furthermore, the phage encode Ankyrin-repeat (ANK) proteins which are thought to mediate protein-protein interactions, act as transcription factors, and modify cell-cycle regulatory activity. ANK proteins are believed to contribute to reproductive parasitism. Most recently, WO phage genes have been associated with inducing cytoplasmic incompatibility in insects in which crosses between infected males and uninfected females result in embryonic lethality (LePage *et al*., 2017). Endosymbionts that are strictly vertically transmitted to offspring (i.e. *Buchnera*) typically lack phage; however, endosymbionts that can switch hosts like *Wolbachia* tend to possess phage and a large percentage of mobile DNA that can change its

position in the genome (Kent and Bordenstein, 2010; Metcalf and Bordenstein, 2013). For instance, *Wolbachia* of *Drosophila melanogaster* has a genome comprised of 14.2% transposable sequences and phage elements (Wu *et al*., 2004). Although phage is not present in *Wolbachia* of nematodes, six genes belonging to *Wolbachia* within *B. malayi* are homologous to phage of the reproductive parasites (Kent and Bordenstein, 2011). This homology suggests that nematodes at one time harbored phage that have since been lost. *Wolbachia* endosymbionts within nematodes consist of isolates with limited host-switching, infrequent genetic exchange, and few co-infections compared to insect endosymbionts (Brown *et al*., 2016). Perhaps a lack of phage within nematode *Wolbachia* suggests these isolates are now primarily limited to vertical transmission. The absence of WO phage, which has been associated with cytoplasmic incompatibility, may also account for why these particular isolates act as nutritional mutualists instead of reproductive parasites.

Recently, a non-*Wolbachia* bacterial endosymbiont has been fully sequenced from *Xiphinema americanum* (dagger nematode) that are well known vectors of plant viruses (Brown *et al*., 2015). The endosymbiont has been named *Xiphinematobacter* and belongs to the phylum *Verrucomicrobia*. The *Xiphinematobacter* genome size has been greatly reduced compared to a typical bacterium and locomotive and chemotaxis functions have been lost suggesting it is an obligate endosymbiont. *Xiphinematobacter* resides in the gut, ovaries, eggs, and gut primordia of embryos. It's possible that this bacterium provides a nutritional advantage to the nematode because of its location in the gut and because *X. americanum* feeds on phloem.

From available data, plant parasitic nematodes appear to host endosymbionts less frequently than sap-feeding insects. If true, the potential exists that PPN stylet openings may

size-exclude against bacterial cells, and PPN may be better adapted to acquire nutrients from plants. Until recently, next generation sequencing projects on nematodes have not focused on searching for endosymbionts. Evolutionarily, nematode relationships with endosymbionts may be different due to stylet size. Feeding canals of sap-feeding insects range in diameter from 0.5 µm for aphids to 0.9 µm for whiteflies (Rosell *et al*., 1995; Auclair, 1963). While estimates on nematode stylet lumen diameters are difficult to find, there is some evidence that at least stunt and cyst nematodes have an opening of 0.1 µm to 0.3 µm (DM Bird, personal communication). There are no measurements available for stylet lumen diameters of the genera that have been found to host endosymbionts; however, it is not improbable that these nematodes may possess larger stylet openings. In contrast, bacterial endosymbionts discovered thus far in marine nematodes have a cell diameter between 0.3 µm and 1.0 µm (Kjeldsen *et al*., 2010), and within the PPN *Xiphinema americanum, Xiphinematobacter* cells are approximately 0.7 µm in diameter (Brown *et al*., 2015). Smaller bacterial cells, or oblong cells, may be capable of entering insect feeding canals and presumably the stylets of *Xiphinema*, *Radopholus,* and *Pratylenchus* spp. However, a whole bacterium would not be expected to pass through the stylet of many plant parasitic nematodes such as cyst and root-knot nematodes that likely have smaller diameter lumens. Contradictory to this idea, a 2006 report described an endosymbiont 0.4 µm to 0.8 µm in width within *Heterodera glycines* (Noel and Atibalentja, 2006). The presence of *Candidatus* Paenicardinium endonii was shown with electron microscopy and by sequencing a 1.5 kb fragment of the 16*S* rRNA. A single *H. glycines* population originating from a single field in Tennessee was examined, and follow-up research to detect the bacterium in additional populations has not yet been reported. Thorough genetic evidence is lacking for *Candidatus* Paenicardinium endonii to

deduce whether this organism has hallmarks of an endosymbiont genome with reductions in locomotion and chemotaxis functions. Hopefully, future research will be conducted to determine if this is a true bacterial endosymbiont which exists within more than one population of *H. glycines* and what its function might be within the host.

Endosymbionts are found frequently in insects that have nutritionally limited diets of plant sap or blood. It has recently been discovered that plant parasitic nematodes belonging to genera *Xiphinema, Pratylenchus,* and *Radopholus* harbor endosymbiotic bacteria (Brown *et al*. 2015; Brown *et al*., 2016). *Xiphinema* has been demonstrated to have a diet derived from phloem nutrients and likewise has a long stylet approximating 170-193 µm in length (Handoo *et al*., 2016). *Xiphinema* must supplement its diet with amino acids produced by its endosymbiont, *Xiphinematobacter*, to survive. The other two genera possess shorter stylets closer to 17 µm long (Tarte and Mai, 1976; Xu *et al*., 2014); however, these worms burrow within the root and may still feed on phloem nutrients. Additionally, lesion and burrowing nematodes do not establish specialized feeding sites, and it is possible that these nematodes do not satisfactorily capture necessary nutrients from the plant without the aid of *Wolbachia*. Conversely, nematodes such as cyst and root-knot develop specialized feeding cells and modify the plant to act as an ideal host. The sedentary feeding behavior of cyst and root-knot nematodes allows them to wait for necessary nutrients to arrive. Moreover, they may be more efficient at capturing nutrients than nematodes and insects that do not create specialized feeding sites as evidenced by root-knot's ability to turn the giant cell into a 'nutrient sink' (Bird and Loveys, 1975; McClure, 1977). The complete dependence these nematodes have on host plants may be a defining factor in comparing endosymbiont acquisition to sap-feeding insects.

There are a number of genes within plant parasitic nematodes that are thought to be horizontally-acquired from endosymbionts despite the apparent absence of these microorganisms within the host nematodes. It is possible that an endosymbiont was acquired by ingestion long ago when these nematodes were still free-living, bacterial feeders (Brown *et al*., 2015) with an open stoma and no stylet. Novel genes were possibly gained via horizontal gene transfer, and the endosymbiont no longer exists due to a long co-evolution and reduction of the bacterial genome to the point of elimination. One notable example of genes acquired via horizontal transfer are nematode cellulases (Danchin *et al*., 2010; Paganini *et al*., 2012; Smant *et al*., 1998). Cellulases promote the breakdown of cell walls when nematodes invade plant roots. Acquisition of cellulase genes from a bacterium likely helped plant parasitic nematodes develop from free-living organisms into plant parasites (Danchin *et al*., 2010). The GH5 cellulase has been reported in numerous Tylenchina species (root-knot, cyst, burrowing, and lesion) and possible bacterial donors have been identified from the Coleopteran and Bacteroidetes groups (Danchin *et al*., 2010). Another example of lateral gene transfer within these nematode species are expansin-like proteins which loosen bonds of the plant cell wall. The expansin gene in nematodes was likely acquired from Actinomycetales bacteria millions of year ago.

In summation, endosymbiosis of plant-feeding invertebrates is common in sap-feeding insects and has recently been discovered in a handful of plant-parasitic nematode species that likely consume a heavily phloem sap-based diet. These endosymbionts supplement the host's diet with essential amino acids that are not readily available within the phloem nutrients. This endosymbiotic relationship is demonstrated by *Buchnera* in pea aphids (Wilson *et al*., 2010) and *Xiphinematobacter* in the dagger nematode (Brown *et al*.,

2015). Insect endosymbionts also manipulate host reproduction, increase heat tolerance, and increase vector competencies; however, these influences have not been noted for nematodes. Insects and nematodes may differ in their cadre of endosymbionts because the nematode's small stylet opening could limit consumption of microorganisms. The origins of *Wolbachia* in PPN remain a mystery but may be a vestige of the evolution of plant parasitism in nematodes. Moreover, many plant parasitic nematodes are highly adapted to host plants and have become masters of capturing nutrients. Their obligate pathogen lifestyle could reduce the need for endosymbiosis which is so prevalent in insects. Nematode species that are better adapted to parasitize plants have likely acquired beneficial genes from the endosymbionts that are now absent from the worm. There is evidence that suggests nematode cellulases and expansin-like proteins were acquired from previous lateral gene transfer events with bacteria. Future next generation sequencing research may uncover additional endosymbionts within plant parasitic nematodes, although it is unlikely that these bacteria will be found as frequently as they are within insects.

VIRUSES INFECTING NEMATODES

Until recent advancements in RNA sequencing technologies, nematodes were largely considered to be immune to viral infections. Although certain nematodes are known to transmit plant viruses (Brown *et al*., 1995), these viruses do not replicate in the worm and are lost while molting to the next life stage. An early study observed that root knot nematode (*Meloidogyne incognita*) was infected with a filterable, virus-like pathogen, but the infective agent was never identified (Loewenberg *et al*., 1959). The 1970s brought a collection of electron microscopy images of virus-like particles in nematodes; however, insufficient

definitive information left the scientific community doubtful (Foor, 1972; Poinar and Hess, 1977; Zuckerman *et al*., 1973). There are several biological reasons why nematologists believed sedentary endoparasitic plant nematodes, in particular, to be non-infected with viruses: the stylet and feeding tube diameters appeared too narrow for viral particles to be ingested, and the tough collagen cuticle should inhibit viral penetration. The more likely scenario for nematodes being 'virus free' is that researchers simply did not have adequate research methodologies available to discover nematode infecting viruses.

In 2005, Lu *et al*. demonstrated that *Caenorhabditis elegans* supports viral replication by artificially infecting the nematode with *Flock house virus* (FHV). FHV was chosen as it is unique in its ability to replicate within yeast, plants, insect, and mammalian cells (Ball and Johnson, 1998; Dasgupta *et al*., 2001; Dasgupta *et al*., 2007; Price *et al*., 1996; Scotti *et al*., 1983; Selling *et al*., 1990). FHV successfully replicated in *C. elegans* because of its ability to inhibit nematode RNA-guided RNA interference (RNAi) via the FHV B2 protein (Lu *et al*., 2005). This work established the possibility of viral replication in a nematode and inspired other researchers to search for viruses within various nematode species. The first naturally occurring viral infections of nematodes were discovered via RNA sequencing within wild populations of *C. elegans* and *C. briggsae* (Felix *et al*., 2011; Franz *et al*., 2012). *Caenorhabditis* nodaviruses are not incorporated in the host genome and are also not vertically transmitted. Instead, *C. elegans* were able to successfully horizontally transmit viruses for six months in culture (or approximately fifty generations). A proposed route of infection is that viral particles are shed from the intestine through the rectum and then ingested during feeding (Felix *et al*., 2011). It appears that viruses are able to invade the host by surpassing RNA inference pathways, as *C. elegans* defective in these pathways

accumulated higher virus titers. Nodaviruses were later shown to be primarily localized in several intestinal cells of the nematode (Franz *et al*., 2014). The viruses alter intestinal cell morphology including elimination of storage granules, increased fluidity of cytoplasm, elongation of nuclei, and fusion of neighboring cells. Despite dramatic morphological changes, adult longevity and progeny size were not affected. However, progeny production was delayed and infected worms took up to two days longer to produce the same number of offspring (Franz *et al*., 2014). Due to the discovery of natural viral infection and an artificial infection method, *C. elegans* are now being considered as an emerging model for studying virus-host interactions (Diogo and Bratanich, 2014; Gammon, 2017).

Additionally, four negative-sense RNA viruses (SbCNV-1, ScPV, ScTV, and ScRV) were reported within research populations of the plant pathogenic soybean cyst nematode (SCN; *Heterodera glycines*) (Bekal *et al*., 2011). The genome structures vary among the SCN viruses, and they are either monopartite or multipartite (single or multiple segments of RNA). This same research group later uncovered a positive-sense RNA virus (SbCNV-5) from several SCN research and field populations (Bekal *et al*., 2014). Interestingly, the nearest known relatives of the SCN specific viruses infect arthropods such as ticks and leafhoppers (Bekal *et al*., 2011). Although there is now evidence for the existence of SCN viruses, very little is known about what these viruses may actually be doing to the nematode host. To date, the SCN viruses have not been detected within plant host tissues (Bekal *et al*., 2011; Ruark *et al*., 2017), but more comprehensive analysis to rule out localized root infection may be a worthwhile endeavor. Thus far, the effects of viruses on SCN are unknown, and nodaviruses discovered in *Caenorhabditis* species are the only nematode viruses in which pathogenic effects have been demonstrated.

A recent study that analyzed transcriptomes of over 220 invertebrate species provided an additional 1,445 viral genome entries into the NCBI database (Shi *et al*., 2016). Included in this analysis were animal parasitic nematodes belonging to *Ascaridia, Ascaris, Romanomermis,* and other unidentified nematode genera providing 32 new nematode viral genomes for further investigation. While there is genomic evidence for these viruses, much like the SCN viruses, ample research needs to be conducted to understand the biological impact of these infections. The emerging field of virus infection of nematodes and the limited data on viruses that infect PPN prompted the studies presented in this dissertation.

In the research presented, we hope to expand upon the limited information currently available on nematode viruses. One over-arching commonality of nematode viruses discovered so far is that they possess single-stranded RNA genomes without a DNA intermediate (Bekal *et al*., 2011; Bekal *et al*., 2014; Felix *et al*., 2011; Franz *et al*., 2012). Thus, these viruses were not initially discovered by genomic sequencing and could not be readily detected without transcriptomic data. As such, we sequenced the transcriptomes of SCN populations with the intention of uncovering more unidentified viruses from this important PPN. From these data, two novel viruses were discovered and temporarily named SCN nyami-like virus (NLV) and SCN bunya-like virus (BLV) until later submission to the International Committee on Taxonomy of Viruses (ICTV) (Ruark *et al*., 2018). These viruses also follow the same trend as previously discovered nematode viruses as they have single-stranded RNA genomes. In this case both new SCN viruses have a negative-sense genome – one monopartite (SCN NLV) and the other multipartite (SCN BLV).

To determine how prevalent the seven known SCN viruses [(4) Bekal *et al*., 2011; (1) Bekal *et al*., 2014; (2) Ruark *et al*., 2018)] are in SCN, we sampled SCN greenhouse research

populations as well as North Carolina (NC) field samples (only the first 5 known viruses have been tested within field samples so far). In the greenhouse populations of SCN, we have detected all seven viruses with high frequency. These greenhouse populations were maintained at the University of Missouri but initially collected from field locations across the United States before selective breeding (Ruark *et al*., 2017). In contrast, only two viruses (SbCNV-1 and ScPV) were detected abundantly in our NC field samples. As mentioned above, field samples have not yet been tested for SCN NLV or SCN BLV; however, infection is a distinct possibility as the transcriptome data used to mine for these viruses originated from research populations (OP25 and OP50) originally isolated from a NC field and then heavily inbred in the laboratory (Dong and Opperman, 1997). Likewise, OP25 and OP50 were positive for only SbCNV-1 (formerly called ScNV) and ScPV from real-time PCR testing (Ruark *et al*., 2017). In this particular situation, the inbred NC lab populations reflected which infections were seen most commonly in fields across the state. Implementing a wider, geographic survey with thorough sequence information may offer insights into the origins of SCN viral infections and whether geography is a key component of viral presence within the nematode.

There is not an obvious relationship between the pathogenicity of a nematode population and its virome composition. A SCN research population that can break all known plant resistance (LY1) has similar infection levels to that of a population susceptible to all forms of resistance (PA3) (Ruark *et al*., 2017). Although it is natural to assume viruses would be detrimental to SCN, there is not yet evidence that this is the case. In fact, these viruses could very well act as commensal or perhaps even beneficial symbionts to the host. At this time, a SCN population has not been found that can confidently be called ‘virus-free’. If an uninfected

population cannot be found, a means of eradicating viruses from the nematode would be essential to understanding the impact of infection.

Thus far, SCN viruses appear to have a narrow host range and have only been detected in the most closely related species (Skantar *et al*., 2012) *H. trifolii* (clover cyst nematode) and occasionally *H. schachtii* (beet cyst nematode) (Ruark *et al*., 2017; Ruark *et al*., 2018). Within clover cyst nematode, five of the seven SCN viruses have been discovered (SbCNV-1, ScPV, ScTV, SCN NLV, and SCN BLV); whereas, only two viruses are detectable in beet cyst nematode (ScPV and ScRV). With the revelation that viruses were present in other cyst nematode species, we analyzed publicly available transcriptome data for the known SCN as well as undiscovered viruses. Within datasets for potato cyst nematodes (PCN), SCN viruses were not detected; however, the genome of a novel virus was assembled. This is this first report of a viral genome within PCN, and it was uncovered from both *Globodera pallida* (pale potato cyst nematode) and *G. rostochiensis* (golden potato cyst nematode) (Ruark *et al*., 2018). Until submission to ICTV, this virus has been named PCN picorna-like virus (PLV) and is a monopartite, positive-sense RNA virus. Much like the SCN viruses, little is known about PCN PLV beyond preliminary genome characterizations. As a small (9.4 kb) positive-sense virus, PCN PLV may be a viable candidate for an expression vector within PPN and warrants further examination.

The SCN and PCN viruses are distantly related to known viruses within public bioinformatic databases. Viruses that do show limited sequence similarity were primarily discovered within a single study that looked to expand knowledge of invertebrate viromes (Shi *et al*., 2016). Although this study provided a wealth of new viral genomes, the biological relevance of these invertebrate viruses is also unknown at this point in time. The viruses that

most closely match the newly discovered SCN and PCN viruses were primarily isolated from the *Arthropoda* subphylum *Chelicerata* (specifically ticks and spiders). The relatedness of *Nematoda* and *Arthropoda* viruses suggests a possible evolutionary linkage between these invertebrate phyla that should be further investigated.

To further understand SCN viruses, fluorescence *in situ* hybridization (FISH) methodology was developed to localize viruses within the nematode host. This protocol is novel to the study of PPN as the fluorescent probes are able to pass through the collagenous nematode cuticle without interfering with the specimen's structural integrity (de Boer *et al*., 1998). Interestingly, viral RNAs of SbCNV-1, SCN NLV, and SCN BLV were identified throughout the J2 with the exception of the intestinal tract. Fluorescence was most intense in those areas of presumably highest metabolic activity including the gland cells, genital primordium, cells within the tip of the tail, longitudinal muscles, and generally the anterior end of the worm. The absence of viral RNAs within the intestinal tract is notable as *C. elegans* nodaviruses were found solely within a few intestinal cells and these viruses are exclusively horizontally transmitted (Franz *et al*., 2014). The presence of viruses throughout the majority of SCN including the genital primordium (preliminary cells that form the reproductive system), but a stark absence of viruses from the intestinal tract, suggests SCN viruses may be vertically transmitted. Further evidence for vertical transmission of SCN viruses includes viral presence and replication within multiple life stages of SCN including the eggs (Ruark *et al*., 2017). Of course, additional means of transmission cannot be dismissed as the SCN viruses appear to have fully functional and non-reduced genomes (Bekal *et al*., 2011; Bekal *et al*., 2014; Ruark *et al*., 2018) that can typically be observed in long-term, obligate symbiosis (Ratzka *et al*., 2012).

Although nematode viruses are new to the research community, it is quite likely these viruses are not new to nematodes. The research presented in this dissertation aims to further elucidate the complex association between an obligate plant pathogenic nematode and a plethora of SCN-specific viruses that researchers have been unaware of until recently. Although great strides have been made in proving the existence of these PPN viruses, an abundant amount of research needs to be conducted to better understand transmission routes, impacts on nematode biology, and potential exploitation of viruses for nematode management.

LITERATURE CITED

1. Auclair JL. Aphid feeding and nutrition. Annual Review of Entomology. 1963; 8(1): 439-490.

2. Ball A, Johnson KL. Nodaviruses of insects. *In:* The insect viruses. Miller LK, Ball LA (eds.), Plenum Publishing, New York. 1998; 225-267.

3. Bekal S, Domier LL, Gonfa B, McCoppin NK, Lambert KN, Bhalerao K. A novel flavivirus in the soybean cyst nematode. J Gen Virol. 2014; 95: 1272-1280.

4. Bekal S, Domier LL, Niblack TL, Lambert KN. Discovery and initial analysis of novel viral genomes in the soybean cyst nematode. J Gen Virol. 2011; 92: 1870-1879.

5. Bird AF, Loveys BR. The incorporation of photosynthates by *Meloidogyne javanica*. J Nematol. 1975; 7(2): 111.

6. Brown AMV, Howe DK, Peetz AB, Wasala SK, Zasada IA, Denver DR. Comparative genomics of an endosymbiont in a plant-parasitic nematode suggest a role in nutritional symbiosis. Gen Biol & Evol. 2015; 7(9): 2727-2746.

7. Brown AMV, Wasala SK, Howe DK, Peetz AB, Zasada IA, Denver DR. Genomic evidence for plant-parasitic nematodes as the earliest *Wolbachia* hosts. Sci Rep. 2016; 6: 34955.

8. Brown AMV. Microevolution of insect-bacterial mutualists: a population genomics perspective. *In:* Evolutionary Biology: Genome Evolution, Speciation, Coevolution and Origin of Life. Pontarotti P. (ed.). Springer International, Switzerland. 2014; 247-259.

9. Brown DJ, Robertson WM, Trudgill DL. Transmission of viruses by plant nematodes. Annu Rev Phytopathol. 1995; 33: 223–249.

10. Chen S, MacDonald DH, Kurle, JE, Reynolds DA. The soybean cyst nematode. University of Minnesota Extension Service. 2001. Available at http://www.soybeans.umn.edu/pdfs/DC3935.pdf [accessed on Dec 4, 2017]

11. Danchin EG, Rosso MN, Vieira P, de Almeida-Engler J, Coutinho PM, Henrissat B, Abad P. Multiple lateral gene transfers and duplications have promoted plant parasitism ability in nematodes. Proc Natl Acad Sci. 2010; 107(41): 17651-17656.

12. Dasgupta R, Garcia BH, Goodman RM. Systemic spread of an RNA insect virus in plants expressing plant viral movement protein genes. Proc Natl Acad Sci. 2001; 98: 4910-4915.

13. Dasgupta R, Free HM, Zietlow SL, Paskewietz SM, Aksoy S, Shi L, Fuchs J, Hu C, Christensen BM. Replication of Flock house virus in three genera of medically important insects. J Med Entomol. 2007; 44 (1) 102-110.

14. de Boer JM, Yan Y, Smant G, Davis EL, Baum TJ. *In-situ* hybridization to messenger RNA in *Heterodera glycines*. J. Nematol. 1998; 30 (3): 309-312.

15. Di Vito M, Cianociotta V, Zaccheo G. The effect of population densities of *Meloidogyne incognita* on yield of susceptible and resistant tomato. Nematologia Mediterranea. 1991; 19: 265-268.

16. Diogo J, Bratanich A. The nematode *Caenorhabditis elegans* as a model to study viruses. Arch Virol. 2014; 159: 2843-2851.

17. Dong K, Opperman CH. Genetic analysis of parasitism in the soybean cyst nematode *Heterodera glycines*. Genetics. 1997; 146: 1311-1318.

18. Felix MA, Ashe A, Piffaretti J, Wu G, Nuez I, Belicard T, Jiang Y, Zhao G, Franz C, Goldstein L, Sanroman M, Miska E, Wang D. Natural and experimental infection of *Caenorhabditis* nematodes by novel viruses related to nodaviruses. PLoS Biol. 2011; 9: e1000586.

19. Foor WE. Virus-like particles in a nematode. J Parasitol. 1972; 1065-1070.

20. Foster J, Ganatra M, Kamal I, Ware J, Makarova K, Ivanova N, Vincze T. The *Wolbachia* genome of *Brugia malayi*: endosymbiont evolution within a human pathogenic nematode. PLoS Biol. 2005; 3(4): e121.

21. Franz CJ, Renshaw H, Frezal L, Jiang Y, Felix MA, Wang D. Orsay, Santeuil and Le Blanc viruses primarily infect intestinal cells in *Caenorhabditis* nematodes. Virol. 2014; 448: 255-264.

22. Franz CJ, Zhao G, Félix MA, Wang D. Complete genome sequence of Le Blanc virus, a third *Caenorhabditis* nematode-infecting virus. J Virol. 2012; 86: 11940-11940.

23. Gammon DB. *Caenorhabditis elegans* as an emerging model for virus-host interactions. J Virol. 2017; 91: e00509-17.

24. Gavotte L, Henri H, Stouthamer R, Charif D, Charlat S, Boulétreau M, Vavre F. A survey of the bacteriophage WO in the endosymbiotic bacteria *Wolbachia*. Mol Biol Evol. 2007; 24(2): 427-435.

25. Gibson CM, Hunter MS. Extraordinarily widespread and fantastically complex: comparative biology of endosymbiotic bacterial and fungal mutualists of insects. Ecol Lett. 2010; 13(2): 223-234.

26. Handoo ZA, Carta LK, Skantar AM, Subbotin SA, Fraedrich SW. Molecular and morphological characterization of *Xiphinema chambersi* population from live oak in Jekyll Island, Georgia, with comments on morphometric variations. J Nematol. 2016; 48(1): 20.

27. Hansen AK, Moran NA. Aphid genome expression reveals host–symbiont cooperation in the production of amino acids. Proc Natl Acad Sci. 2011; 108(7): 2849-2854.

28. Hewitt WB, Raski DJ, Goheen AC. Nematode vector of soil-borne fanleaf virus of grapevines. Phytopathol. 1958; 48: 586-595.

29. Jones MG, Payne HL. Early stages of nematode-induced giant-cell formation in roots of *Impatiens balsamina*. J Nematol. 1978; 10(1): 70-84.

30. Jones JT, Haegeman A, Danchin EG, Gaur HS, Helder J, Jones MG, *et al.* Top 10 plant-parasitic nematodes in molecular plant pathology. Mol Plant Path. 2013; 14(9): 946-61.

31. Kent BN, Bordenstein SR. Phage WO of *Wolbachia*: lambda of the endosymbiont world. Trends Microbiol. 2010; 18(4): 173-181.

32. Kjeldsen KU, Obst M, Nakano H, Funch P, Schramm A. Two types of endosymbiotic bacteria in the enigmatic marine worm *Xenoturbella bocki*. Appl Environ Microbiol. 2010; 76(8): 2657-2662.

33. LePage DP, Metcalf JA, Bordenstein SR, On J, Perlmutter JI, Shropshire JD, Bordenstein SR. Prophage WO genes recapitulate and enhance *Wolbachia*-induced cytoplasmic incompatibility. Nature. 2017; 543(7644): 243-247.

34. Loewenberg JR, Sullivan T, Schuster ML. A virus disease of *Meloidogyne incognita*, the southern root knot nematode. Nature. 1959; 184: 1896.

35. Lu R, Maduro M, Li F, Li HW, Broitman-Maduro G, Li WX, Ding SW. Animal virus replication and RNAi-mediated antiviral silencing in *Caenorhabditis elegans*. Nature. 2005; 436: 1040 –1043.

36. Metcalf JA, Bordenstein SR. The complexity of virus systems: the case of endosymbionts. Curr Opin Microbiol. 2012; 15(4): 546-552.

37. Moorman GW. Foliar nematodes. PennState Extension. 2017. Available at https://extension.psu.edu/foliar-nematodes [accessed Dec 13, 2017]

38. Noel GR, Atibalentja N. '*Candidatus Paenicardinium endonii'*, an endosymbiont of the plant-parasitic nematode *Heterodera glycines* (*Nemata: Tylenchida*), affiliated to the phylum *Bacteroidetes*. Int J Syst Evol Microbiol. 2006; 56(7): 1697-1702.

39. Paganini J, Campan-Fournier A, Da Rocha M, Gouret P, Pontarotti P, Wajnberg E, Danchin EG. Contribution of lateral gene transfers to the genome composition and parasitic ability of root-knot nematodes. PLoS ONE. 2012; 7(11): e50875.

40. Palomares-Rius JE, Archidona-Yuste A, Cantalapiedra-Navarrete C, Prieto P, Castillo P. Molecular diversity of bacterial endosymbionts associated with dagger nematodes of the genus *Xiphinema* (*Nematoda: Longidoridae*) reveals a high degree of phylogenetic congruence with their host. Mol Ecol. 2016; 25(24): 6225-6247.

41. Poinar GO, Hess R. Virus-like particles in the nematode *Romanomermis culicivorax* (*Mermithidae*). Nature. 1977; 266: 256-257.

42. Price BD, Rueckert RR, Ahlquist P. Complete replication of an animal virus and maintenance of expression vectors derived from it in *Saccharomyces cerevisiae*. Proc Natl Acad Sci. 1996; 93: 9465-9470.

43. Ratzka C, Gross R, Feldhaar H. Endosymbiont tolerance and control within insect hosts. Insects. 2012; 3(2): 553-572.

44. Rosell RC, Lichty JE, Brown JK. Ultrastructure of the mouthparts of adult sweetpotato whitefly, *Bemisia tabaci Gennadius* (*Homoptera: Aleyrodidae*). Int J Insect Morph Embryol. 1995; 24(3): 297-306.

45. Ruark CL, Koenning SR, Davis EL, Opperman CH, Lommel SA, Mitchum MG, Sit TL. Soybean cyst nematode culture collections and field populations from North Carolina and Missouri reveal high incidences of infection by viruses. PLOS ONE. 2017; 12 (1): e0171514.

46. Ruark CL, Gardner M, Mitchum MG, Davis EL, Sit TL. Novel RNA viruses within plant parasitic cyst nematodes. PLOS ONE. 2018; 13 (3): e0193881.

47. Russo G, Greco N, D'errico FP, Brandonisio A. Impact of the root-knot nematode, *Meloidogyne incognita*, on potato during two different growing seasons. Nematologia Mediterranea. 2007; 35: 29-34.

48. Scotti PD, Dearing S, Mossop DW. Flock house virus: a nodavirus isolated from *Costelytra zealandica* (White) (Coleoptera: *Scarabaeidae*). Arch Virol. 1983; 75: 181-189.

49. Selling BH, Allison RF, Kaesberg P. Genomic RNA of an insect virus directs synthesis of infectious virions in plant. Proc Natl Acad Sci. 1990; 87: 434-438.

50. Shi M, Lin XD, Tian JH, Chen LJ, Chen X, Li CX, *et al*. Redefining the invertebrate RNA virosphere. Nature. 2016; 540: 539-543.

51. Skantar AM, Handoo ZA, Zanakis GN, Tzortzakakis EA. Molecular and morphological characterization of the corn cyst nematode, *Heterodera zeae*, from Greece. J Nematol. 2012; 44 (1): 58-66.

52. Smant G, Stokkermans JP, Yan Y, De Boer JM, Baum TJ, Wang X, Hussey RS, Gommers FJ, Henrissat B, Davis EL, Helder J. Endogenous cellulases in animals: isolation of β-1, 4-endoglucanase genes from two species of plant-parasitic cyst nematodes. Proc Natl Acad Sci USA. 1998; 95(9): 4906-11.

53. Taylor CE, Brown DJF. Nematode Vectors of Plant Viruses. 1997; Wallingford, Oxfordshire: CAB International.

54. Taylor MJ, Voronin D, Johnston KL, Ford L. *Wolbachia* filarial interactions. Cell Microbiol. 2013; 15(4): 520-526.

55. Turner SJ, Rowe JA. Cyst nematodes. *In:* Plant Nematology. 2006. (Perry, R.N. and Moens, M., eds), Wallingford, Oxfordshire; CAB International: 90-122.

56. Vandekerckhove TT, Coomans A, Cornelis K, Baert P, Gillis M. Use of the *Verrucomicrobia*-specific probe EUB338-III and fluorescent *in situ* hybridization for detection of "*Candidatus Xiphinematobacter*" cells in nematode hosts. Appl Env Microbiol. 2002; 68(6): 3121-3125.

57. Voronin D, Bachu S, Shlossman M, Unnasch TR, Ghedin E, Lustigman S. Glucose and glycogen metabolism in *Brugia malayi* is associated with *Wolbachia* symbiont fitness. PLoS ONE. 2016; 11(4): e0153812.

58. White JA, Giorgini M, Strand MR, Pennacchio F. Arthropod endosymbiosis and evolution. *In:* Arthropod Biology and Evolution. 2013. Springer Berlin Heidelberg: 441-477.

59. Wilson AC, Ashton PD, Calevro F, Charles H, Colella S, Febvay G, Thomas GH. Genomic insight into the amino acid relations of the pea aphid, *Acyrthosiphon pisum*, with its symbiotic bacterium *Buchnera aphidicola*. Insect Mol Biol. 2010; 19(s2): 249-258.

60. Wu M, Sun LV, Vamathevan J, Riegler M, Deboy R, Brownlie JC, Wiegand C. Phylogenomics of the reproductive parasite *Wolbachia pipientis* w Mel: a streamlined genome overrun by mobile genetic elements. PLoS Biol. 2004; 2(3): e69.

61. Zuckerman BM, Himmelhoch S, Kisiel M. Virus-like particles in *Dolichodorus heterocephalus*. Nematologica. 1973; 19: 117.

CHAPTER 2

Soybean Cyst Nematode Culture Collections and Field Populations from North Carolina and Missouri Reveal High Incidences of Infection by Viruses

Published in *PLOS ONE*:

Citation:

Ruark CL, Koenning SR, Davis EL, Opperman CH, Lommel SA, Mitchum MG, and Sit TL. Soybean cyst nematode culture collections and field populations from North Carolina and Missouri reveal high incidences of infection by viruses. PLOS ONE. 2017; 12(1): e0171514. https://doi.org/10.1371/journal.pone.0171514.

ABSTRACT

Five viruses were previously discovered infecting soybean cyst nematodes (SCN; *Heterodera glycines*) from greenhouse cultures maintained in Illinois. In this study, the five viruses [ScNV, ScPV, ScRV, ScTV, and SbCNV-5] were detected within SCN greenhouse and field populations from North Carolina (NC) and Missouri (MO). The prevalence and titers of viruses in SCN from 43 greenhouse cultures and 25 field populations were analyzed using qRT-PCR. Viral titers within SCN greenhouse cultures were similar throughout juvenile development, and the presence of viral anti-genomic RNAs within egg, second-stage juvenile (J2), and pooled J3 and J4 stages suggests active viral replication within the nematode. Viruses were found at similar or lower levels within field populations of SCN compared with greenhouse cultures of North Carolina populations. Five greenhouse cultures harbored all five known viruses whereas in most populations a mixture of fewer viruses was detected. In contrast, three greenhouse cultures of similar descent to one another did not possess any detectable viruses and primarily differed in location of the cultures (NC versus MO). Several of these SCN viruses were also detected in *Heterodera trifolii* (clover cyst) and *Heterodera schachtii* (beet cyst), but not the other cyst, root-knot, or reniform nematode species tested. Viruses were not detected within soybean host plant tissue. If nematode infection with viruses is truly more common than first considered, the potential influence on nematode biology, pathogenicity, ecology, and control warrants continued investigation.

INTRODUCTION

Until recently, plant parasitic nematodes (PPN) of the genera *Longidorus*, *Trichodorus*, and *Xiphinema* were the only nematodes known to harbor viruses, but these genera serve as

vectors of plant viruses and replication does not occur within the worm [1,2,3]. Few studies have attempted to demonstrate viral replication in nematodes. An early study observed that root knot nematode (*Meloidogyne incognita*) was infected with a filterable, virus-like pathogen, but the infective agent was never identified [4]. The 1970s brought a collection of electron microscopy images of virus-like particles in nematodes; however, insufficient definitive information left the scientific community doubtful [5,6,7]. More recently, *Caenorhabditis elegans* were experimentally infected with the insect-infecting *Flock house virus* (FHV), and successful replication within the nematode was demonstrated [8]. Natural infection by Orsay virus in *C. elegans* and Santeuil virus in *C. briggsae* were subsequently discovered by high throughput sequencing [9]. Le Blanc virus infection was also discovered in *C. briggsae* [10] shortly afterwards. Another study localized Orsay, Santeuil, and Le Blanc viruses primarily to a small number of intestinal cells of *C. elegans* and *C. briggsae* [11]. The effect of these viruses on *Caenorhabditis* species is yet to be determined.

The first viruses confirmed to infect plant-parasitic nematodes were discovered by serendipity within the soybean cyst nematode (SCN; *Heterodera glycines*) via transcriptome pyrosequencing [12]. SCN is the leading pathogen of soybean in the United States [13]. The four viruses initially discovered in SCN possess negative-sense, single-stranded RNA genomes [12]. An additional virus, SCN virus-5 (SbCNV-5), was later discovered [14] which has a positive-sense, single-stranded RNA genome. The five viruses were detected within TN10, an inbred SCN line from single-cyst descent, and several other greenhouse populations of SCN that also originated from single-cyst descent [15]. SbCNV-5 was the only virus also documented within field samples of SCN in Illinois [14]. Thus far, the negative-sense RNA viruses have not been reported within field populations of SCN.

The objective of the investigation here was to assess if virus infection of SCN is more widespread than originally demonstrated [12,14]. A large-scale survey was conducted for SCN to determine if virus infection could be detected and to assess the relative levels of potential SCN viral infections. Both field and greenhouse populations were examined to deduce whether viruses infect nematodes directly in agricultural systems and are not artifacts of heavily inbred greenhouse populations. The study focused on the known viruses in SCN to confirm previous reports [12,14] as well as additional nematode species that have not yet been investigated for virus infection. Plant host tissue was tested to determine if viruses could potentially infect host plants as well as nematodes. A critical component of this study was to determine if viruses are actively replicating in SCN and if these viruses are detectable in multiple nematode life stages. As SCN is the predominant pathogen of soybean, further knowledge of nematode viruses could prove useful in understanding nematode ecology and implementing successful management strategies.

MATERIALS AND METHODS

Sample collection

Total RNA was extracted from 0.1 g of tissue from the leaves, stems, roots, and pods of 1 to 3-month-old soybean plants non-infected with SCN in a greenhouse at North Carolina State University (NCSU). Soybean cultivars tested include Bedford, Hartwig, Jake, NC Raleigh, NC Roy, and Williams 82. Additionally, a split root trial of NC Roy was repeated twice where half the root system was infected with either LY1 (infected with five known viruses) or MM21 (no known viral infection). Roots tested for viruses were selected from the non-infected half of the root system to avoid possible contamination of nematodes. In addition

to roots, leaves, stems, and pods were also sampled for SCN viral content. ELF1B was used as a measure of soybean plant levels via qRT-PCR, and SCN internal controls GAPDH and 18*S* were tested to further rule out contamination via nematodes (Table 2.2). The backgrounds of inbred SCN populations used in this study are documented in Table 2.1. Field SCN populations were collected from infested soybean fields in North Carolina (NC) and Missouri (MO); multiple soil cores were collected and pooled from each field. Distributions of SCN in NC have been documented by [16] and in MO by [17]. NC samples were propagated in the greenhouse for several months on roots of susceptible soybean cultivars, and field samples of SCN from MO were tested directly in the assays below without further propagation of the populations. SCN cysts were extracted from soil via water flotation and collection on nested sieves of screen sizes 20 (850 µm) and 60 (250 µm). SCN eggs were extracted by crushing cysts with a Tenbroeck homogenizer and further separated from soil debris by centrifugation in 70% sucrose and collection on a size 500 screen (25 µm). To minimize contamination, extraction equipment was bleached and/or autoclaved between SCN populations.

RNA extraction and cDNA synthesis

RNA was extracted from approximately 10,000 eggs of SCN greenhouse cultures as well as MO field samples and 5 to 10 cysts of NC field populations. Samples were prepared for total RNA extraction by homogenization with three 3-mm glass beads in a 1.5 ml tube on a Silamat S6 (Ivoclar Vivadent, Amherst, NY). Alterations in sample preparation were made for cysts in which a motorized pestle was first used to improve sample destruction. When extracting total RNA from plant tissue, a different modification was made as it was flash frozen in liquid nitrogen immediately before bead beating. The samples were then processed for total

RNA using TRIzol® Reagent (Invitrogen, Carlsbad, CA) under the guidelines of the manufacturer's protocol adapted from [18]. Total RNA concentrations were analyzed via Nanodrop 1000 (Thermo Fisher Scientific, Waltham, MA). cDNA was synthesized by incubating approximately 1 µg RNA with 0.06 µg random primers (Invitrogen) for 10 minutes at 70°C followed by rapid cooling on ice. Next, 4 µl GeneAmp® 10X PCR Buffer II (Applied Biosystems, Foster City, CA), 5.5 mM $MgCl_2$, 0.5 µM deoxynucleotide solution mix, 32 U Murine RNase Inhibitor (New England BioLabs, Ipswich, MA), and 50 U Multiscribe™ Reverse Transcriptase (Applied Biosystems) were added before additional incubations of 42°C and 70°C for 15 minutes each.

Virus detection via qRT-PCR

NCBI GenBank accession numbers for SCN viral sequences are HM849038 (ScNV), HM849039 (ScRV), HM849040 (ScPV), HM849041 (ScTV) and KF726084 (SbCNV-5). All primers used in this research were synthesized by Eurofins Genomics (Huntsville, AL). Viral primers originating from [12,14] were used to amplify fragments of the respective viral polymerases (Table 2.2). [Note: SCN negative-sense virus reverse (R) primers are oriented to the viral genome and reverse universal (RU) primers are oriented to the mRNA]. HgFAR1 was used as an internal control for SCN as this gene was used by [14] for qRT-PCR. Additionally, a primer pair for GAPDH (NCBI Genbank accession number CA939315) was designed as this gene is validated for steady expression throughout different SCN life stages by [19]. When testing soybean plants for virus, the *Glycine max* internal control gene ELF1B was amplified via primers from [20] listed in Table 2.2. qRT-PCR products were amplified using 0.5 µM of each appropriate primer pair, 10 µl iTaq™ Universal SYBR® Green Supermix (Bio-Rad,

Hercules, CA), and 1 µl cDNA. Applied Biosystems 7000 Real-Time PCR System was used at the following settings: 95°C, 10 minutes; 95°C, 15 seconds; 60°C, 1 minute for a total of 40 amplification cycles with a melt curve of 60°C for 20 seconds and 95°C for 15 seconds. Plant products were amplified utilizing the same methodology but with the newer technology of the Applied Biosystems QuantStudio™ 6 Flex Real-Time PCR system on the following settings: 95°C, 20 seconds; 95°C, 2 seconds; 60°C, 25 seconds repeated for 40 amplification cycles with a continuous melt curve of 95°C, 20 seconds; 60°C, 1 minute; and 94°C for 20 seconds.

Cycle threshold values (Ct; amplification cycle in which fluorescence emitted exceeds background fluorescence) equal to or greater than 35 were considered non-detectable. DNase treatments yielded insignificant results between Ct values of treated and untreated samples and was not necessary for analysis. The average normalized abundance ratios (i.e. relative amount of virus in each SCN sample) were determined for each population sample. Ct values of SCN viruses were normalized against the mean Ct values of SCN internal reference genes (GAPDH and/or HgFAR1) using the equation $E_{internal}^{Ct(internal)}/E_{target}^{Ct(target)}$ where E equals the efficiency of a primer pair [21]. Further modifications were made for addressing viral titer compared with host internal control genes [22]. Primer efficiencies were calculated by the equation $2^{(-1/slope)}$ via a five-point 1:2 dilution series. The efficiencies of primer pairs are E_{ScNV}=1.91 (91%), E_{ScPV}=1.92 (92%), E_{ScRV}=1.88 (88%), E_{ScTV}=1.89 (89%), $E_{SbCNV\text{-}5}$=1.98 (98%), E_{HgFAR1}=2.05 (105%), and E_{GAPDH}=2.07 (107%). Average normalized abundance of field populations was calculated using HgFAR1 as the internal control due to limited sample material; greenhouse populations were analyzed with both HgFAR1 and GAPDH. The average difference between GAPDH and HgFAR1 mean Ct values for greenhouse populations of SCN eggs was 0.83, less than one amplification cycle. Field samples for which both internal controls were amplified

had Ct values that differed by a mean of 0.37. Further statistical analysis of samples was conducted via GraphPad Prism 6 software (GraphPad Software, La Jolla, CA).

Viral presence and replication in different SCN life stages

OP50 and PA3 populations of SCN were analyzed for viral titer and replication within different life stages; these SCN lines were maintained at an NCSU greenhouse on susceptible soybean hosts. For each biological replication, four plants grown in individual cone planters were pooled for nematode extraction one month after inoculation with SCN eggs. Eggs were extracted from SCN females and collected via stacked sieves and sucrose centrifugation as previously described. Approximately half of the collected eggs were reserved for RNA extraction. The remaining eggs were hatched for three days at 27°C using a Baermann pan method [23] and the cohort of hatched J2 were collected. The remaining infected soybean roots were pulverized in a blender to remove J3 and J4 stages of SCN and the nematode sample was cleaned via stacked sieves and sucrose centrifugation. Pooled J3 and J4 samples of SCN were further concentrated by pelleting the collected nematodes in a microcentrifuge tube. RNA extraction from the collected SCN eggs, hatched J2, and J3/J4 life stages was completed as described above.

First strand cDNA synthesis was initiated with either random, genomic sense, or anti-genomic sense primers. Genomic sense primers used to initiate cDNA were ‘F500’ series and anti-genomic sense primers were ‘RU’ series. ‘Q’ primer pairs were utilized for qRT-PCR analysis as these primers are nested between the ‘F500’ and ‘RU’ primers (Table 2.2). OP50 samples were analyzed on an Applied Biosystems 7000 Real-Time PCR System, while PA3 samples were analyzed on an Applied Biosystems QuantStudio™ 6 Flex Real-Time PCR

System under the previously described settings. qRT-PCR average relative abundance ratios were quantified using the SCN internal control GAPDH as previously described via the Pfaffl method [21]. Pooled technical triplicates were electrophoresed on a 2% TAE agarose gel for further analysis.

Virus detection in other PPN species via qRT-PCR

New viral primers were designed to account for a potentially high degree of sequence dissimilarity for viruses in other PPN species. Therefore, viral 'Q' primers were designed within conserved regions of 500 nucleotide sequences of viral polymerases (Table 2.2). The nematode species *Heterodera schachtii* (beet cyst), *H. trifolii* (clover cyst), *Vittatidera zeaphila* (corn cyst) [24], *Globodera rostochiensis* (golden potato cyst), *G. tabacum* (tobacco cyst) were tested for viruses. Additionally, *Meloidogyne arenaria* (peanut root-knot), *M. hapla* (northern root-knot), *M. incognita* (southern root-knot), *M. javanica* (Javanese root-knot), and *Rotylenchus reniformis* (reniform) were examined. Due to either unavailable or dissimilar GAPDH sequences across nematode species, internal control primers were designed from conserved regions of the 18*S* ribosomal RNA gene among sequences available from NCBI Genbank including *H. glycines* (AY043247), *H. schachtii* (KJ636284), *Meloidogyne javanica* (AF442193) and *Aphelenchoides besseyi* (AY508035). The resulting primers are also listed in Table 2.2. Products were analyzed on an Applied Biosystems QuantStudio™ 6 Flex Real-Time PCR System under the previously described settings. Samples positive for viruses were electrophoresed on a 2% TAE agarose gel.

Confirmation of viral presence via endpoint PCR and Sanger sequencing

To confirm positive qRT-PCR results, a 500 bp region of the appropriate viral polymerases were amplified. The reverse universal (RU) primers from [12] and SbCNV-5-R primer [14] were used in conjunction with newly designed 'F500' primers (Table 2.2) to amplify an approximately 500 bp PCR product. OneTaq® 2X Master Mix with standard buffer (New England BioLabs) and appropriate primers were used according to manufacturer's protocol to amplify products from cDNA in the Bio-Rad C1000 Touch Thermal Cycler under the following conditions: 94°C, 5 minutes; 94°C, 30 seconds; 60°C, 30 seconds; 68°C, 40 seconds for 40 amplification cycles followed by a final extension of 68°C for 5 minutes. Products were electrophoresed on a 1% TAE agarose gel with 1X TAE buffer. PCR products were purified for sequencing with the QIAquick® PCR Purification Kit (Qiagen, Valencia, CA) according to manufacturer's instructions. In the case of low viral titers, PCR products were cloned into the pGEM®-T Easy Vector System (Promega, Madison, WI) and purified from transformed *Escherichia coli* via QIAprep® Spin Miniprep Kit (Qiagen). Sanger sequencing was performed by Eurofins Genomics with sequence primers listed on S2.1 Table. Sequence results were analyzed using Vector NTI Advance® 11.5.3 software (Invitrogen).

RESULTS

Viruses are not detectable in soybean plants

The SCN viruses are most closely related to viruses that are transmitted from insects to plants, but these specific viruses have not been reported to infect plants. Because of this potential, the pods, leaves, stems, and roots of SCN infected and noninfected soybean plants were collected for analysis via qRT-PCR. The soybean cultivars Bedford, Hartwig, Jake, NC

Raleigh, NC Roy and Williams 82 were tested for viruses via qRT-PCR (roots were tested only for soybean noninfected with SCN). Furthermore, split root trials with the soybean variety NC Roy were conducted where one-half of the root system was exposed to SCN. Roots were infected with either LY1 (harbors five known SCN viruses) or MM21 (noninfected with viruses), and roots from the noninfected half of the root system were tested for SCN viruses. The internal control gene ELF1B (eukaryotic elongation factor I-beta) [20] was used as a measure of soybean genetic material via qRT-PCR. Additionally, SCN primers (GAPDH and 18*S*) were utilized to further rule out nematode contamination; all attempts to amplify GAPDH and 18*S* were unsuccessful. SCN viruses were not detectable in any quantity within soybean plant tissues suggesting that these viruses are not passed from nematode to soybean plant or vice versa. If roots are capable of being infected by SCN viruses, infection would most likely be localized and not move throughout the root system or plant. Future testing of the root closer to a nematode feeding site may determine if a small site of localized infection exists.

Viruses are present and actively replicating in different SCN life stages

The egg, J2, and pooled J3/J4 stages of SCN were examined via qRT-PCR to see if viruses are detectable within multiple nematode life stages. Two different greenhouse lines of SCN (OP50 and PA3) were used in this experiment as these populations are commonly used for research purposes. OP50 (population originating from an NCSU greenhouse) was found to be infected with ScNV and ScPV via qRT-PCR (Fig 2.1A) whereas, PA3 harbors viral infections of ScNV, ScPV, ScRV and ScTV (Fig 2.1B). Viruses were detected in all SCN life stages tested and there were no significant differences in viral titers when comparing across multiple life stages of OP50 or PA3. Within a particular life stage, there was also no single

virus that was expressed at a significantly higher or lower titer than another virus. These data suggest that the viruses detected are stably present throughout the life stages of SCN. The Ct values and average normalized abundance ratios are reported for OP50 (S2.2 Table) and PA3 (S2.3 Table).

To deduce whether viruses (ScNV, ScPV, ScRV and ScTV) actively replicate within the nematode, first strand cDNA synthesis was initiated with primers specific to either the genomic or anti-genomic sense strand of RNA. qRT-PCR products internal to the cDNA primer initiation sites were amplified (S2.4 Table), and an electrophoresis gel of viral PCR products from OP50 demonstrated that both RNA-sense strands are amplified for ScNV and ScPV (Fig 2.1C). ScNV genomic and anti-genomic products are visible at relatively similar concentrations while anti-genomic RNA of ScPV is present at a visibly lower concentration in OP50. Typically, non-symmetric replication of the viral genome versus the anti-genome is expected. In the case of ScNV, viral titer may be high enough that differences in abundance cannot be visualized via electrophoresis of qRT-PCR products. Normalized abundance ratios were not calculated for this experiment as different cDNA was used to amplify specific orientations of viral products and internal controls were only amplified from cDNA initiated with random primers. The experiment was also replicated with PA3 (Fig 2.1D; S2.5 Table) and similar results are observable. For the four viruses present in PA3, both genomic and anti-genomic sense RNAs are detectable in egg, J2, and J3/J4 life stages. Anti-genomic RNA is visibly lower for ScRV within the PA3 J3/J4 life stages as compared with genomic RNA. ScNV, ScPV and ScTV titers are high for both negative and positive-sense RNAs in PA3. The presence of anti-genomic RNAs demonstrates that negative-sense RNA viruses are actively replicating within multiple life stages of SCN.

Viruses are prevalent in NC and MO greenhouse cultures and field populations of SCN

Forty-seven SCN greenhouse populations were surveyed for viruses to expand upon previous work in which viruses were detected in a limited number of SCN inbred greenhouse lines [12,14]. A small subset of the SCN lines - OP20, OP25, OP50 [25] - had been inbred and maintained in NCSU greenhouses for almost twenty years. The remaining greenhouse SCN populations tested were maintained within greenhouses at the University of Missouri (MU) and had originated from different field sites and inbred over time (Table 2.1). Total RNAs were extracted from SCN eggs followed by first strand cDNA synthesis and qRT-PCR analysis. Fig 2.2 displays the SCN greenhouse populations surveyed and heat map of the approximate viral titer (i.e. average normalized abundance ratio) within nematode egg samples relative to internal nematode control genes HgFAR1 and GAPDH. Average Ct values for greenhouse populations are listed in S2.6 Table. Each of the five SCN viruses were found frequently in inbred SCN greenhouse populations. Five SCN populations (TN7, TN22, LY1, MM2 and LY2) harbored infections with all five viruses known for SCN. Contrastingly, several SCN populations (MM21, MM23 and MM24) of similar descent (Table 2.1) have no detectable viral infections. A mixture of viral infections was present in the majority of SCN populations that were tested. There does not appear to be a distinct pattern of viral infections correlated with nematode virulence. For example, PA3 is SCN Hg type 0 and MM10, which possesses similar viral titers, is Hg type 1.2.3.4.5.6.7. ScRV and ScTV were only detected in SCN cultures originating in MO, and SbCNV-5 was also detected in greater frequency in SCN cultures from MO compared with SCN cultures originating from NC.

In addition to greenhouse populations, 25 field populations of SCN in NC and MO were sampled to deduce whether viral infections exist and are prevalent in an agricultural

setting. Due to the geography and climate of NC, soybeans are grown profitably almost exclusively in the eastern third of the state. The distribution of NC counties sampled for SCN viruses are mapped in Fig 2.3A. Twenty field samples, each from twenty different NC counties, yielded enough total RNA to reliably detect SCN internal control genes. There does not appear to be any clear pattern of viral distribution across NC; however, there does appear to be natural viral infections of SCN in agricultural fields. Approximate viral titers of county samples measured by qRT-PCR are listed and heat mapped in Fig 2.3. ScNV was the most common and highest titer virus found in SCN from NC fields followed by ScPV. The majority of viral titers in NC field samples of SCN were considered as non-detectable (ND), falling below the expression level of the reference SCN gene (GAPDH). Additionally, five field samples of SCN from MO were sampled to deduce whether viruses were present within another geographic area and if frequencies of viral infections differed. In the MO field samples of SCN tested, ScNV was the only virus detectable within one of five populations and is lower titer than the majority of NC samples. qRT-PCR Ct values for field samples are provided in S2.7 Table.

The percentage of SCN samples infected with ScNV or ScPV is similar for both greenhouse and field populations (Table 2.3). The biggest discrepancy in viral presence between these population sources is that ScTV is detectable within a high percentage of greenhouse populations but is not found within any NC or MO field samples. ScRV and SbCNV-5 are less frequently detected within field samples of SCN. These results suggest these viruses, with the exception of perhaps ScTV, are not artifacts of inbreeding greenhouse populations of SCN. Moreover, there are no significant differences between mean SCN viral titers of field and greenhouse populations of ScRV (Fig 2.4). Conversely, mean viral titer levels are significantly higher for ScNV, ScPV and SbCNV-5 in SCN greenhouse populations. Thus,

the replication process of ScRV does not appear to be hindered within field isolates of SCN. ScNV, ScPV and SbCNV-5 titers were lower in SCN field populations. However, for SbCNV-5 this could be a statistical result from relatively few samples being infected by this virus. Notably, ScTV was not detected within field samples from NC or greenhouse populations of NC origin [OP20, OP25 and OP50] even when maintained in MU greenhouses. Future work will examine if NC populations of SCN have innate immunity to ScTV or if these populations simply have not yet been exposed to this virus.

Other cyst nematode species are infected with SCN viruses

Other PPN species were sampled for the presence of the known five viruses to see if viral host ranges extended beyond SCN. Each nematode sample was tested for viruses via qRT-PCR using the "Q" primer sets (Table 2.2) and conditions that were used for SCN. No viruses were detectable in the majority of tested PPN species. Only clover cyst nematode (*H. trifolii*) and beet cyst nematode (*H. schachtii*) harbor three or two SCN viruses, respectively (Table 2.4) as detected by the PCR assay used here. Additional cyst (*Globodera rostochiensis, G. tabacum, Vittatidera zeaphila*), root-knot (*Meloidogyne arenaria, M. hapla, M. incognita, M. javanica*), and reniform (*Rotylenchus reniformis*) nematode species did not possess SCN viruses at detectable levels. Normalized abundance ratios were not calculated for this experiment as a new internal control (18*S*) was utilized due to sequence dissimilarity among PPN species. Positive qRT-PCR results were then confirmed by endpoint PCR amplification and Sanger sequencing of a 500 bp region of the RNA-dependent RNA polymerase (RdRP). *H. trifolii* was confirmed to possess ScNV, ScPV and ScTV (Fig 2.5) sequences. In two separate *H. schachtii* samples, a faint band for the 500 bp product was seen for either ScPV or

ScRV (images not shown). The PCR products of *H. schachtii* were also confirmed to be the correct virus products by Sanger sequencing.

DISCUSSION

Until recently, nematodes were widely considered noninfected by viruses primarily due to a scarcity of convincing published reports. High-throughput genomic and transcriptomic sequencing has enabled discovery of naturally occurring viruses within *C. elegans* and *C. briggsae* [9] and SCN [12,14]. This study confirms via qRT-PCR and Sanger sequencing of viral RdRP segments, the reports [12,14] that five viruses are present within SCN from different geographic regions. The results demonstrated that viruses are present within greenhouse populations of SCN, including extensive analysis of greenhouse populations commonly used in research. We report the presence of negative-sense viruses for the first time in field populations of SCN from two different states, NC and MO. Moreover, the negative-sense viruses are shown to actively replicate within the SCN host throughout egg, J2, and J3/J4 life stages. Finally, viruses are reported for the first time within the closely related cyst nematode species *H. trifolii* and *H. schachtii*.

Viruses are present within both greenhouse and field populations of SCN. Infection rates of ScNV and ScPV were similar for greenhouse and NC field samples (Table 2.3). The starkest difference in viral presence is ScTV that was detected in 58.1% of greenhouse populations but is not found in field samples. Future studies could examine whether NC SCN can be infected if introduced to ScTV or if the tested field populations are immune to infection by this particular virus. Interestingly, for those samples that tested positive, viral titers were not significantly different between field and greenhouse samples for ScRV (Fig 2.4). However,

titers were higher for ScNV, ScPV and SbCNV-5 in greenhouse populations. SbCNV-5 values do not cluster which may be a result of a small sample size or variation within SbCNV-5 replication itself. These data are similar to the findings of [14] who found SbCNV-5 in greenhouse populations but detected the virus less commonly in the field. Previously [12], field samples were not analyzed for the four negative-sense RNA viruses but did detect these viruses in several greenhouse lines of SCN. Preliminary results suggest SCN viruses could be more common in NC than in MO field samples as ScNV is the only virus detected in one of the five MO field samples. One possible explanation for this observation is that NC field samples were introduced to viruses when population levels were amplified in NCSU greenhouses for several months. However, this scenario is unlikely as several NC field samples tested positive for ScNV and ScPV when sampled directly from the field. A larger sampling of fields in MO and other geographic areas may illustrate a clearer picture of SCN viral infections. Moreover, viral titers are lower for SCN populations maintained in NCSU greenhouses as compared with those at MU. OP20, OP25 and OP50 are maintained at both locations, but virus levels are higher in MU populations. Greater inbreeding of greenhouse populations (i.e. TN, MM lines) among the MU SCN lines seemed to increase both virus frequency and titer, while the opposite seemed true for the inbred (OP) lines at NCSU. These discrepancies raise questions about how SCN viruses are transmitted and if different greenhouse conditions and research techniques can alter viral composition. Further confounding the issue, viral titers may vary within a particular population because of time of sample collection, soil temperature or host plant.

Related groups of nematodes seem to harbor similar infections. For instance, TN20 and PA3 are the parent lines of MM7, MM8 and MM10 (Fig 2.2) [26]. Subsequent populations are similar to PA3 in viral content and possess high titers of the negative-sense RNA viruses.

Similarly, the related populations MM16, MM18, MM19, MM21, MM23 and MM24 represent a relatively recent inbred MO field population and these nematodes have low amounts or no virus present. Although the titers are lower, the types of viral infections are different for MM16, MM18 and MM19. This inconsistency may arise because additional viruses are actually present but are below the detection limits of qRT-PCR. Another possibility is that viral titers are similar because these particular nematode populations have a genetic disposition to limit viral replication. Much of the available literature examines viruses of non-pathogenic *C. elegans* and *C. briggsae* [9,10] and makes it difficult to determine if viruses could affect nematode virulence. However, from this study it does not appear that viral infection is related to SCN virulence. As noted earlier, SCN lines with similar types and amounts of viral infection can have dissimilar HG types. One of the least virulent lines, PA3, has an HG type of 0 and one of the most virulent lines, MM10, has an Hg type of 1.2.3.4.5.6.7; yet, PA3 and MM10 are infected with ScNV, ScPV, ScRV and ScTV at similar titers.

Negative-sense RNA viruses are present within egg, J2, and J3/J4 stages of SCN. There are no significant differences in viral titers between life stages (Fig 2.1A and 1B). Furthermore, RNA viruses actively replicate within immature life stages of SCN (Fig 2.1C and 2.1D). Anti-genomic sense RNAs are detectable for ScNV, ScPV, ScRV and ScTV denoting that the viral genomes are being replicated. These data agree and expand upon the work of [12] who used a positive strand specific qRT-PCR assay to suggest that SCN negative-sense viruses replicate in the host. Although viral production did not increase within immature stages, future studies will examine if viral titers are higher within males or virgin females just prior to mating. Additionally, if the virus is nonpathogenic to SCN, then a stable, low titer of virus may be tolerated by the nematode innate immune system.

Since variation was observed among the 500 bp sequences of viral polymerases, new qRT-PCR primers were designed within conserved regions of the known SCN viruses to increase potential detection of these viruses within other PPN species. Additional PPN species were tested for viruses (Table 2.4) with only cyst nematode species *H. schachtii* and *H. trifolii* harboring detectable viruses. An approximately 500 bp region of each viral RdRP was confirmed to be the correct PCR product via Sanger sequencing. Three viruses were found within *H. trifolii*: ScNV, ScPV and ScTV. The viruses ScPV and ScRV are present in two separate *H. schachtii* population samples from 2008 and an unknown date (Table 2.4). It is not unrealistic to believe SCN viruses are present within *H. schachtii* and *H. trifolii*. The phylogenic relationship of the *Schachtii* lineage is reported [27] based upon ITS regions of ribosomal DNA sequences. Coincidentally, *H. glycines* is most closely related to *H. trifolii* followed by *H. mediterranea* (not tested) and *H. schachtii*. These data suggest SCN viruses may have evolved within this subset of cyst nematodes before the species split from one another. Additional analysis of viral genomes in PPN may resolve relationships between different virus isolates. Furthermore, it is possible that viruses discovered in SCN exist in additional nematode species but the titers are below detectable limits, primers cannot bind due to genetic dissimilarity or they simply have not yet been tested. More objective analyses to detect potential virus infection of other PPN species are certainly warranted given the extent of virus infection that occurs in SCN.

Predicting why there is variance in viral infections among populations and environments without knowing the mode of transmission or tropisms is challenging. There may be a dilution effect if the viruses are localized to only a few cells in comparison to the internal control (GAPDH) that expresses a single copy in each cell. The information available

on *Caenorhabditis* viruses may help to localize SCN viral infections within the nematode. Viruses that infect *Caenorhabditis* species were discovered to possess tropism to several intestinal cells [11]. Methods of natural transmission have not been clearly deduced; however, experimental infection of *C. elegans* with FHV is possible by microinjection of *C. elegans* and FHV plasmids into the gonad [8]. Unfortunately, this technique does not explain how viruses naturally establish infection in nematodes.

Future work will determine if nematode viruses are contributing factors to host development or pathogenicity. Relatedly, treating human infections of the nematode species *Onchocerca volvulus* with doxycycline in conjunction with ivermectin enables greater treatment success. The antibiotic sterilizes female nematodes by attacking an endosymbiotic bacterium, *Wolbachia spp.*, which controls host development [28]. If viruses can function similarly in other parasitic nematodes, targeting viruses could help to disrupt the parasitic cycles of important nematode species. More in depth studies of microbial symbionts of nematodes may yield interesting results that can further development of novel control strategies, and it is likely that future next-generation sequencing projects will continue to unveil additional novel viral sequences within nematode species. Although SCN viruses were not detectable in soybean plant tissue, more intensive testing of SCN weed hosts may yield interesting results as to additional hosts for these viruses. From the presented research, we hope to demonstrate that nematode viruses are more widespread than previously thought and may have important impacts on nematode biology. Thus, in the future, viruses could prove useful for development of novel biological controls to target nematodes. Upcoming studies include examining how viral transmission occurs and localizing cellular and tissue tropisms.

ACKNOWLEDGEMENTS

Funding was provided by NC Soybean Producers Association, Grant 12-13, http://ncsoy.org/. This material is based upon work supported by the National Science Foundation Graduate Research Fellowship under Grant No. DGE-1252376 to CLR, https://www.nsfgrfp.org/. We would like to thank the following technicians for their invaluable support of this research: Chunying Li, Jim Cole, Jack Ward, Jeff Spivey, Amanda Howland, John Dempsher and Robert Heinz. A special thank you is extended to Xiaohong Wang and Shiyan Chen of Cornell University for their contribution of *G. rostochiensis* total RNA.

LITERATURE CITED

1. Brown DJ, Robertson WM, Trudgill DL. Transmission of viruses by plant nematodes. Annu Rev Phytopathol. 1995; 33: 223–249.

2. Gray SM, Banerjee N. Mechanisms of arthropod transmission of plant and animal viruses. Microbiol Mol Biol Rev. 1999; 63: 128–148.

3. Hooper DJ. Virus vector nematodes – taxonomy and general introduction. In: Lamberti F, Taylor CE, Seinhorst JW, editors. Nematode vectors of plant viruses. London: Plenum Press; 1974. pp 1-14.

4. Loewenberg JR, Sullivan T, Schuster ML. A virus disease of *Meloidogyne incognita*, the southern root knot nematode. Nature. 1959; 184: 1896.

5. Foor WE. Virus-like particles in a nematode. J Parasitol. 1972; 1065-1070.

6. Poinar GO, Hess R. Virus-like particles in the nematode *Romanomermis culicivorax* (Mermithidae). Nature. 1977; 266: 256-257.

7. Zuckerman BM, Himmelhoch S, Kisiel M. Virus-like particles in *Dolichodorus heterocephalus*. Nematologica. 1973; 19: 117.

8. Lu R, Maduro M, Li HW, Broitman-Maduro G, Li WX, Ding SW. Animal virus replication and RNAi-mediated antiviral silencing in *Caenorhabditis elegans.* Nature. 2005; 436: 1040-1043.

9. Felix MA, Ashe A, Piffaretti J, Wu G, Nuez I, Belicard T, Jiang Y, Zhao G, Franz C, Goldstein L, Sanroman M, Miska E, Wang D. Natural and experimental infection of

Caenorhabditis nematodes by novel viruses related to nodaviruses. PLoS Biol, 2011; 9: e1000586.

10. Franz CJ, Zhao G, Félix MA, Wang D. Complete genome sequence of Le Blanc virus, a third *Caenorhabditis* nematode-infecting virus. J Virol. 2012; 86: 11940-11940.

11. Franz CJ, Renshaw H, Frezal L, Jiang Y, Felix MA, Wang D. Orsay, Santeuil and Le Blanc viruses primarily infect intestinal cells in *Caenorhabditis* nematodes. Virology. 2013; 448: 255-264.

12. Bekal, S, Domier LL, Niblack TL, Lambert KN. Discovery and initial analysis of novel viral genomes in the soybean cyst nematode. J Gen Virol. 2011; 92: 1870-1879.

13. Wrather JA, Koenning SR. Estimates of disease effects on soybean yields in the United States 2003 to 2005. J Nematol. 2006; 38: 173-180.

14. Bekal S, Domier LL, Gonfa B, McCoppin NK, Lambert KN, Bhalerao K. A novel flavivirus in the soybean cyst nematode. J Gen Virol. 2014; 95: 1272-1280.

15. Colgrove AL, Niblack TL. Correlation of female indices from virulence assays on inbred lines and field populations of *Heterodera glycines*. J Nematol. 2008; 40: 39-45.

16. Koenning SR, Barker KR. Survey of *Heterodera glycines* races and other plant-parasitic nematodes on soybean in North Carolina. J Nematol. 1998; 30: 569-576.

17. Mitchum MG, Wrather JA, Heinz RD, Shannon JG, Danekas G. Variability in distribution and virulence phenotypes of *Heterodera glycines* in Missouri during 2005. Plant Dis. 2007; 91: 1473-1476.

18. Chomczynski P, Sacchi N. Single step method of RNA isolation by acid guanidinium thiocyanate-phenol-chloroform extraction. Anal Biochem. 1987; 162: 156-159.

19. Ithal N, Recknor J, Nettleton D, Hearne L, Maier T, Baum TJ, Mitchum MG. Parallel genome-wide expression profiling of host and pathogen during soybean cyst nematode infection of soybean. Mol Plant-Microbe Interact. 2007; 20: 293-305.

20. Jian B, Liu B, Bi Y, Hou W, Wu C, Han T. Validation of internal control for gene expression study in soybean by quantitative real-time PCR. BMC Mol Biol. 2008; 9: 59.

21. Pfaffl MW. A new mathematical model for relative quantification in real-time RT–PCR. Nucleic Acids Res. 2001; 29: 2002-2007.

22. Rotenberg D, Krishna Kumar NK, Ullman DE, Montero-Astúa M, Willis DK, German TL, Whitfield AE. Variation in Tomato spotted wilt virus titer in *Frankliniella occidentalis* and its association with frequency of transmission. Phytopathology. 2009; 99: 404-410.

23. Townshend JL. A modification and evaluation of the apparatus for the Oostenbrink direct cottonwool filter extraction method. Nematologica. 1963; 9: 106–110.

24. Bernard EC, Handoo ZA, Powers TO, Donald PA, Heinz RD. *Vittatidera zeaphila* (Nematoda: *Heteroderidae*), a new genus and species of cyst nematode parasitic on corn (*Zea mays*). J Nematol. 2010; 42: 139-150.

25. Dong K, Opperman CH. Genetic analysis of parasitism in the soybean cyst nematode *Heterodera glycines*. Genetics. 1997; 146: 1311-1318.

26. Gardner M, Heinz R, Wang J, Mitchum MG. Genetics and adaption of soybean cyst nematode to broad spectrum resistance. G3. 2017; doi: 10.1534/g3.116.035964.

27. Skantar AM, Handoo ZA, Zanakis GN, Tzortzakakis EA. Molecular and morphological characterization of the corn cyst nematode, *Heterodera zeae*, from Greece. J Nematol. 2012; 44: 58-66.

28. Hoerauf A, Mand S, Adjei O, Fleischer B, Büttner DW. Depletion of wolbachia endobacteria in *Onchocerca volvulus* by doxycycline and microfilaridermia after ivermectin treatment. Lancet. 2001; 357: 1415-1416.

TABLES

Table 2.1. Inbreeding protocol, date of origin and HG type of SCN greenhouse populations used in this study.

Population	Inbreeding protocol	Origin date	HG type at time of sample collection	Citation
LY1	Synthetic isolate, selected for reproduction on 'Hartwig' by Lawrence Young.	1998	1–7	[15]
LY2	Field isolate from Tennessee mass selected on 'Hartwig' by Lawrence Young.	2000	1-7	
MM1	PA3 mass-selected on susceptible Essex x Forrest 63 (EXF63) recombinant inbred line	2006	0	M. Mitchum, unpubl.
MM2	PA3 mass-selected on resistant Essex x Forrest 67 (EXF67) recombinant inbred line	2006	1.2.3.5.6.7	
MM3	PA3 mass-selected on susceptible Evans x PI 209332 near-isogenic line 7923S	2006	2.5.7	
MM4	PA3 mass-selected on resistant Evans x PI 209332 near-isogenic line 7923R	2006	2.5.7	
MM7	PA3 x TN20 outselected on Peking	2006	1.2.3.5.6.7	[26]
MM8	PA3 x TN20 outselected on PI 88788	2006	2.5.7	
MM10	PA3 x TN20 outselected on PI 437654	2006	1-7	
MM16	Mass-selection of cysts recovered from a Mississippi, MO field population on PI 437654.	2013	1-7	M. Mitchum, unpubl.
MM18	Mississippi County, MO field population HG 1.2.3.5.6.7 (Race 4) subjected to rotation on susceptible soybean cvs. Lee74, Essex, Macon and Williams 82.	2013	1.2.3.5.6.7	
MM19	Mississippi County, MO field population HG 1.2.3.5.6.7 (Race 4) subjected to rotation on soybeans with PI 88788 type resistance.	2013	1.2.3.5.6.7	
MM21	Mississippi County, MO field population HG 1.2.3.5.6.7 (Race 4) subjected to rotation on soybeans with Hartwig type resistance.	2013	1.2.3.-	
MM23	Mississippi County, MO field population HG 1.2.3.5.6.7 (Race 4) subjected to rotation on soybeans with PI 88788, Peking and Hartwig type resistance.	2013	1.2.3.-	
MM24	Mississippi County, MO field population HG 1.2.3.5.6.7 (Race 4) subjected to rotation on soybeans with PI 88788, Peking and Hartwig type resistance and susceptible soybeans.	2013	1.2.3.-	
OP20[a]	Field isolate from North Carolina selected by single cyst decent on PI 88788.	-	1.2.3.5.6.7	[25]
OP25[a]	Field isolate from North Carolina selected by single cyst decent on Lee 68.	-	0	
OP50[a]	Field isolate from North Carolina selected by single cyst decent on PI 90763.	-	1.2.3.5.6.7	
PA3	Prakash Arelli "Race 3" maintained on Williams 82.	-	0	[15]
TN1	Terry Niblack, Gene pool isolate originally prepared by V. Dropkin maintained on Macon soybean.	1980	1.2.3.5.6.7	
TN2/tomato	Isolate from a potato field inbred by mass selection on Tiny Tim tomato.	1990	0	
TN2/soybean	TN2 inbred by mass selection on soybean Williams 82.	1990	0	
TN6	TN1 selected by single-cyst descent on Peking.	1996	1.2.3.5.6.7	

Table 2.1 (continued)

TN7	TN1 selected by single-cyst descent on PI 88788.	1996	2.5.7	
TN8	TN1 selected by single-cyst descent on PI 90763.	1996	1.3.6.7	
TN12	TN1 inbred by mass selection on Pickett.	1988	1.2.3.5.6.7	
TN13	TN1 inbred by mass selection on Peking.	1988	1.3.5.6.7	
TN14	TN1 inbred by mass selection on PI 88788.	1988	1.2.5.7	
TN15	TN1 inbred by mass selection on PI 90763.	1988	1-7	
TN19	LY1 selected by single-cyst descent on Hartwig.	1988	1-7	
TN20	LY1 selected by single-cyst descent on PI 437654.	1999	1–7	
TN21	Field isolate from Missouri mass selected on Hartwig.	2001	1–7	
TN22	TN2 mass selected on PI 88788.	1999	1.2.5.7	
VL1	Virgil Leudders 'Hg1' (high on 89008, low on 209332); mass selected on PI 89008.	1985	2.5.7	

Unless otherwise noted, populations were maintained at University of Missouri (MU) greenhouses. LY = Lawrence Young; MM = Melissa Mitchum; OP = Charlie Opperman; PA = Prakash Arelli; TN = Terry Niblack; VL = Virgil Leudders.
[a] Maintained in both NCSU and MU greenhouses

Table 2.2. Primers used for amplifying selected regions of virus RNA-dependent RNA polymerases (RdRPs) from total RNA samples.

Primer	Sequence [5' to 3']	Source
ELF1B-F [a]	GTTGAAAAGCCAGGGGACA	[20]
ELF1B-R [a]	TCTTACCCCTTGAGCGTGG	
ScNV-R [a]	ACGAGCAGCGGATGAGTTTAA	[12]
ScNV-RU [a,b]	GGTCCTCCGCTGCCCTATGGTGGCCACTTCCTGTGCTTCT	
ScPV-R [a]	CAGTGGGACGGCAAAATCTT	
ScPV-RU [a,b]	GGTCCTCCGCTGCCCTATGGCAGTGGGACGGCAAAATCTT	
ScRV-R [a]	TTGACAAGTGCGGGTTTGAG	
ScRV-RU [a,b]	GGTCCTCCGCTGCCCTATGGGTCCCCCTGCCCCATTATC	
ScTV-R [a]	AGCCCCAAGGACCTGGTTT	
ScTV-RU [a,b]	GGTCCTCCGCTGCCCTATGGCTTCCGGTGTAGCAGGGAGAT	
SbCNV-5-F [a]	GGAACTGTGTCGCGGTTTG	[14]
SbCNV-5-R [a,b]	TGCACTGAGGCATTTCACAAC	
HgFAR1-F [a]	CCATTTGCCGCCTTTGGA	
HgFAR1-5-R [a]	GGGATCAATTCGCGGTATTCG	
GAPDH-F [a]	TCCAAGGCATAGAAAGACGACG	Designed for this study
GAPDH-R [a]	AACAAGTCATTGGACGGCATCA	
ScNV-F500 [b]	ACATAGTCAGTGGCCGATTC	
ScPV-F500 [b]	CTCGTCGAAGAGCTGTGTTAC	
ScRV-F500 [b]	GCGACTGTTCTCGCTCCTGA	
ScTV-F500 [b]	TGTGTTTTACATGCCGGCCTC	
SbCNV-5-F500 [b]	CTTGTTCGAGGTGAGTGTGG	
ScNVQ-F [a]	GGTCCTGCTTAGCTTGTGA	
ScNVQ-R [a]	CATCTGTGGTGATTGGAC	
ScPVQ-F [a]	CGCAAGATGGAAGACCAG	
ScPVQ-R [a]	GGTGATGGTGGAGAATTTAG	
ScRVQ-F [a]	GGCATACCCGTCGGCAAC	
ScRVQ-R [a]	GTCCAACCGGGACACAGCC	
ScTVQ-F [a]	CTCATGTCACCGTCTCTGTGC	
ScTVQ-R [a]	GCAGTTACGCAAGACTGGTCTAG	
SbCNV5Q-F [a]	CATGACAGCAAAGTGTGCCG	
SbCNV5Q-R [a]	CGGTCCAACTTCGCGCCAC	
PPN18S-F [a]	GGTAGTGACGAGAAATAACG	
PPN18S-R [a]	CTGCTGGCACCAGACTTG	

RNAs were extracted from *Glycine max* (internal control ELF1B), *Heterodera glycines* (internal controls HgFAR1, GAPDH and PPN18*S*) or other nematode species (internal control PPN18*S*).

[a] Used for qRT-PCR detection

[b] PCR amplification of approximately 500 bp segment of RdRP

Table 2.3. Number and percent of North Carolina SCN greenhouse and NC field population samples infected with viruses as detected with qRT-PCR.

	Greenhouse populations		NC field populations	
Virus	**Number infected**	**Percent infected**	**Number infected**	**Percent infected**
ScNV	38/43	88.4%	16/20	80.0%
ScPV	25/43	58.1%	13/20	65.0%
ScRV	31/43	72.1%	3/20	15.0%
ScTV	25/43	58.1%	0/20	0.0%
SbCNV-5	14/43	32.6 %	3/20	15.0%

Table 2.4. Detection of known SCN viruses in other species of plant-parasitic nematodes via qRT-PCR.

				Average Ct value[a]					
PPN species	**Life stage**	**Location**	**Date collected**	**ScNV**	**ScPV**	**ScRV**	**ScTV**	**SbCNV-5**	**18S[b]**
Globodera rostochiensis	egg	CU	2015	ND[c]	ND	ND	ND	ND	13.22
	J2	CU	2015	ND	ND	ND	ND	ND	13.30
G. tabacum	egg	MU	2015	ND	ND	ND	ND	ND	11.51
	J2	NCSU	1997a	ND	ND	ND	ND	ND	11.17
			1997b	ND	ND	ND	ND	ND	9.435
Heterodera schachtii	J2	NCSU	2008	ND	30.75	ND	ND	ND	12.90
			2009a	ND	ND	ND	ND	ND	15.65
			2009b	ND	ND	ND	ND	ND	12.88
			NA[d]	ND	ND	34.60	ND	ND	11.60
H. trifolii	egg	MU	2014	25.81	23.25	ND	26.97	ND	13.45
Meloidogyne arenaria	J2	NCSU	1997	ND	ND	ND	ND	ND	14.16
			NA	ND	ND	ND	ND	ND	9.489
M. hapla	J2	NCSU	1997	ND	ND	ND	ND	ND	7.688
M. incognita	J2	NCSU	1994a	ND	ND	ND	ND	ND	15.46
			1994b	ND	ND	ND	ND	ND	6.926
			2001	ND	ND	ND	ND	ND	12.70
			NAa	ND	ND	ND	ND	ND	9.114
			NAb	ND	ND	ND	ND	ND	8.072
M. javanica	J2	NCSU	1995	ND	ND	ND	ND	ND	7.403
Rotylenchus reniformis	J2	NC field	2003	ND	ND	ND	ND	ND	13.79
			NA	ND	ND	ND	ND	ND	12.49
Vittatidera zeaphila	egg	MU	2015	ND	ND	ND	ND	ND	10.93

[a] average of technical triplicates
[b] internal control
[c] not detectable
[d] date not available

FIGURES

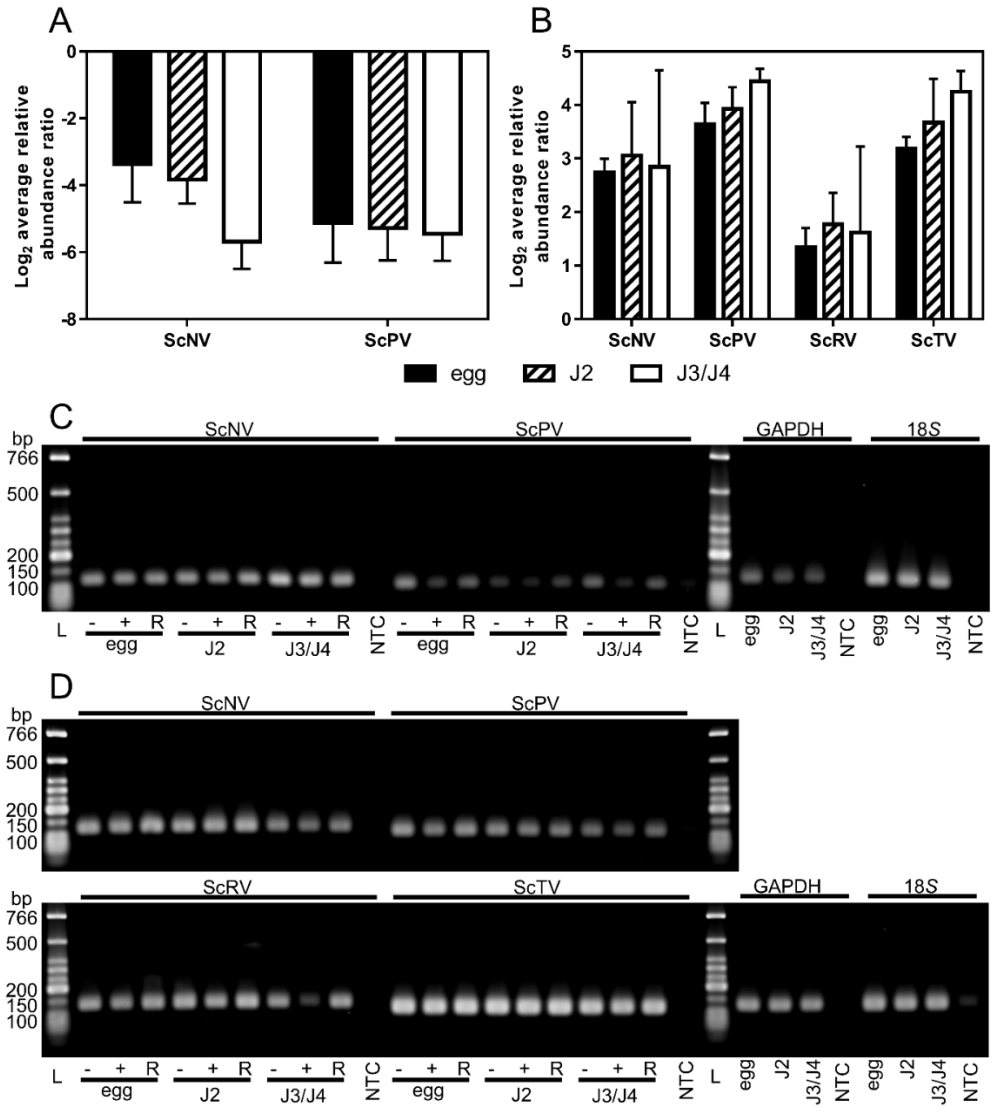

Fig 2.1. Titer and replication of negative-sense RNA viruses within SCN life stages measured with qRT-PCR. Log_2 average relative abundance of viruses within SCN OP50 (A) and PA3 (B) populations for egg, J2 and J3/J4 stages. Each experiment was conducted in technical triplicates and two different biological replicates. Error bars represent the SEM. Analysis of the means was conducted with 2-way ANOVA (GraphPad Prism 6). Active replication of viruses is shown for OP50 (C) and PA3 (D) by analyzing qRT-PCR products on a 2% agarose gel. The following abbreviations are explained: low molecular weight ladder (L; New England BioLabs), no template control (NTC), genomic RNA (-), anti-genomic RNA (+) and both genomic and anti-genomic RNA control initiated with random primers. Internal controls for SCN are GAPDH and 18*S*.

SCN population	ScNV	ScPV	ScRV	ScTV	SbCNV-5
MM16[c]	ND	ND	-9.56	ND	ND
MM18[c]	-6.17	-5.41	ND	ND	ND
MM19[c]	-4.49	ND	-8.41	-6.13	ND
MM21[c]	ND	ND	ND	ND	ND
MM23[c]	ND	ND	ND	ND	ND
MM24[c]	ND	ND	ND	ND	ND
OP20[a,d]	-6.47	ND	ND	ND	ND
OP25[a,d]	-5.91	-6.63	ND	ND	ND
OP50[a,d]	-7.85	-7.9	ND	ND	ND
OP20[d]	1.85	ND	ND	ND	ND
OP25[d]	-1.22	1.02	ND	ND	1.98
OP50[d]	4.71	ND	ND	ND	ND
TN1[e]	3.59	ND	1.31	2.21	5.09
TN6[e]	-4.75	ND	ND	ND	-4.86
TN7(a)[e]	1.83	1.27	-1.24	1.83	3.29
TN7(b)[e]	1.98	0.56	1.26	2.17	4.11
TN8(a)[e]	-5.83	ND	0.94	ND	1.18
TN8(b)[e]	ND	ND	-6	ND	3.82
TN12[e]	3.69	0.28	0.36	2.91	ND
TN13[e]	3.4	ND	0.7	2.49	3.27
TN14[e]	3.37	ND	-0.96	ND	ND
TN15[e]	3.2	ND	-0.42	2.56	ND
TN2/soybean[f]	2.23	ND	ND	-5.04	ND
TN2/tomato[f]	2.51	ND	-1.93	ND	-13.13
TN22[f]	2.9	1.3	-2.87	1.62	-10.71
LY1[g]	4.2	1.73	0.17	3.29	6.14
TN19[g]	2.93	-2.53	-0.16	2.16	ND
TN20[g,h]	ND	ND	-3.49	ND	-2.68
PA3[h]	3.21	1.78	-0.22	3.36	ND
MM7[h]	3.91	2.05	0.08	-8.83	ND
MM7/Williams82[h]	3.29	1.58	-0.73	ND	ND
MM8[h]	0.49	0.56	-1.11	0.52	ND
MM8/Peking[h]	1.95	0.76	-0.71	1.14	ND
MM8/Williams82[h]	1.49	1.05	-2.44	1.21	ND
MM10[h]	4.1	2.35	1.04	3.33	ND
MM10/Williams82[h]	4.7	2.96	1.75	3.48	ND
MM4[h]	2.58	1.31	0.77	2.59	ND
MM3[h]	1.3	1.76	-1.15	1.16	ND
MM1[h]	1.67	0.66	-1.94	1.71	ND
MM2[h]	1.27	1.2	-7.43	0.52	3.29
LY2	1.69	0.5	-0.44	-1.29	1.9
TN21	2.81	0.67	-0.68	1.06	ND
VL1	-6.31	ND	-1.58	2.73	ND

Fig 2.2. Log$_2$ average relative abundance ratios of respective viruses in SCN egg samples from populations maintained in research greenhouses. Viral presence and level were determined by relative quantification of qRT-PCR values normalized against SCN internal control genes HgFAR1 and GAPDH. Experiments were conducted in technical triplicates. The color gradient represents a heat map of variance in viral titers.

A

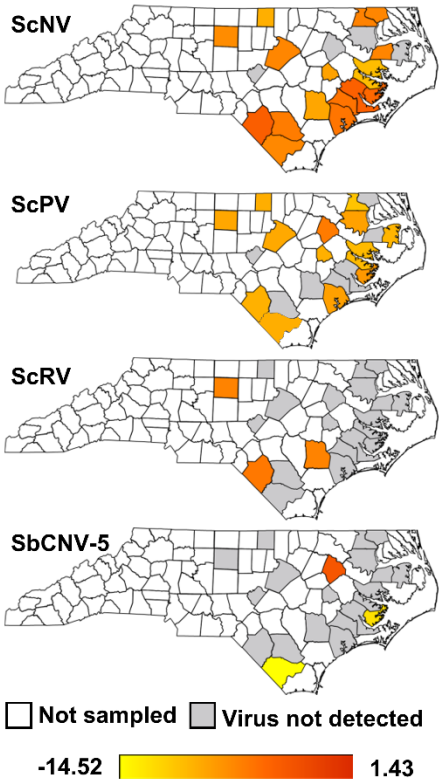

B

SCN population	ScNV	ScPV	ScRV	ScTV	SbCNV-5
Beaufort	-7.93	-7.66	ND[b]	ND	ND
Bertie	ND	-5.22	ND	ND	ND
Bladen	-1.56	ND	ND	ND	ND
Columbus	-2.73	-6.48	ND	ND	-14.52
Craven	0.89	ND	ND	ND	ND
Duplin	-5.71	ND	-2.23	ND	ND
Edgecombe	ND	-1.43	ND	ND	1.43
Gates	-2.54	ND	ND	ND	ND
Greene	-5.29	-6.73	ND	ND	ND
Guilford	-3.20	-5.76	-2.29	ND	ND
Hertford	-2.12	-8.64	ND	ND	ND
Jones	-0.68	ND	ND	ND	ND
Lee	ND	ND	ND	ND	ND
Onslow	-0.86	-5.09	ND	ND	ND
Pamlico	0.36	-4.29	ND	ND	-11.45
Person	-6.60	-6.50	ND	ND	ND
Robeson	1.00	-6.77	-1.18	ND	ND
Tyrell	ND	-7.16	ND	ND	ND
Wake	-2.60	-5.98	ND	ND	ND
Washington	-2.47	ND	ND	ND	ND
Barton[a]	-8.70	ND	ND	ND	ND
Dunklin 1[a]	ND	ND	ND	ND	ND
Dunklin 2[a]	ND	ND	ND	ND	ND
Scott 1[a]	ND	ND	ND	ND	ND
Scott 2[a]	ND	ND	ND	ND	ND

[a] Samples are collected from infested fields in MO; all other samples are from NC fields
[b] virus not detected.

Fig 2.3. Log$_2$ average relative abundance ratios of respective viruses in SCN egg samples from NC and MO infested fields. Viral titers are represented spatially (A) and numerically for NC county field samples (B). Virus presence and level are determined by relative quantification of qRT-PCR values normalized to SCN internal control gene HgFAR1. Experiments were conducted in technical triplicates. The color gradient accentuates differences in viral titers.

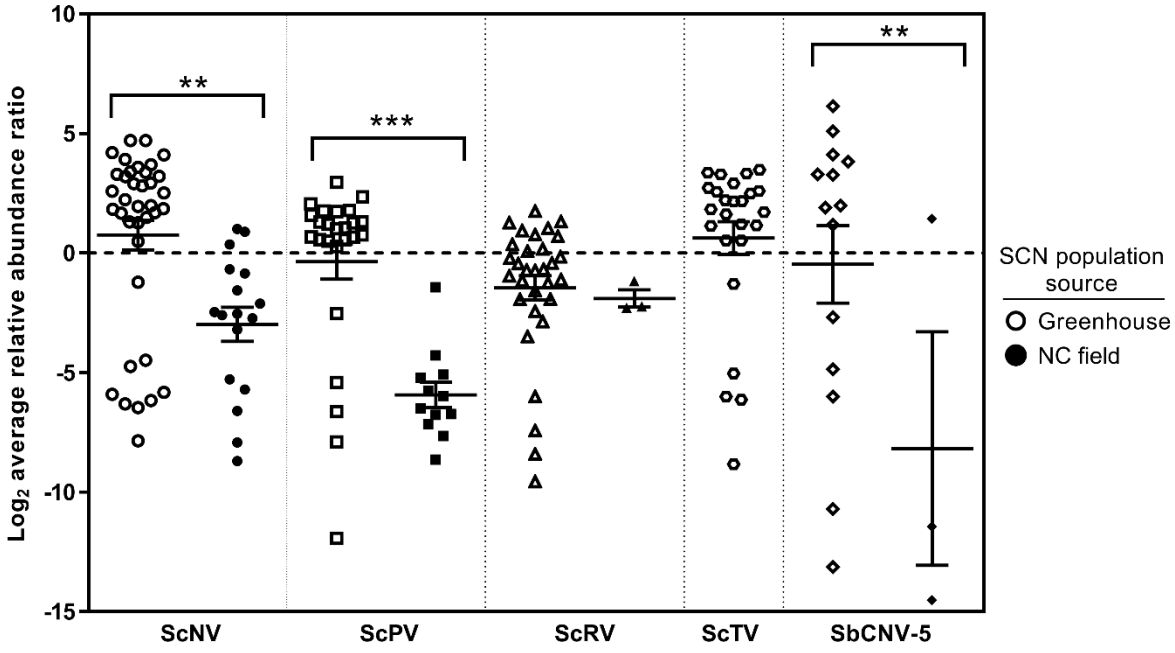

Fig 2.4. Log_2 average relative abundance ratios of SCN samples in which virus is detectable via qRT-PCR. Both SCN greenhouse and NC field population values are shown except for ScTV as this virus was not detected in field samples. The center line denotes the mean and error bars represent the SEM. Analysis of the means was conducted with 2-way ANOVA (GraphPad Prism 6) and asterisks demonstrate significant differences at p = .01 (**) and p = .001 (***) levels.

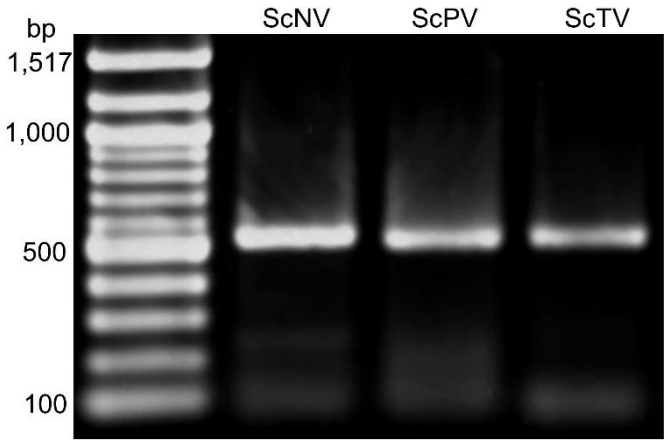

Fig 2.5. Amplification of SCN viruses within *Heterodera trifolii*. PCR products of the approximately 500 bp RdRP region for ScNV, ScPV and ScTV were amplified from total RNA extracted from *H. trifolii* and electrophoresed on a 1% agarose gel with 100 bp molecular ladder (New England BioLabs).

CHAPTER 3

Novel RNA Viruses within Plant Parasitic Cyst Nematodes

Published within *PLOS ONE*

Citation: **Ruark CL**, Gardner M, Mitchum MG, Davis EL, and Sit TL. Novel RNA viruses within plant parasitic cyst nematodes. PLOS ONE. 2018; 13(3): e0193881. https://doi.org/10.1371/journal.pone.0193881.

ABSTRACT

The study of invertebrate – and particularly nematode – viruses is emerging with the advancement of transcriptome sequencing. Five single-stranded RNA viruses have now been confirmed within the economically important soybean cyst nematode (SCN; *Heterodera glycines*). From previous research, we know these viruses to be widespread in greenhouse and field populations of SCN. Several of the SCN viruses were also confirmed within clover (*H. trifolii*) and beet (*H. schachtii*) cyst nematodes. In the presented study, we sequenced the transcriptomes of several inbred SCN populations and identified two previously undiscovered viral-like genomes. Both of these proposed viruses are negative-sense RNA viruses and have been named SCN nyami-like virus (NLV) and SCN bunya-like virus (BLV). Finally, we analyzed publicly available transcriptome data of two potato cyst nematode (PCN) species, *Globodera pallida* and *G. rostochiensis.* From these data, a third potential virus was discovered and called PCN picorna-like virus (PLV). PCN PLV is a positive-sense RNA virus, and to the best of our knowledge, is the first virus described within PCN. The presence of these novel viruses was confirmed via qRT-PCR, endpoint PCR, and Sanger sequencing with the exception of PCN PLV due to quarantine restrictions on the nematode host. While much work needs to be done to understand the biological and evolutionary significance of these viruses, they offer insight into nematode ecology and the possibility of novel nematode management strategies.

INTRODUCTION

Specific genera of plant parasitic nematodes (PPN) are non-propagative vectors of plant viruses [1], but PPN themselves were thought to be immune to viral infections. Recent

advances in whole transcriptome sequencing, however, have led to the discovery of novel viruses infecting nematodes. The first nematode viruses, belonging to the family *Nodaviridae,* were identified within natural populations of *Caenorhabditis elegans* and *C. briggsae* [2,3]. Soon afterward, the first viruses infecting PPN were found within *Heterodera glycines* (soybean cyst nematode; SCN) belonging to families *Bunyaviridae, Bornaviridae, Rhabdoviridae,* and *Flaviviridae* [4,5]. Additionally, a novel nodavirus element has recently been described within the plant parasitic pinewood nematode, *Bursaphelenchus xylophilus* [6]. Previous research has demonstrated the widespread prevalence of the known SCN viruses within inbred and field populations as well as other *Heterodera* species including beet and clover cyst nematode [7]. In addition, we confirmed that these viruses replicate within the nematode host and are found in multiple life stages. Recently, a comprehensive paper analyzing over 220 invertebrate species provided an additional 1,445 viral genome entries into the NCBI database [8]. Included in this analysis were animal parasitic nematodes belonging to *Ascaridia, Ascaris, Romanomermis,* and other unidentified nematode genera providing 32 new viral genomes for further investigation. One over-arching commonality of nematode viruses discovered so far is that they possess single-stranded RNA genomes. These viruses were not initially discovered by genome sequencing as there is no DNA intermediate and thus, cannot be readily detected without RNA sequencing technology.

The study presented here analyzed nematode transcriptome data to identify and describe novel viral genomes via de novo assembly with the assistance of the VirFind toolset (virfind.org) [9]. Nematode species analyzed for viruses in this study include *Heterodera glycines, H. schachtii, H. avenae, H. trifolii, Globodera pallida, G. rostochiensis, G. tabacum,* and *Vittatidera zeaphila.* These cyst nematode species cause significant destruction

to agricultural crops and are thus of economic importance [10,11]. Moreover, a limited toolset currently exists for growers to defend their crops against these pests. Identification of novel viral genomes will provide a greater understanding of nematode biology and potentially provide innovative management strategies.

MATERIALS AND METHODS

Processing of biological samples for RNAseq

Two inbred populations of *Heterodera glycines,* OP25 and OP50 [12], were cultured on roots of 'Hutcheson' soybean plants grown under greenhouse conditions. The SCN cysts were extracted from plant roots with water pressure and soil via water flotation and collected on nested sieves of screen sizes 20 (850 µm) and 60 (250 µm). SCN eggs were extracted by crushing cysts with a Tenbroeck homogenizer and further separated from soil debris by centrifugation through 70% sucrose and collection on a size 500 screen (25 µm). Equipment was sterilized and stored separately for each SCN population. Eggs were surface sterilized in 2% (w/v) sodium azide for 30 minutes. Eggs were hatched at 27°C using the Baermann pan method [13] and the hatched pre-parasitic second-stage juveniles (ppJ2s) were collected within 48 hours of hatch on a size 500 screen. Nematode samples were prepared for total RNA extraction by vibration homogenization for 20 seconds with 3-mm glass beads in a 1.5 ml tube on a Silamat S6 (Ivoclar Vivadent, Amherst, NY). Total RNA from approximately 10,000 pooled ppJ2s was extracted via TRIzol® Reagent (Invitrogen, Carlsbad, CA) under the guidelines of the manufacturer's protocol adapted from [14]. The nematode total RNA samples were prepared and processed for sequencing at the NC State University Genomic Sciences Laboratory (NCSU GSL; Raleigh, NC). Sample concentration was measured via the

2100 BioAnalyzer (Agilent Technologies, Santa Clara, CA). To enrich for sequence coverage of viruses, samples were treated for ribosomal depletion by preparation with NEBNext® Ultra™ Directional RNA Library Prep Kit for Illumina® (New England BioLabs, Ipswich, MA). OP25 and OP50 RNA were run via paired-end Illumina MiSeq 300x300bp at the NCSU GSL. Raw sequence reads are available under the NCBI Short Read Archive (SRA) accession numbers SRR6269844 and SRR6269845.

The SCN inbred population MM8 (HG Type 2.5.7) was propagated under greenhouse conditions on plant introduction 88788 [15]. Freshly hatched ppJ2 were inoculated onto 10-day old seedlings and the inoculated plants were placed in the greenhouse. Five days post-inoculation, parasitic second-stage juveniles (pJ2) nematodes were isolated from the roots by blending the roots for 30 seconds in a kitchen blender. Following this, the root homogenate was poured over a nested stack of sieves with pore sizes of 850µm, 250µm, and 25µm before purifying the nematodes from the sample using sucrose centrifugal flotation [16]. RNA was isolated from frozen nematode pellets using the PerfectPure Fibrous Tissue Kit (5Prime) and a modified version of the manufacturer's extraction protocol [17]. RNA quality was determined using a Fragment Analyzer (Advanced Analytical) and quantified using a Qubit Fluorometer prior to library preparation. RNAseq libraries were constructed using the TruSeq mRNA Stranded Library Prep Kit (Illumina) and sequenced on the Illumina HiSeq 2500 platform in a paired-end manner (2x50). Library preparation and high-throughput sequencing services were performed at the University of Missouri DNA Core Facility. Three biological replicates of each sample were sequenced. Raw sequence reads are available under the NCBI SRA accession numbers SRR6232814-SRR623816 and SRX3341252-SRX3341254.

Transcriptome data (Roche 454) of *H. schachtii* J2s (SRR1125017) are publicly available on the NCBI SRA database from the University of Murdoch [18]. Transcriptome data (Illumina Genome Analyzer II) of pooled J2s and females of *H. avenae* are available under accession number ERR414136 and is provided by the Indian Agricultural Research Institute. *G. pallida* (PCN) transcriptome files (Illumina Genome Analyzer II) of males (ERR202422) and females (ERR202423) are publicly available from the Wellcome Trust Sanger Institute [19]. *G. rostochiensis* (PCN) female RNAseq data (Illumina HiSeq 2000) are available from the University of Dundee (ERR1173512).

Bioinformatic analysis

RNA sequencing fastq files were uploaded onto the VirFind server [9] (virfind.org). Blastx and Blastn E-values were set at 1.0E-2 with no trimming of contigs. De novo assembled contigs were uploaded into Geneious version 9.1.7 (Biomatters, Auckland, New Zealand) [20] and contigs ≥ 3kb were further analyzed for viral signatures. The contigs were first screened for predicted open reading frames (ORFs) within Geneious software; those assemblies that had ORFs with similar organization to viruses were translated into amino acids. Translated proteins were screened for predicted function via NCBI PSI-BLAST (position-specific iterated BLAST) of non-redundant protein sequences (nr). Additional filtering to find true viral sequences was conducted with the InterProScan [21] plug-in within Geneious software. Each recovered viral genome was independently de novo assembled via VirFind.

To determine coverage of viruses within nematode datasets, genomes were reassembled in Geneious with BBMap using the VirFind de novo assembly as a reference

sequence (Table 3.1). Phylogenetic trees were built by compiling the closest hits to the novel virus translated polymerase or polyprotein based upon NCBI PSI-BLAST. Proteins were aligned with ClustalW [22] BLOSUM cost matrix (gap open cost=10, gap extend cost=0.1). Trees were constructed from the protein alignment with Geneious Tree Builder using the Jukes-Cantor genetic distance model and a neighbor-joining tree method. No outgroup was selected, and the tree was resampled via bootstrap method with 1000 replicates (50% support threshold). To further characterize SCN nyami-like virus (NLV), conserved transcription initiation/termination sites were identified by aligning non-coding regions with MAAFT version 7.222 [23] (200PAM/k=2 scoring matrix; 1.53 gap open penalty; 0.123 offset value) and selecting conserved domains with similarity to other *Nyamiviridae* [24]. Additionally, putative protease cleavage sites of PCN picorna-like virus (PLV) were predicted via the NetPicoRNA 1.0 Server (http://www.cbs.dtu.dk/services/NetPicoRNA/) [25].

Confirmation of viral presence in nematodes

Nematode eggs maintained at the University of Missouri and juveniles maintained at Cornell University and North Carolina State University were collected similarly to the process described for RNAseq. The inbreeding protocol, date of origin, and HG type of SCN populations used for this manuscript can be viewed in a previous publication from our laboratory [7]. Total RNA was extracted as described previously via an adapted TRIzol® Reagent protocol (Invitrogen, Carlsbad, CA) [14]. Total RNA concentrations were analyzed via Nanodrop 1000 (Thermo Fisher Scientific, Waltham, MA). cDNA was synthesized by incubating approximately 1 µg RNA with 0.06 µg random primers (Invitrogen) for 10 minutes at 70°C followed by rapid cooling on ice. Next, 4 µl GeneAmp® 10X PCR Buffer II

(Applied Biosystems, Foster City, CA), 5.5 mM $MgCl_2$, 0.5 µM deoxynucleotide solution mix, 32 U Murine RNase Inhibitor (New England BioLabs, Ipswich, MA), and 50 U Multiscribe™ Reverse Transcriptase (Applied Biosystems) were added before additional incubations of 42°C and 70°C for 15 minutes each.

All primers used for viral detection and analysis were synthesized by Eurofins Genomics (Louisville, KY) and are listed on Table 3.2. qRT-PCR was conducted to determine if the proposed viral genomes were detectable in nematode samples. The SCN-specific internal control genes GAPDH (Glyceraldehyde 3-phosphate dehydrogenase) [7] and HgFAR1 (*H. glycines* fatty acid and retinol binding protein-1) [5] were used to determine the relative quantification of viral titers. Across PPN species, 18*S* rRNA was used as an internal control as other regions tested were too variable. qRT-PCR products were amplified using 0.5 µM of each appropriate primer pair, 10 µl iTaq™ Universal SYBR® Green Supermix (Bio-Rad, Hercules, CA), and 1 µl cDNA. Applied Biosystems QuantStudio™ 6 Flex Real-Time PCR system was used with the following settings: 95°C, 20 seconds; 95°C, 2 seconds; 60°C, 25 seconds repeated for 40 amplification cycles with a continuous melt curve of 95°C, 20 seconds; 60°C, 1 minute; and 94°C for 20 seconds.

Cycle threshold values (Ct; amplification cycle in which fluorescence emitted exceeds background fluorescence) equal to or greater than 35 were considered non-detectable. DNase treatments yielded insignificant results between Ct values of treated and untreated samples and was not necessary for analysis. The average normalized abundance ratios (i.e. relative amount of virus in each nematode sample) were determined for each population sample. Ct values of viruses were normalized against the mean Ct values of nematode internal reference genes (18*S* or an average of GAPDH and HgFAR1) using the

equation $E_{internal}^{Ct(internal)}/E_{viral}^{Ct(viral)}$ where E equals the efficiency of a primer pair [26]. Further modifications were made for addressing viral abundance compared with host internal control genes [7,27]. Primer efficiencies were calculated by the equation $2^{(-1/slope)}$ via a five-point 1:2 dilution series. The efficiencies of primer pairs are E_{NLV}=2.01 (101%), E_{BLV}=1.94 (94%), E_{HgFAR1}=2.05 (105%), E_{GAPDH}=2.07 (107%), and in *H. glycines* E_{18S}=1.95 (95%) versus E_{18S}=1.81 (81%) in *H. trifolii*.

To confirm positive qRT-PCR results, approximately 0.8 kb regions of viral RdRPs were amplified via endpoint PCR. OneTaq® 2X Master Mix with standard buffer (New England BioLabs) and appropriate primers (Table 3.2) were used according to manufacturer's protocol to amplify products from cDNA in the Bio-Rad C1000 Touch Thermal Cycler under the following conditions: 94°C, 5 minutes; 94°C, 30 seconds; 60°C, 30 seconds; 68°C, 60 seconds for 40 amplification cycles followed by a final extension of 68°C for 5 minutes. Primers pairs were designed within additional ORFs (I, II, III, and IV) of SCN NLV to demonstrate correct assembly size. Products were electrophoresed on a 2% TAE agarose gel with 1X TAE buffer. PCR products were purified for Sanger sequencing with DNA Clean & Concentrator™ (Zymo Research Corp., Irvine, CA). Sanger sequencing was performed by Eurofins Genomics (Louisville, KY) via nested sequence primers listed in Table 3.2. Nucleotide sequences were translated and aligned with Geneious version 9.1.7 (Biomatters) using ClustalW (Blosum cost matrix, gap open cost of 10, gap extend cost of 0.1).

RESULTS

VirFind [9] (virfind.org) analysis of cyst nematode transcriptomes identified three novel viral genomes. The names and NCBI Genbank accession numbers for the nematode viruses identified in this report are listed in Table 3.3. Two of these viruses were embedded within the transcriptomes obtained from SCN populations OP25 and OP50 maintained in NC State University greenhouses [12] and SCN population MM8 maintained in University of Missouri greenhouses [15]. A nearly complete genome of nyami-like virus (SCN NLV), likely belonging to the family *Nyamiviridae*, was recovered as well as the RNA dependent RNA polymerase (RdRP) gene of a bunya-like virus (SCN BLV). SCN NLV and BLV are negative-sense RNA viruses; NLV is monopartite and BLV is most similar to known multipartite viruses. Viral genome coverage was not high in MM8 likely due to differences in RNA sample preparation and sequencing methodology. Moreover, a partial sequence related to the SCN NLV RdRP was recovered from transcriptome data of the greenhouse culture of *Heterodera schachtii* (beet cyst nematode; BCN). The viral-like RdRP sequence from BCN is approximately 1.8kb long and has 67% nucleotide identity to NLV originating from SCN. An additional viral genome was identified from *Globodera pallida* (potato cyst nematode; PCN) transcriptome data [19]. The virus is a picorna-like virus (PCN PLV) and is a positive-stranded RNA virus that typically generates a single polyprotein [28]. In addition to *G. pallida*, the PLV genome was also assembled from transcriptome data of the other PCN species, *G. rostochiensis*, at low levels. The presence of novel viruses was confirmed via qRT-PCR, endpoint PCR, and Sanger sequencing with the exception of PCN PLV. The host species with high read coverage of PCN PLV, *Globodera pallida*, could not be obtained for testing due to quarantine restrictions. To compensate for this hindrance, viral genomes were

independently *de novo* assembled from multiple data sets. This same process was applied to SCN NLV and SCN BLV assemblies as well.

SCN nyami-like virus (NLV)

SCN NLV is suggested to be a negative-sense RNA virus belonging to the *Mononegavirales* order and *Nyamiviridae* family. Thus far, there are three genera and five viral species within the *Nyamiviridae* family, and these viruses were isolated from invertebrate hosts [29]. The SCN NLV genome possesses five ORFs and is approximately 11.7kb in length (Fig 3.1A). Based upon conserved protein motifs, ORF I is 410 amino acids (AA) in length and encodes a predicted nucleoprotein - the function of which is to encapsidate the viral genome. Functions for the proteins encoded by ORFs II and III cannot definitively be determined due to lack of sequence similarity. However, when comparing SCN NLV to other *Mononegavirales*, is it likely that ORF II is a phosphoprotein (346 AA) and ORF III is a matrix protein (92 AA) [30]. Generally, phosphoproteins stabilize the RdRP to the RNA templates, and matrix proteins aid in viral particle budding. ORF IV consists of a 567 AA glycoprotein that is predicted to aid in attachment to host cells. The largest encoded protein (2060 AA) is the RdRP generated from ORF V. Notably, a single-nucleotide polymorphism (SNP) (C to U) was observed at position 5,328 of the SCN NLV sequence recovered from the SCN MM8 transcriptome data. The SNP alters the codon sequence to UUG, a start codon, and could potentially extend the RdRP protein by 4 amino acids (MCKS). From these results, conclusions cannot be drawn about the frequency of this mutation or if there is truly any effect on protein size or virus function; however, this discrepancy may be worth exploring in the future. Additionally, putative transcription

initiation and termination sequences for each ORF have been identified within non-coding regions of SCN NLV (Fig 3.1B). The predicted initiation sequences of SCN NLV are similar for each ORF while the termination sequences are nearly identical. Overall, the conserved initiation motif is highly similar to that found in SCN virus 1 (SbCNV-1); midway virus (MIDWV), a member of the same family, is also similar but possesses a truncated sequence with six fewer nucleotides. The termination motifs for SCN NLV, SbCNV-1, and MIDWV were nearly identical to one another. This relatedness provides additional support for the placement of SCN NLV within the *Nyamiviridae* family.

SCN NLV, is most closely related to SbCNV-1 (Fig 3.1C) but does not belong to the *Socyvirus* genus according to a proposal describing the *Nyamiviridae* family [29]. Criteria for inclusion of SCN NLV within the *Socyvirus* genus requires the full-length genome sequence be <30% different from SbCNV-1. The genome sequences of SbCNV-1 and SCN NLV differ by approximately 50% suggesting that SCN NLV either requires a new genus for classification or the species definition will need to be expanded. The protein AA identity of NLV compared to SbCNV-1 ranges from 55.1% (RdRP; ORF V) to 23.5% (putative phosphoprotein; ORF II). The virus with the second-most similarity to SCN NLV (after SbCNV-1) is the tick-transmitted nyamanini nyavirus (35% genome identity), which is also the type species for the *Nyamiviridae* family. SCN NLV is similar to a number of invertebrate viruses, many of which come from a single, large-scale study [8]. Many of these related viruses were isolated from other nematode species (non-plant pathogens), a tapeworm species, and a range of arthropod hosts including those belonging to *Chelicerata*, *Crustacea*, and *Insecta*.

SCN bunya-like virus (BLV)

SCN BLV is proposed to be a multipartite, negative-sense RNA virus belonging to the order *Bunyavirales*. The RdRP portion of the genome was recovered and used for bioinformatic analysis of transcriptome data (Fig 3.2A). Incomplete non-coding regions were also recovered on either side of the RdRP ORF. The ORF of the RdRP is approximately 9.45 kb long and produces a protein 3150 AA in length. This virus was identified within SCN transcriptome data for OP25, OP50, and MM8. The RdRP protein of SCN BLV appears truncated from OP25 and MM8 samples (3140 versus 3149 AA). However, this is probably a result of poor read coverage of the terminal end, and the ORF likely extends to the same point as the assembly originating from OP50. Much like SCN NLV, viruses most closely related to SCN BLV infect other nematode species and arthropods – specifically crustaceans and insects (Fig 3.2B) [8]. The polymerase of SCN BLV groups with four other viruses originating from nematode hosts. The most closely related viral RdRP protein, Xingshan nematode virus 3 (APG79357), is 27.44% identical and originates from a mixture of *Spirurian* nematodes. The classifications of these nematode viruses have not yet been determined, and so it is difficult to predict where SCN BLV belongs beyond the Order taxon. Although SCN BLV and the most closely related nematode viruses vary greatly from one another, conserved protein motifs were identified to correctly characterize the genome. An alignment of the RdRP with that of other related viruses shows conserved motifs as demonstrated by Donaire *et al.* [31] for Bunya-like viruses (S3.1 Fig).

PCN picorna-like virus (PLV)

A novel potential viral genome was also identified from PCN transcriptome data of the species *Globodera pallida* and *G. rostochiensis*. The virus likely belongs within *Picornavirales*, has a positive-sense RNA genome of approximately 9.4 kb, and produces a singular predicted polyprotein (3090 AA) (Fig 3.3A). There is likely a large portion of 5' untranslated region (UTR) unrecovered from the transcriptome data as picorna-like viruses typically have 5' UTRs upwards of 0.5 kb that contain an internal ribosome entry site (IRES) [28]. Putative cleavage sites of the polyprotein were computationally predicted via the NetPicoRNA 1.0 Server [25] and have not been experimentally verified (Fig 3.3B). Furthermore, these sites were compared to those mentioned in other reports characterizing *Picornavirales* cleavage sites [32-34]. The predicted regions have a conserved Q/G (glutamine/glycine) cleavage site as well as a valine (V) in the -4 position for each site except between the leader (L) and viral particle (VP) proteins. Without further experimentation, it is not clear whether this virus truly has an L protein that can sometimes be found within *Picornavirales* species [35].

PCN PLV is distantly related to other NCBI database entries (Fig 3.3C). The order of encoded cleaved proteins is similar to that of *Iflaviridae*; however, there is not enough resolution in the phylogenetic tree to determine the genus at this time. The most closely related virus, Burke-Gilman virus (AOX15251) [36], has a polyprotein that is 13.61% identical followed by Hubei picorna-like virus 46 (YP_009330031) [7] at 13.49% identity. Interestingly, both of these viruses were isolated from spiders. PCN PLV does not clearly group with other viruses in the database and may ultimately require its own genera for proper classification. Conserved motifs of picorna-like viruses were identified for the protease,

helicase, and RdRP (S3.2 Fig) [37,38]. The helicase alignment shows the most dissimilarity; however, much of this occurrence can be attributed to the plant viruses: rice tungro spherical virus (RTSV), bellflower vein chlorosis virus (BVCV), and maize chlorotic dwarf virus (MCDV).

Confirmation of viral presence in nematodes

To demonstrate whether these newly assembled viral genomes truly exist in nature, qRT-PCR analysis was conducted on eggs of 17 SCN research populations maintained at the University of Missouri. SCN NLV was detectable in 12 of these samples (71%) at levels ranging from 7.26-fold lower than the SCN internal controls to 3.12-fold higher (Table 3.4). Moreover, SCN BLV was detectable in 15 populations (88%) with consistently higher titers than SCN NLV. SCN BLV relative titers were primarily present at a level higher than the internal controls and spanned 1.18-fold lower to 5.44-fold higher. The prevalence of these viruses across SCN populations of different type and location demonstrates that the RNAseq generated assemblies are not artifacts and suggests a potential importance to nematode biology.

In addition to SCN populations, other cyst nematode species were tested for viruses via qRT-PCR. From the limited population size tested, SCN NLV and SCN BLV were detectable in clover cyst nematode (*H. trifolli*) at levels comparable to the SCN population MM8 (Table 3.5). PCN PLV was not detectable with qRT-PCR within an available *G. rostochiensis* RNA sample; *G. rostochiensis* and *G. pallida* isolates could not be acquired as a result of quarantine restrictions. It is important to note that relative titers between Table 3.4 and Table 3.5 should not be directly compared as the internal controls that were utilized are

different. Despite a large difference in 18*S* Ct values when compared to viruses, it was necessary to use 18*S* as a control across cyst nematode species as GAPDH and HgFAR1 primers did not work well outside of SCN.

PCR primers were designed within the five ORFs of SCN NLV, and the resulting products (from SCN population MM8) are the anticipated size based upon the predicted RNAseq assembly (S3.3A Fig): ORF I (405 bp), ORF II (327 bp), ORF III (181 bp), ORF IV (448 bp), and ORF V (838 bp). The PCR products of ORF V (viral RdRP) were purified and Sanger sequenced; likewise, sequencing was conducted on SCN BLV RdRP products of approximately the same size. Nucleotides were translated into amino acids and aligned for SCN NLV (S3.3B Fig) and SCN BLV (S3.3C Fig). SCN NLV was Sanger sequenced from ten different SCN populations as well as clover cyst nematode. There are six sites where single nucleotide polymorphisms (SNPs) are present (99.2% identical) resulting in a single amino acid variation from one SCN sample (TN21). SCN BLV was sequenced from eight different SCN populations and clover cyst nematode. SCN BLV has 48 SNPs within the sequenced region of the RdRP (94.2% identical) resulting in four sites of amino acid variation. qRT-PCR detection and Sanger sequencing of these viral RdRPs confirms that these novel SCN viruses exist in nature. Furthermore, these viruses can be detected in the majority of cultured SCN research populations tested as well as in a second species, clover cyst nematode.

DISCUSSION

This report describes three novel RNA viruses within cyst nematodes. Within SCN, two new negative-stranded RNA viruses have been identified. In addition, a proposed

positive-stranded RNA virus was recovered from existing PCN data. To the best of our knowledge, this is the first viral genome identified from PCN. The use of the VirFind [9] application to mine cyst nematode transcriptome data that was generated in-house or publicly available was key to the identification of these three new nematode viruses. Viral infection of cyst nematodes demonstrates the ecological complexity within an agricultural system. This host-pathogen interaction includes a nematode parasitizing a plant while being infected with a combination of viruses that have currently unknown functions. To date, the viruses reported within nematodes [2-8] are all single-stranded RNA viruses but can contain quite different genome organizations.

SCN NLV was assembled from three sets of SCN J2 transcriptome data (OP25, OP50, and MM8) and partially assembled from BCN. If improved read coverage was available for BCN, it is probable that the viral-like segment identified may belong to an unidentified, but closely related, viral species due to sequence dissimilarity. SCN NLV is a potential sixth member of the family *Nyamiviridae* and is most closely related to viruses which infect nematodes and arthropods (Fig 3.1C). Additionally, the polymerase of a bunya-like virus (SCN BLV) was extracted from SCN J2 transcriptome data for OP25, OP50, and MM8. Recovery of the full genomes of multipartite viruses can be conducted via repeats on terminal, non-coding ends. However, the terminal sequences of the SCN BLV RdRP segment could not be assembled. Placement of SCN BLV within a genus is difficult as related viruses are primarily unclassified. However, four viruses exist which show some similarity to SCN BLV and originate from nematode hosts (Fig 3.2B). Both SCN NLV and SCN BLV were detected in SCN research populations and a clover cyst nematode sample via qRT-PCR, endpoint PCR, and Sanger sequencing (Tables 3.4 and 3.5, S3.3 Fig). SCN NLV and SCN

BLV appear to be prevalent in research SCN populations, infecting 71% and 88% of samples tested, respectively. It is possible with more extensive testing of cyst nematode species that these viruses, or variants of these viruses, will be detected. Finally, a new picorna-like virus was recovered from three PCN transcriptome data sets: *G. pallida* (males and females) and *G. rostochiensis* (females). This is a positive-sense virus that encodes a single polyprotein which undergoes proteolytic cleavage (Figs 3.3A and 3.3B). PCN PLV aligns most closely with arthropod viruses, and it will likely belong to an undescribed genus as it is distantly related to other NCBI Genbank entries (Fig 3.3C). Unfortunately, we were unable to sufficiently test PCN species for virus via qRT-PCR and Sanger sequencing due to quarantine measures against these nematodes.

It is unclear exactly how and when these nematodes originally became infected with viruses; preliminary testing of soybean plants did not reveal the presence of these viruses. Viral infection is prevalent within tested SCN populations (Table 3.4), and it is probable that samples can appear virus-free but simply possess titers below the detectable limits of qRT-PCR. Likewise, viruses were detected in both egg and juvenile life stages suggesting vertical transmission is a possible route of infection. This is a similar result to what was observed in previously discovered SCN viruses [7] as these viruses are present and actively replicate within multiple life stages (including egg and J2) of the nematode. These groups of RNA viruses do not have a DNA intermediary stage, and therefore, should not be capable of integrating into the host genome. Instead, it is plausible that viruses are maternally transmitted through eggs and could be transmitted paternally as well. As this is an emerging field of research, vertical transmission has not been well studied for nematode viruses; however, it has been evidenced for viral endosymbionts of insects [39]. These SCN viruses

appear to have a narrow host range, and thus, may have evolved alongside *Heterodera spp.*, specifically SCN (*H. glycines*) and *H. trifolii*. Within the *Heterodera spp., H. trifolii* and *H. mediterranea* (not tested) are the most closely related to SCN [40].

This study contributes further knowledge to the new and evolving field of nematode virology. With additional mining of transcriptome data using appropriate informatics tools such as VirFind [9], it is likely that more viruses will be discovered within more nematode species. Elucidating the role of nematode viruses may provide insight into nematode biology and result in additional forms of pest control. Future work will focus on the impact viruses have on the nematode host, localization and transmission of viruses in nematodes, and explore the potential applications of viral infection of nematodes.

ACKNOWLEDGEMENTS

This work was supported by the National Science Foundation, DGE-1252376 (www.nsf.gov). The funder had no role in study design, data collection and analysis, decision to publish, or preparation of the manuscript. The authors would like to acknowledge the NC State University Genomic Sciences Laboratory for RNA sequencing as well as Ioannis Tzanetakis at the University of Arkansas for granting access to VirFind (http://virfind.org). Gratitude is extended towards Xiaohong Wang and Shiyan Chen of Cornell University for their contribution of *G. rostochiensis* total RNA. We thank the NC State University College of Agricultural and Life Sciences' North Carolina Agricultural Research Service for providing their facilities and support in this work. Lastly, we would like to thank the researchers from which we utilized public transcriptome data.

LITERATURE CITED

1. Brown DJ, Robertson WM, Trudgill DL. Transmission of viruses by plant nematodes. Annu Rev Phytopathol. 1995; 33: 223–249. PMID: 18999960.

2. Felix MA, Ashe A, Piffaretti J, Wu G, Nuez I, Belicard T, *et al*. Natural and experimental infection of *Caenorhabditis* nematodes by novel viruses related to nodaviruses. PLOS Biol, 2011; 9: e1000586. PMID: 21283608.

3. Franz CJ, Zhao G, Félix MA, Wang D. Complete genome sequence of Le Blanc virus, a third *Caenorhabditis* nematode-infecting virus. J Virol. 2012; 86: 11940. PMID: 23043172.

4. Bekal, S, Domier LL, Niblack TL, Lambert KN. Discovery and initial analysis of novel viral genomes in the soybean cyst nematode. J Gen Virol. 2011; 92: 1870-1879. PMID: 21490246.

5. Bekal S, Domier LL, Gonfa B, McCoppin NK, Lambert KN, Bhalerao K. A novel flavivirus in the soybean cyst nematode. J Gen Virol. 2014; 95: 1272-1280. PMID: 24643877.

6. Cotton JA, Steinbiss S, Yokoi T, Tsai IJ, Kikuchi T. Expressed, endogenous Nodavirus-like element captured by a retrotransposon in the genome of the plant parasitic nematode *Bursaphelenchus xylophilus*. Sci Rep. 2016; 6: 39749. PMID: 28004836.

7. Ruark CL, Koenning SR, Davis EL, Opperman CH, Lommel SA, Mitchum MG, *et al*. Soybean cyst nematode culture collections and field populations from North Carolina

and Missouri reveal high incidences of infection by viruses. PLOS ONE. 2017; 12: e0171514. PMID: 28141854.

8. Shi M, Lin XD, Tian JH, Chen LJ, Chen X, Li CX, *et al*. Redefining the invertebrate RNA virosphere. Nature. 2016; 540: 539-543. PMID: 27880757.

9. Ho T, Tzanetakis IE. Development of a virus detection and discovery pipeline using next generation sequencing. Virology. 2014; 471–473: 54–60. PMID: 25461531.

10. Nicol JM, Turner SJ, Coyne DL, Den Nijs L, Hockland S, Maafi ZT. Current nematode threats to world agriculture. In: Genomics and molecular genetics of plant-nematode interactions. 2011; 21-43. Springer Netherlands.

11. Jones JT, Haegeman A, Danchin EG, Gaur HS, Helder J, Jones MG, *et al*. Top 10 plant-parasitic nematodes in molecular plant pathology. Mol Plant Pathol. 2013; 14: 946-961. PMID: 23809086.

12. Dong K, Opperman CH. Genetic analysis of parasitism in the soybean cyst nematode *Heterodera glycines*. Genetics. 1997; 146: 1311-1318. PMID: 9258676.

13. Townshend JL. A modification and evaluation of the apparatus for the Oostenbrink direct cottonwool filter extraction method. Nematologica. 1963; 9: 106–110.

14. Chomczynski P, Sacchi N. Single step method of RNA isolation by acid guanidinium thiocyanate-phenol-chloroform extraction. Anal Biochem. 1987; 162: 156-159. PMID: 17406285.

15. Gardner M, Heinz R, Wang J, Mitchum MG. Genetics and adaption of soybean cyst nematode to broad spectrum resistance. G3. 2017; 7: 835-841. PMID: 28064187.

16. de Boer JM, Yan YT, Wang XH, Smant G, Hussey RS, Davis EL, *et al*. Developmental expression of secretory β-1,4-endoglucanases in the subventral esophageal glands of *Heterodera glycines*. Mol Plant Microbe Interact. 1999; 12: 663–669. PMID: 10432634.

17. Gardner M, Dhroso A, Johnson N, Davis EL, Baum TJ, Korkin D, *et al*. Novel global effector mining from the transcriptome of early life stages of the soybean cyst nematode *Heterodera glycines*. Sci Rep. 2018; 8: 2505. PMID: 29410430.

18. Fosu-Nyarko J, Nicol P, Naz F, Gill R, Jones MGK. Analysis of the transcriptome of the infective stage of the beet cyst nematode, *H. schachtii*. PLOS ONE. 2016; 11: e0147511. PMID: 26824923.

19. Cotton JA, Lilley CJ, Jones LM, Kikuchi T, Reid AJ, Thorpe P, *et al*. The genome and life-stage specific transcriptomes of *Globodera pallida* elucidate key aspects of plant parasitism by a cyst nematode. Genome Biol. 2014; 15: R43. PMID: 24580726.

20. Kearse M, Moir R, Wilson A, Stones-Havas S, Cheung M, Sturrock S, *et al*. Geneious Basic: an integrated and extendable desktop software platform for the organization and analysis of sequence data. Bioinformatics. 2012; 28: 1647-1649. PMID: 22543367.

21. Quevillon E, Silventoinen V, Pillai S, Harte N, Mulder N, Apweiler R, *et al*. InterProScan: protein domains identifier. Nucleic Acids Res. 2005; 33: W116-W120. PMID: 15980438.

22. Larkin MA, Blackshields G, Brown NP, Chenna R, McGettigan PA, McWilliam H, *et al*. ClustalW and ClustalX version 2. Bioinformatics. 2007; 23: 2947-2948. PMID: 17846036.

23. Katoh K, Misawa K, Kuma KI, Miyata T. MAFFT: a novel method for rapid multiple sequence alignment based on fast Fourier transform. Nucleic Acids Res. 2002; 30: 3059-66. PMID: 12136088.

24. Rogers MB, Cui L, Fitch A, Popov V, Travassos da Rosa APA, Vasilakis N, *et al*. Short report: whole genome analysis of Sierra Nevada virus, a novel mononegavirus in the family Nyamiviridae. Am J Trop Med. 2014; 91: 159-164. PMID: 24778199.

25. Blom N, Hansen J, Blaas D, Brunak S. Cleavage site analysis in picornaviral polyproteins: discovering cellular targets by neural networks. Protein Science. 1996; 5: 2203-2216. PMID: 8931139.

26. Pfaffl MW. A new mathematical model for relative quantification in real-time RT–PCR. Nucleic Acids Res. 2001; 29: 2002-2007. PMID: 11328886.

27. Rotenberg D, Krishna Kumar NK, Ullman DE, Montero-Astúa M, Willis DK, German TL, Whitfield AE. Variation in Tomato spotted wilt virus titer in *Frankliniella occidentalis* and its association with frequency of transmission. Phytopathology. 2009; 99: 404-410. PMID: 19271982.

28. Le Gall O, Christian P, Fauquet CM, King AM, Knowles NJ, Nakashima N, *et al*. Picornavirales, a proposed order of positive-sense single-stranded RNA viruses with a pseudo-T= 3 virion architecture. Arch Virol. 2008; 153: 715. PMID: 18293057.

29. Kuhn JH, Bekal S, Caì Y, Clawson AN, Domier LL, Herrel M, *et al*. Nyamiviridae: proposal for a new family in the order Mononegavirales. Arch Virol. 2013; 158: 2209-2226. PMID: 23636404.

30. Mihindukulasuriya KA, Nguyen NL, Wu G, Huang HV, da Rosa AP, Popov VL, *et al*. Nyamanini and midway viruses define a novel taxon of RNA viruses in the order Mononegavirales. J Virol. 2009; 83: 5109-16. PMID: 19279111.

31. Donaire L, Pagán I, Ayllón MA. Characterization of *Botrytis cinerea* negative-stranded RNA virus 1, a new mycovirus related to plant viruses, and a reconstruction of host pattern evolution in negative-sense ssRNA viruses. Virology. 2016; 499: 212-218. PMID: 27685856.

32. Lanzi G, de Miranda JR, Boniotti MB, Cameron CE, Lavazza A, Capucci L, *et al*. Molecular and biological characterization of deformed wing virus of honeybees (*Apis mellifera* L.). J Virol. 2006; 80: 4998-5009. PMID: 16641291.

33. Geng P, Li W, Lin L, de Miranda JR, Emrich S, *et al*. Genetic characterization of a novel Iflavirus associated with vomiting disease in the Chinese Oak Silkmoth *Antheraea pernyi*. PLOS ONE. 2014; 9: e92107. PMID: 24637949.

34. Mann KS, Walker M, Sanfacon H. Identification of cleavage sites recognized by the 3C-like cysteine protease within the two polyproteins of strawberry mottle virus. Front Microbiol. 2017; 8: 745. PMID: 28496438.

35. Zell R, Delwart E, Gorbalenya AE, Hovi T, King AM, Knowles NJ, *et al*. ICTV virus taxonomy profile: Picornaviridae. J Gen Virol. 2017; 2421-2422. PMID: 28884666.

36. Shean RC, Makhsous N, Crawford RL, Jerome KR, Greninger AL. Draft genome sequences of six novel picorna-like viruses from Washington State spiders. Genome Announc. 2017; 5: e01705-16. PMID: 28254976.

37. Ongus J, Peter D, Bonmatin JM, Bengsch E, Vlak JM, van Oers MM. Complete sequence of a picorna-like virus of the genus Iflavirus replicating in the mite *Varroa destructor*. J Gen Virol. 2004; 85: 3747-3755. PMID: 15557248.

38. Yinda CK, Zell R, Deboutte W, Zeller M, Conceicao-Neto N, Heylen E, *et al*. Highly diverse population of Picornaviridae and other members of the Picornavirales, in Cameroonian fruit bats. BMC Genomics. 2016; 18: 249. PMID: 28335731.

39. Longdon B, Jiggins FM. Vertically transmitted viral endosymbionts of insects: do sigma viruses walk alone? Proc Biol Sci. 2012; 279(1744): 3889-3898. PMID: 22859592.

40. Skantar AM, Handoo ZA, Zanakis GN, Tzortzakakis EA. Molecular and morphological characterization of the corn cyst nematode, *Heterodera zeae*, from Greece. J Nematol. 2012; 44: 58-66. PMID: 23482617.

TABLES

Table 3.1. Number of sequence reads and mean read coverage of viral genomes from mined transcriptome data sets. Sequence coverage was determined in Geneious software version 9.1.7 with BBMap using de novo assemblies generated by VirFind [9]. Abbreviations: J2 (second-stage juvenile), SCN (soybean cyst nematode), BCN (beet cyst nematode), CCN (cereal cyst nematode), PCN (potato cyst nematode), *Gp* (*Globodera pallida*), *Gr* (*G. rostochiensis*), NLV (nyami-like virus), BLV (bunya-like virus), PLV (picorna-like virus). Mean describes average sequence read coverage for each nucleotide position. ND (not detected) denotes the virus was not found in the specified nematode sample.

			SCN NLV		SCN BLV		PCN PLV	
Sample	**Run ref #**	**Reads**	**Reads**	**Mean**	**Reads**	**Mean**	**Reads**	**Mean**
SCN OP25 J2s	SRR6269844	11.4 mil	22,989	557	5845	168	ND	ND
SCN OP50 J2s	SRR6269845	12.7 mil	34,351	820	5619	161	ND	ND
SCN MM8 J2s	SRR6232814-16	71.3 mil[a]	7391	50	305[b]	3	ND	ND
BCN J2s	SRR1125017	184,024	1714	3	ND	ND	ND	ND
CCN J2s + females	ERR414136	46.1 mil	ND	ND	ND	ND	ND	ND
PCN (*Gr*) females	ERR1173512	41.2 mil	ND	ND	ND	ND	1751	19
PCN (*Gp*) males	ERR202422	33.7 mil	ND	ND	ND	ND	88,829	731
PCN (*Gp*) females	ERR202423	33.5 mil	ND	ND	ND	ND	12,138	99

[a] Read information represents three pooled biological replicates.

[b] Sequence data spans the length of the genome; however, there is poor coverage within A-T rich regions creating several large, undermined gaps in the genome.

Table 3.2. Primers used for this research study and their application. Abbreviations: NLV (nyami-like virus), BLV (bunya-like virus), PLV (picorna-like virus), SCN (soybean cyst nematode), PPN (plant parasitic nematode).

Primer	Application	Sequence [5' to 3']
NLV_QF	qRT-PCR	GTTGACGGCACTTGAACACC
NLV_QR	qRT-PCR	GGGATTCAACTCAAGCCGGA
NLV_ORF1_F	Endpoint PCR	GACCAAGTGCCTCGTTCTCA
NLV_ORF1_R	Endpoint PCR	CCAAAGCCATCCCGTTGTTG
NLV_ORF2_F	Endpoint PCR	CCTCTTCTTCTTCTGCCGCA
NLV_ORF2_R	Endpoint PCR	TTGTGCTTGGTGTTAACGCG
NLV_ORF3_F	Endpoint PCR	CCCAGACCGAGCCTATGAAC
NLV_ORF3_R	Endpoint PCR	GGTCACGGGAAAGGGGAATT
NLV_ORF4_F	Endpoint PCR	TTGTCTTGACACTCGCCCTC
NLV_ORF4_R	Endpoint PCR	CTCCGACATACACCGAGTCG
NLV_ORF5_F	Endpoint PCR	CAGGAGCATTCGTGATTGCG
NLV_ORF5_R	Endpoint PCR	GAGCACCGACAACTACACCA
NLV_SEQ_F	Sanger sequencing	TAGGGCCACAATTGCTCGTT
NLV_SEQ_R	Sanger sequencing	TCGTGCGGACTTCAAGACAA
BLV_QF	qRT-PCR	GCCAGCCAGCATTTACAAGG
BLV_QR	qRT-PCR	CCAGGGGACATGAGAATCACC
BLV_F	Endpoint PCR	GCTGCTTCAGATCCAACAGC
BLV_R	Endpoint PCR	GCACCAGGACCCCATTTAGT
BLV_SEQ_F	Sanger sequencing	TGGTTGTTGTGTTTCGGATCAC
BLV_SEQ_R	Sanger sequencing	GGCACCACCCCATTGAACTT
PLV_QF	qRT-PCR	ACATGCGGCCAAAACATTCC
PLV_QR	qRT-PCR	AGCGCGTCATAAGCAAATGC
SCN_HgFAR1_F	qRT-PCR	CCATTTGCCGCCTTTGGA
SCN_HgFAR1_R	qRT-PCR	GGGATCAATTCGCGGTATTCG
SCN_GAPDH_F	qRT-PCR	TCCAAGGCATAGAAAGACGACG
SCN_GAPDH_R	qRT-PCR	AACAAGTCATTGGACGGCATCA
PPN_18*S*_F	qRT-PCR	GGTAGTGACGAGAAATAACG
PPN_18*S*_R	qRT-PCR	CTGCTGGCACCAGACTTG

Table 3.3. Genbank accession numbers for partial viral genomes. De novo assemblies were generated from transcriptome data via VirFind [9]. Abbreviations: J2 (second-stage juvenile), SCN (soybean cyst nematode), BCN (beet cyst nematode), PCN (potato cyst nematode), *Gp* (*Globodera pallida*), *Gr* (*Globodera rostochiensis*), NLV (nyami-like virus), BLV (bunya-like virus), PLV (picorna-like virus), RdRP (RNA-dependent RNA polymerase).

Virus	Accession	Assembly length	Sample source	Source accession
SCN NLV	MG550265	11,736	SCN OP50 J2s	SRR6269845
	MG550266	11,733	SCN OP25 J2s	SRR6269844
	MG550267	11,728	SCN MM8 J2s	SRR6232814-16
	MG550268	1,815[b]	BCN J2s	SRR1125017
SCN BLV[a]	MG550269	9,478	SCN OP50 J2s	SRR6269845
	MG550270	9,478	SCN OP25 J2s	SRR6269844
	MG550271	9,469	SCN MM8 J2s	SRR6232814-16
PCN PLV	MG550272	9,321[c]	PCN (*Gr*) females	ERR1173512
	MG550273	9,371	PCN (*Gp*) males	ERR202422
	MG550274	9,334	PCN (*Gp*) females	ERR202423

[a] SCN BLV is a multipartite virus; the recovered sequences represent the RdRP region.
[b] Only a partial sequence of the viral RdRP was recovered with 67% nt identity to the virus within SCN.
[c] The coding region was recovered with the exception of 3 nt from the 3' end.

Table 3.4. qRT-PCR Ct values and relative titers of soybean cyst nematode (SCN) viruses within SCN research populations. Mean qRT-PCR cycle threshold (Ct) values are shown for SCN nyami-like virus (NLV), SCN bunya-like virus (BLV), and internal SCN control (HgFAR1 and GAPDH). Relative viral titers were calculated and log_2 adjusted by comparison against internal controls using a modified Pfaffl method [7,26,27]. Negative log_2 relative titers denote a value below the internal control; whereas, positive values represent titers higher than the internal controls. ND (not detected) demonstrates that virus was not found in the sample. Experiments were conducted in technical triplicates and standard deviations are shown.

	SCN NLV		SCN BLV		HgFAR1	GAPDH
SCN Population	**Mean Ct**	**Rel titer (log_2)**	**Mean Ct**	**Rel titer (log_2)**	**Mean Ct**	**Mean Ct**
MM3	23.66 ± 0.075	**0.54**	21.09 ± 0.089	**4.21**	21.76 ± 0.047	23.96 ± 0.023
MM4	27.01 ± 0.181	**2.27**	27.57 ± 0.114	**3.12**	27.00 ± 0.009	28.77 ± 0.093
MM7	29.26 ± 0.114	**-0.94**	28.75 ± 0.235	**1.04**	27.00 ± 0.053	27.57 ± 0.078
MM8	18.75 ± 0.042	**1.86**	20.62 ± 0.140	**1.03**	18.81 ± 0.035	20.4 ± 0.199
MM16	ND	**ND**	19.88 ± 0.045	**0.97**	18.37 ± 0.056	19.57 ± 0.061
MM18	ND	**ND**	22.98 ± 0.086	**1.48**	21.43 ± 0.270	22.97 ± 0.189
MM19	30.11 ± 0.066	**-7.26**	21.86 ± 0.056	**2.17**	20.84 ± 0.061	22.66 ± 0.036
MM21	ND	**ND**	25.73 ± 0.027	**1.80**	24.63 ± 0.048	25.68 ± 0.029
PA3	23.97 ± 0.024	**0.97**	22.66 ± 0.035	**3.45**	22.78 ± 0.056	24.61 ± 0.067
TN2	22.97 ± 0.138	**0.74**	ND	**ND**	21.89 ± 0.067	23.36 ± 0.050
TN6	ND	**ND**	ND	**ND**	25.91 ± 0.064	28.4 ± 0.003
TN12	30.54 ± 0.188	**2.62**	31.92 ± 0.196	**2.86**	30.34 ± 0.278	32.56 ± 0.478
TN13	20.74 ± 0.037	**3.12**	26.35 ± 0.095	**-1.18**	21.92 ± 0.080	23.52 ± 0.058
TN14	26.43 ± 0.095	**2.10**	28.21 ± 0.168	**1.74**	26.58 ± 0.046	27.97 ± 0.164
TN19	28.41 ± 0.152	**1.65**	27.01 ± 0.018	**4.44**	26.62 ± 0.061	29.68 ± 0.064
TN20	ND	**ND**	27.36 ± 0.147	**5.44**	28.89 ± 0.049	30.82 ± 0.341
TN21	19.25 ± 0.074	**1.89**	19.06 ± 0.068	**3.05**	18.80 ± 0.031	21.01 ± 0.035

Table 3.5. qRT-PCR Ct values and relative titers of cyst nematode viruses within plant parasitic nematode (PPN). Mean qRT-PCR cycle threshold (Ct) values are shown for soybean cyst nematode (SCN) nyami-like virus (NLV), SCN bunya-like virus (BLV), potato cyst nematode (PCN) picorna-like virus (PLV), and internal PPN control (18*S*). Relative viral titers were calculated and log_2 adjusted by comparison against internal control using a modified Pfaffl method [7,26,27]. Negative log_2 relative titers denote a value below the internal control; whereas, positive values represent titers higher than the internal controls. ND (not detected) demonstrates that virus was not found in the sample. Experiments were conducted in technical triplicates and standard deviations are shown. Abbreviations: J2 (second-stage juvenile), CU (Cornell University), MU (University of Missouri), NCSU (North Carolina State University).

			SCN NLV		**SCN BLV**		**PCN PLV**	**PPN 18S**
PPN species	**Life stage**	**Location**	**Mean Ct**	**Rel titer (log_2)**	**Mean Ct**	**Rel titer (log_2)**	**Mean Ct**	**Mean Ct**
Globodera rostochiensis	J2	CU	ND	**ND**	ND	**ND**	ND	14.03 ± 0.199
Globodera tobacum	egg	MU	ND	**ND**	ND	**ND**	ND	9.37 ± 0.085
Heterodera glycines (MM8)	egg	MU	21.19 ± 0.191	**-15.10**	21.20 ± 0.033	**-11.78**	ND	8.80 ± 0.311
Heterodera schachtii	J2	NCSU	ND	**ND**	ND	**ND**	ND	16.04 ± 0.058
Heterodera trifolii	egg	MU	25.51 ± 0.096	**-15.59**	25.55 ± 0.034	**-14.32**	ND	11.80 ± 0.055
Vittatidera zeaphila	egg	MU	ND	**ND**	ND	**ND**	ND	12.27 ± 0.075

FIGURES

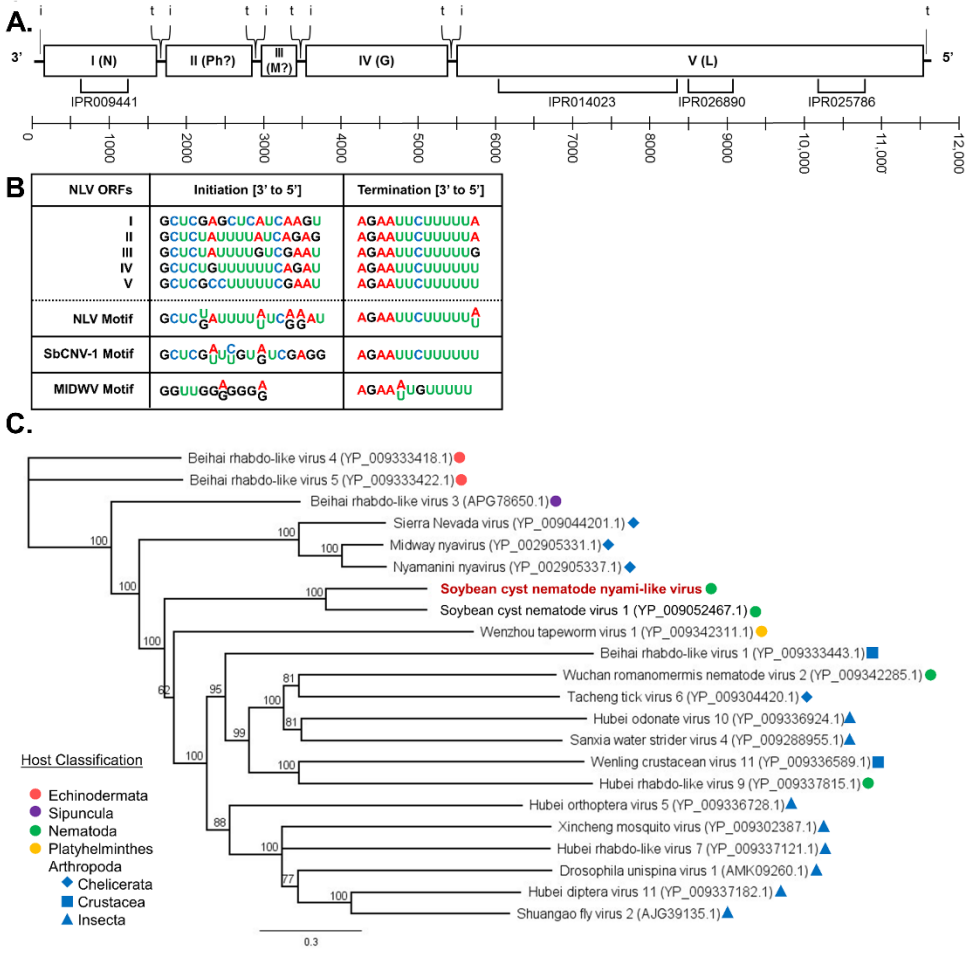

Fig 3.1. Characterization of soybean cyst nematode (SCN) nyami-like virus (NLV). (**A**) Genome organization of NLV. Putative encoded proteins are as follows: ORF I nucleocapsid (N), ORF II phosphoprotein (P), ORF III matrix protein (M), ORF IV glycoprotein (G), and ORF V RNA-dependent-RNA polymerase (RdRP) (L). Identified InterProScan regions are denoted below the genome. Locations of ORF transcription initiation (i) and termination (t) sites are shown above the genome. The scale bar represents the nucleotide length of the genome. (**B**) Initiation and termination sequences for each NLV ORF were identified by aligning non-coding regions with MAAFT version 7.222. Conserved initiation and termination motifs for NLV, soybean cyst nematode virus 1 (SbCNV-1; NC_024702.1), and Midway virus (MIDWV; FJ554525) are also provided. (**C**) Phylogenetic tree of SCN NLV RdRP in relation to RdRPs of the most closely related viruses within the NCBI database via PSI-BLAST. Proteins were aligned with ClustalW and trees constructed with Geneious Tree Builder (Jukes-Cantor genetic distance model; neighbor-joining tree method; no outgroup; 1000 replicates; 50% support threshold). Branch labels display consensus support (%).

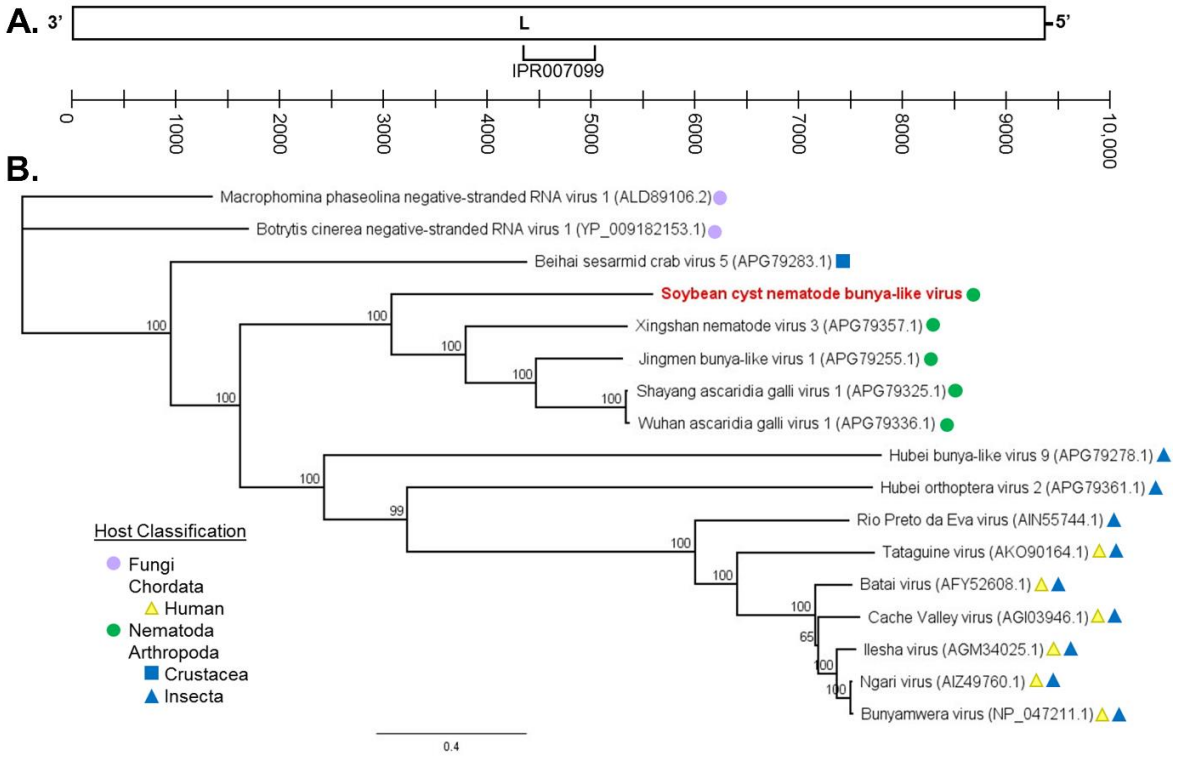

Fig 3.2. Characterization of soybean cyst nematode (SCN) bunya-like virus (BLV). (**A**) RNA-dependent RNA polymerase (RdRP; L) of SCN BLV. An identified InterProScan region is shown below the ORF. The scale denotes nucleotide length. (**B**) Phylogenetic tree of SCN BLV RdRP in relation to polymerases of closely related viruses via NCBI PSI-BLAST. Proteins were aligned with ClustalW and trees constructed with Geneious Tree Builder (Jukes-Cantor genetic distance model; neighbor-joining tree method; no outgroup; 1000 replicates; 50% support threshold). Branch labels display consensus support (%).

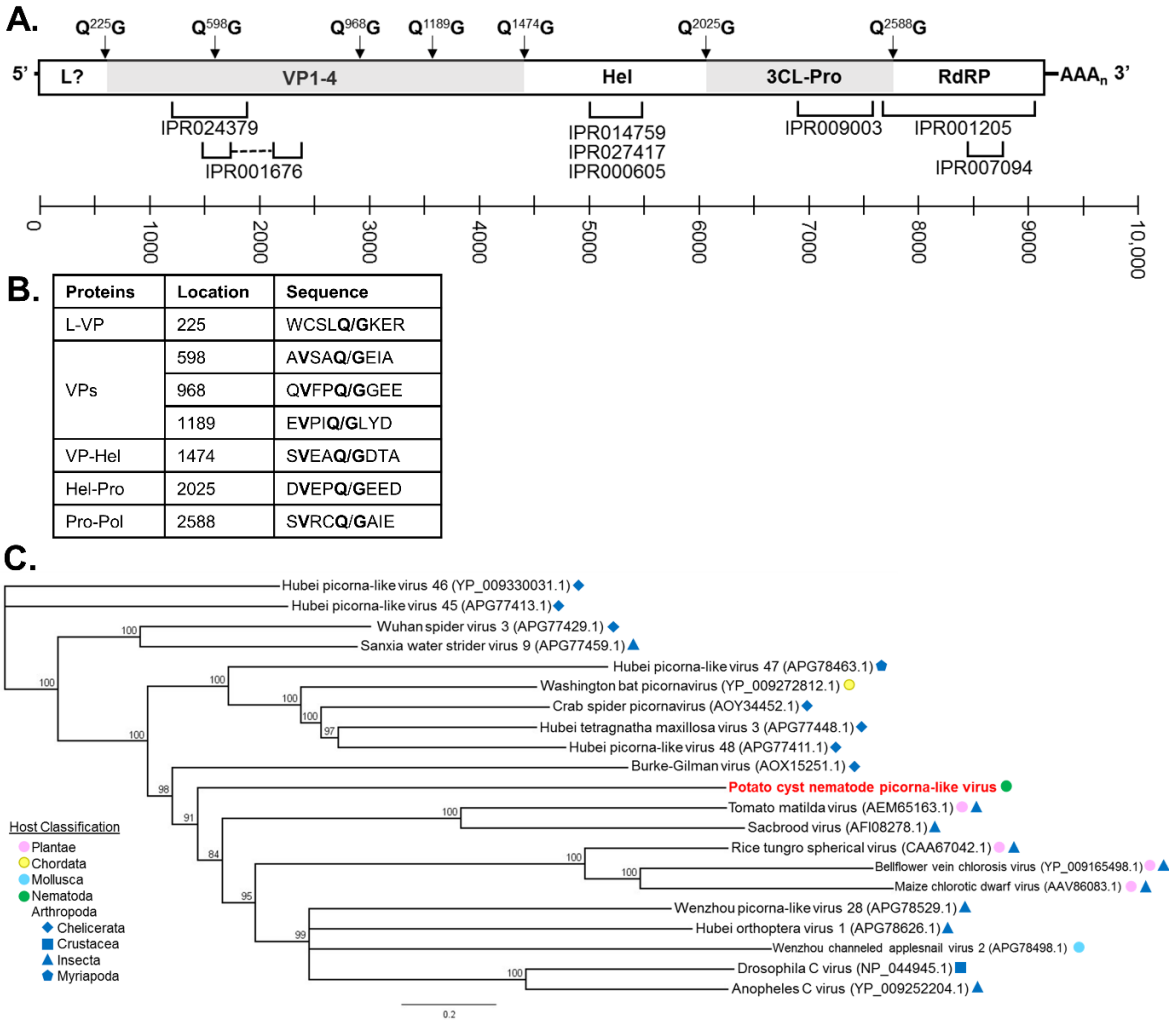

Proteins	Location	Sequence
L-VP	225	WCSL**Q**/**G**KER
VPs	598	A**V**SA**Q**/**G**EIA
	968	Q**V**FP**Q**/**G**GEE
	1189	E**V**PI**Q**/**G**LYD
VP-Hel	1474	S**V**EA**Q**/**G**DTA
Hel-Pro	2025	D**V**EP**Q**/**G**EED
Pro-Pol	2588	S**V**RC**Q**/**G**AIE

Fig 3.3. Characterization of potato cyst nematode (PCN) picorna-like virus (PLV). (**A**) Genome organization of PCN PLV. Putative proteins cleaved from the polyprotein include leader (L), four viral particle (VP1-4) proteins, helicase (hel), 3C-like protease (3CL-Pro), and RNA-dependent RNA polymerase (RdRP). Putative protease cleavage sites are shown above the genome (-1 and +1 positions); InterProScan regions are below the genome. The scale represents nucleotide length of the genome. (**B**) Putative protease cleavage sites of PCN PLV as predicted by the NetPicoRNA 1.0 Server (http://www.cbs.dtu.dk/services/NetPicoRNA/). Conserved amino acids are in bold type. (**C**) Phylogenetic tree of PCN PLV polyprotein in relation to closely related viral polyproteins identified via NCBI PSI-BLAST. Polyproteins were aligned with ClustalW and trees constructed with Geneious Tree Builder (Jukes-Cantor genetic distance model; neighbor-joining tree method; no outgroup; 1000 replicates; 50% support threshold). Branch labels display consensus support (%).

CHAPTER 4

Localization of Viral RNA and Host mRNA within Soybean Cyst Nematode via Whole-Mount Fluorescence *in situ* Hybridization

Citation:

Ruark-Seward CL, Davis EL, and Sit TL. Localization of Viral RNA and Host mRNA within Soybean Cyst Nematode via Whole-Mount Fluorescence *in situ* Hybridization. *In prep.*

ABSTRACT

Nematode-infecting RNA viruses have recently been discovered via transcriptome sequencing. In soybean cyst nematode (SCN; *Heterodera glycines*), seven single-stranded RNA viruses have been identified from transcriptome data and experimentally confirmed with qRT-PCR and Sanger sequencing. Presently, there is still much unknown about the relationship between these viruses and the nematode host. In this study, we localize three viruses within the nematode: SCN socyvirus-1 (SbCNV-1), SCN nyami-like virus (NLV), and SCN bunya-like virus (BLV). To visually locate the viruses, whole-mount fluorescence *in situ* hybridization (FISH) methodology was developed for SCN second-stage juveniles (J2s). Two SCN populations with differing viral titers (LY1 and MM21) were used as a comparison for viral probe fluorescence. Viral RNAs for all three viruses appear throughout most of the J2 of the highly infected population but appear absent within the majority of the intestinal tract. Moreover, viral RNAs were colocalized with host mRNA including glyceraldehyde 3-phosphate dehydrogenase (GAPDH) and a secretory ubiquitin protein specific to the subventral glands. Finally, viral replication was confirmed in SCN eggs and J2s via qRT-PCR detection of the anti-genomic RNA strands. With the presented research, the authors hope to build upon the knowledge of nematode infecting viruses as well as provide useful FISH methodology for studying localized RNA expression in nematodes.

INTRODUCTION

Several nematode genera are known to vector plant viruses; however, these plant viruses do not replicate within the nematode and are lost during molting (Brown *et al*., 1995). Interestingly, nematodes themselves were thought to be uninfected with viruses until Lu *et*

al. (2005) demonstrated *Caenorhabditis elegans* could support viral replication via artificial infection with *Flock house virus* (FHV). This finding lead to the discovery of natural viral infections in wild populations of *C. elegans* and *C. briggsae* from nematode transcriptome data (Felix *et al*., 2011; Franz *et al*., 2012). In total, three nodaviruses have been discovered in *Caenorhabditis* spp. and infections from all three viruses localize to a few intestinal cells (Franz *et al*., 2014). The location of these viral infections in nematode hosts was determined via immunofluorescence assays. These positive-sense RNA viruses are not transmitted vertically and are instead horizontally transmitted for up to 50 generations within cultured *C. elegans*. Currently, the nodaviruses are the only identified nematode viruses demonstrated to have a pathogenic phenotype on the host. Viral infections were observed to cause unusual intestinal cell morphologies in the form of abnormal intestinal granule distribution, nuclear elongation or degradation, a less viscous cytoplasm, and cellular fusions (Franz *et al*., 2014).

Five RNA viruses were also discovered in the soybean cyst nematode (SCN; *Heterodera glycines*) through transcriptome analyses (Bekal *et al*., 2011; Bekal *et al*., 2014). SCN are plant pathogenic nematodes (PPN) of significant importance to global soybean production (Jones *et al*., 2013). In the United States alone, SCN damages result in over a billion dollars of yield loss annually (Wrather and Koenning, 2006) The five original RNA viruses detected within SCN include Socyvirus-1 (SbCNV-1), a phlebovirus (ScPV), a rhabdovirus (ScRV), a tenuivirus (ScTV), and Virus-5 (Bekal *et al*., 2011; Bekal *et al*., 2014). Recently, two additional novel negative-sense RNA viruses were discovered within SCN [a nyami-like virus (NLV) and a bunya-like virus (BLV)] as well as a new positive-sense RNA virus in potato cyst nematode [a picorna-like virus (PLV)] via nematode transcriptome analyses (Ruark *et al*., 2018). The RNA genome structures vary greatly

amongst the SCN viruses with both monopartite and multipartite viruses represented. Additionally, replication of negative-sense viruses has been confirmed within SCN eggs, second-stage juvenile (J2), and pooled J3 and J4 life stages collected from infected plant roots (Ruark *et al*., 2017). Although the genomes have been identified and viral presence has been experimentally confirmed within nematode populations, little is known in regards to both where the viruses are localized within SCN and potential effects the viruses may have on the host.

The microscopic size and tough cuticle of PPN provide a challenge to traditional molecular localization experiments such as mRNA *in situ* hybridizations (ISH). The primary ISH protocol available for SCN J2 involves chemical fixation, cutting, and several permeabilization steps in order to gain probe entry into nematode cells and tissues (de Boer *et al*., 1998). When beginning the experiments described below, it was unknown where the viruses would be localized, and so segmenting the nematode was not an ideal option. Therefore, a fluorescence *in situ* hybridization (FISH) protocol was adapted for SCN from research localizing endosymbiotic bacteria within *Xiphinema* nematodes (Brown *et al*., 2015). Using this protocol, the *Wolbachia* endosymbiont was also localized within *Radopholus similis* and *Pratylenchus penetrans* (Brown *et al*., 2016). This technique overcomes some of the largest obstacles for FISH assays in nematodes: fluorescent probes are introduced in one step and are small enough in size (approximately 6.8 kDa) to pass through the cuticle, and the fluorescent dye utilized has a higher emission wavelength (633 nm) to avoid the intense autofluorescence of nematode tissues observed at lower wavelengths.

In this report, we describe a modified, whole-mount FISH protocol for SCN J2s that allows for colocalization of two targets in one specimen. In addition to the protocol adapted from Brown *et al*. (2015), an alternative methodology was developed for probe entry into nematodes using square-wave electroporation. With these modified protocols, three RNA viruses [SbCNV-1 (formerly ScNV, from Bekal *et al*., (2011) and SCN NLV and SCN BLV from Ruark *et al*. (2018)] were localized in SCN in addition to mRNA of a SCN gene expressed exclusively in the nematode's subventral esophageal gland cells (Gao *et al*., 2003) In addition, viral replication in eggs and J2s was confirmed via detection of the anti-genomic RNA strands with qRT-PCR. The modified FISH techniques presented here provide a more sensitive, combinatorial, and efficient whole-mount method to localize expression of SCN genes in nematode tissues and the first data on localization of viruses that infect a plant-parasitic nematode.

MATERIALS AND METHODS

Nematode Sample Collection

Two SCN (*Heterodera glycines*) populations were used for comparison of the FISH methods below: one with higher viral titers (LY1) and another with lower viral titers (MM21) as previously determined with qRT-PCR (Ruark *et al*., 2017; Ruark *et al*., 2018). The inbred research populations (LY1 and MM21) of SCN were cultured on roots of susceptible 'Hutcheson' soybean plants grown under greenhouse conditions for 2-3 months. The SCN-breeding methodologies to develop the LY1 (Lawrence Young, USDA, MS) and MM21 (Melissa Mitchum, Univ. MO) populations used in this study are described in more detail within Colgrove and Niblack (2008) as well as Ruark *et al*. (2017). SCN cysts were extracted

from plant roots with water pressure and soil via water flotation. Nematodes were then collected on stacked sieves sizes 20 (850 µm) and 60 (250 µm). Cysts were crushed with a Tenbroeck homogenizer to release eggs, and samples were further purified by centrifugation with 70% sucrose and collection on a size 500 sieve (25 µm). Separate equipment was maintained for the LY1 and MM21 nematode populations to avoid potential cross-contamination of nematode viruses. Eggs were hatched via the Baermann pan method (Townshend, 1963) at 27°C and hatched J2s were collected over a size 500-mesh sieve within 72 hours of hatch.

Whole-mount fluorescence *in situ* hybridization (FISH)

Hatched cohorts of SCN J2s were pelleted in a 1.5 ml microcentrifuge tube for 2 minutes at low speed (4000 x *g*). A minimum of 100 J2s were used per hybridization reaction. Excess water was removed from tubes via pipette leaving approximately 10 µl of fluid around the nematode pellet. Mild surface sterilization of nematodes was achieved by adding 200 µl of 0.1% benzalkonium chloride solution to the sample, incubated for 1 minute and then centrifuged for 1 minute at 6000 x *g*. Following centrifugation, roughly 200 µl of supernatant was carefully drawn off and discarded. Two different methodologies (chemical and electropermeabilization) were developed to facilitate probe entry within the nematode (detailed below). Both permeabilization techniques were efficient to achieve hybridization to the desired RNA within whole nematode specimens and two targets can be colocalized at the same time (ATTO-565 and ATTO-647N) when viewed on an appropriate confocal fluorescence microscope.

FISH Chemical Permeabilization Option

The FISH chemical permeabilization protocol described in this section was adapted from Brown *et al*. (2015). After surface sterilization (described above), a series of incubations and rinses of SCN J2 were conducted at room temperature by adding 100 µl of each solution into the 1.5 ml tube followed by centrifugation at 6000 x *g* for 1 minute and then discarding all but 10 µl of the supernatant each time. The incubations were performed in the following order: 1) two incubations for 2 minutes each with 0.85% w/v NaCl, 2) one incubation with 1:1 v/v of glacial acetic acid and 100% ethanol for 15 minutes, 3) two incubations with 100% ethanol for 5 minutes each, 4) one incubation with 1:1 v/v 100% methanol and sterile PBT (phosphate buffered Tween 20; 150 mM NaCl, 10 mM Na_3PO_4, 0.1% w/v Tween 20, pH 7.4) for 10 minutes, 5) one incubation with 1% v/v formaldehyde in PBT for 30 minutes, and 6) two incubations with PBT for 2 minutes each. Samples of SCN J2 following chemical permeabilization were held in a final volume of approximately 10 µl of PBT solution prior to addition of the hybridization probe(s).

FISH Electropermeabilization Option

Following surface sterilization with 0.1% benzalkonium chloride, nematodes were rinsed with 200 µl of sterile water, pelleted for 2 minutes at 4000 x *g*, and excess liquid was removed. Samples were resuspended in 50 µl sterile water for each reaction/probe combination. 50 µl of nematode suspension in water was pipetted into an electroporation cuvette (0.4 cm gap distance), and then 150 µm of each probe [(1.5 µl of 100 µm concentrated probe in TE (10 mM Tris–HCl, 1 mM EDTA, pH 7.4)] was added (Table 4.1). Nematodes suspended in probe solution were electroporated on a GenePulser Xcell^{TM} (Bio-

Rad; Hercules, CA, USA) with a single-pulse square wave at 125 V for 20 milliseconds (Kines *et al*., 2010).

FISH Hybridization

Probes for FISH of SCN specimens were developed for SbCNV-1 (formerly called ScNV, Bekal *et al*., 2011), SCN NLV, and SCN BLV (Ruark *et al*., 2018) as indicated in Table 4.1. For comparison, probes were also developed for SCN host mRNA targeted for a secretory ubiquitin protein (4G06 clone from Gao *et al*., 2003) to specifically localize within the SCN subventral esophageal gland cells. Glyceraldehyde 3-phosphate dehydrogenase (GAPDH) was used as an additional SCN internal control as it should be expressed in all nematode cells because of its involvement in glycolysis. DNA probes (20-mer) complementary to the target sequences were custom synthesized by Eurofins Genomics (Louisville, KY, USA) and were conjugated with either ATTO-647N or ATTO-565 fluorophores (ATTO-TEC; Siegen, Germany) at the 5' end (Table 4.1). Negative controls included samples with no probes added and a probe derived from FHV sequence that was not complementary to any known target sequence in the nematode. Identical treatments and controls were conducted on J2 of the MM21 SCN population for comparisons since lower SCN virus titers were previously detected in MM21 by qRT-PCR (Ruark *et al*., 2017; Ruark *et al*., 2018). [Note: A hybridization incubator was utilized for these protocols (Model 1000, Robbins Scientific; San Diego, CA, USA); however, a stationary heat block will generate similar results if a specialized oven is not available.]

Hybridization of Chemically Permeabilized Samples: Hybridizations were performed immediately after J2 permeabilization by adding 90 µl of hybridization buffer prewarmed to

46°C [20 mM Tris–HCl, pH 7.4, 0.02% w/v sodium dodecyl sulfate (SDS), 0.9 M NaCl, 5 mM ethylenediaminetetraacetic acid (EDTA), 60% v/v formamide]. Next, 100 µm of each probe (10 µl total volume in TE) was added to the nematode suspension and incubated ≥4 hours at 46°C on a gently rocking platform in the dark.

Hybridization of Electropermeabilized Samples: Following electroporation, 100 µl of prewarmed (46°C) hybridization buffer (same as above) was added to the nematode suspension, and the total volume was transferred to a 1.5 ml microcentrifuge tube. Samples were incubated ≥4 hours at 46°C in the dark on a gently rocking platform.

Removal of Excess Probe for Both Chemically Treated and Electroporated Samples: Following hybridizations, samples were centrifuged for 1 minute at 6000 x *g* and excess liquid was removed. Three incubations were performed at 50°C in 100 µl of pre-warmed hybridization wash buffer (20 mM Tris–HCl, 0.02% w/v SDS, 8 mM NaCl, 5 mM EDTA) for 20 minutes each on a rocking platform at a slightly higher rocking speed than the hybridization step. A final centrifugation was again conducted at 6000 x *g* for 1 minute and excess liquid was removed from the nematode pellet. Treated nematodes were pipetted onto glass microscope slides in a small volume of remaining wash buffer (approximately 5 µl). 10 µl of ProLong Diamond Antifade Mountant (Thermo Fisher Scientific; Waltham, MA, USA) was pipetted onto the drying sample and sealed with a coverslip. Slides were dried horizontally in the dark at 25°C for 24 hours and then stored at 4°C in the dark. Nematode specimens on slides were viewed on a Zeiss LSM 880 confocal microscope with an Apochromat 40x water immersion objective (1.2 W Corr FCS M27) and analyzed with Zen

version 2.3 software at North Carolina State University's Cellular and Molecular Imaging Facility (CMIF). The ATTO-565 and ATTO-647N fluorophores were checked for bleed-through between laser channels and no cross-over was detected.

RNA extraction and cDNA synthesis

Samples of approximately 10,000 J2s or eggs from the LY1 SCN population were prepared for total RNA extraction by homogenization with three 3-mm glass beads in a 1.5 ml tube on a Silamat S6 (Ivoclar Vivadent; Amherst, NY, USA). The homogenized samples were processed for total RNA using the Direct-zol™ RNA Microprep kit (Zymo Research; Irvine, CA, USA). Total RNA concentrations were analyzed via Nanodrop 1000 (Thermo Fisher Scientific).

First strand cDNA synthesis was initiated with either random, genomic sense, or anti-genomic sense primers complementary to the SbCNV-1, SCN NLV, or SCN BLV sequences (Table 4.2). cDNA was synthesized by incubating approximately 1 µg RNA with 0.06 µg of the appropriate primer for 10 minutes at 70°C followed by rapid cooling on ice. Next, 4 µl GeneAmp® 10X PCR Buffer II (Thermo Fisher Scientific), 5.5 mM $MgCl_2$, 0.5 µM deoxynucleotide solution mix, 32 U Murine RNase Inhibitor (New England BioLabs; Ipswich, MA, USA), and 50 U Multiscribe™ Reverse Transcriptase (Thermo Fisher Scientific) were added before additional incubations of 42°C and 70°C for 15 minutes each.

qRT-PCR

qRT-PCR primers complementary to SbCNV-1, SCN NLV, or SCN BLV sequences were synthesized by Eurofins Genomics and GAPDH primers (Table 4.3) were used as a SCN

internal control as this gene is validated for steady expression throughout different SCN life stages by Ithal *et al*. (2007). qRT-PCR products were amplified using 0.5 µM of each appropriate primer pair, 10 µl iTaq™ Universal SYBR® Green Supermix (Bio-Rad), and 1 µl cDNA. Samples were analyzed with the Applied Biosystems QuantStudio™ 6 Flex Real-Time PCR system on the following settings: 95°C, 20 seconds; 95°C, 2 seconds; 60°C, 25 seconds repeated for 40 amplification cycles with a continuous melt curve of 95°C, 20 seconds; 60°C, 1 minute; and 94°C for 20 seconds. Pooled technical triplicates were electrophoresed on a 2% 1X TAE (40 mM tris-acetate, pH 8.3, 1 mM EDTA) agarose gel for further analysis.

RESULTS

FISH Protocol Development

In order to clearly localize SCN mRNA and viral RNA, development of FISH methodology in which the nematode was left wholly intact was necessary. Efficient probe entry was achieved by using a small, 20-mer DNA oligo probe with an ATTO fluorophore attached at the 5' end. The protocol described by Brown *et al*. (2015) was improved for SCN by increasing the permeabilization time (acetic acid/ethanol wash step) by 5 minutes for a total time of 15 minutes. Additionally, an alternative permeabilization protocol was devised in which nematodes are electroporated with probes. A comparison of SCN J2s labelled via the two different permeabilization protocol options can be seen in Figure 4.1. These images are a comparison of the same probe that is specific to a SCN secretory ubiquitin protein mRNA localized within the subventral glands. This particular mRNA (4G06 clone) was previously localized to the single dorsal esophageal gland cell (Gao *et al*., 2003), but the new

protocol clearly detected the *4G06* transcript within only the two subventral esophageal glands.

To overcome background autofluorescence within SCN J2s, higher wavelength fluorophores were utilized to conjugate to DNA probes. Viewing unlabeled individuals with a laser scanning confocal microscope (Zeiss LSM 880) demonstrated that fluorophores with an absorption value of 565 nm or higher are optimal. Two different fluorophores were deemed suitable for these experiments: ATTO-565 and ATTO-647N had minimal issues competing with host autofluorescence and are far enough apart on the wavelength spectrum to be used simultaneously to provide differential localization of multiple probes. Additional attempts were made to localize RNAs within egg life stages. Unfortunately, the chitinous eggshell autofluoresces at the higher wavelengths in addition to the lower wavelengths. Thus, the ATTO-565 and ATTO-647N conjugated probes were not distinguishable within SCN eggs. A comparison of an egg versus a J2 with the same confocal microscope settings used to visualize 565 nm and 647 nm dyes is demonstrated in Figure 4.2. Efforts were made to degrade the eggshell with chitinase and various concentrations of sodium hypochlorite; however, attempts which compromised the eggshell also damaged the cellular integrity and endogenous nucleic acids.

FISH localization of host mRNA

SCN mRNA was targeted to optimize the FISH protocols using a probe with a predicted tissue localization and to make these methodologies useful for the study of other SCN localized gene expression. Thus far, two DNA probes have been successfully utilized to hybridize host mRNA (Table 4.1). host-specific FISH probes are conjugated with ATTO-

647N, and any colors represented in the provided images are artificially colored with the microscopy software. The hybridization targets were mRNA encoding a 4G06 ubiquitin protein specific to the esophageal gland cells (Gao *et al*., 2003) and GAPDH (Table 4.1). The 4G06 transcript localized to the two subventral esophageal gland cells using the current protocol (Figures 4.1 and 4.3A) contrary to the original report of expression in the single dorsal esophageal gland cell (Gao *et al*., 2003). GAPDH is involved in glycolysis and should be present within every cell for ATP production. The rationale for selecting GAPDH is that mRNA should be more abundant in metabolically active cells, thus following a similar distribution pattern to an actively replicating virus. Localization for GAPDH hybridization to expressed mRNA within SCN J2 confirmed ubiquitous expression throughout the nematode and greater expression in metabolically-active tissues such as the esophageal gland cells (Figure 4.3B).

FISH colocalization of viral RNAs with host mRNA

Three negative-sense RNA viruses that infect SCN were localized in J2s by the improved FISH assay using probe delivery via the electroporation protocol. One of the targeted viruses is the monopartite SCN Socyvirus-1 (SbCNV-1) first identified by Bekal *et al*. (2011) (virus previously known as ScNV). The other two viruses localized via FISH are SCN nyami-like virus (NLV) and SCN bunya-like virus (BLV) initially identified by Ruark *et al*. (2018). SCN NLV is a monopartite virus most closely related to SbCNV-1, but it is distinct enough (approximately 50% identical) to warrant a separate genus. SCN BLV is a multipartite virus, and thus far, only the polymerase region of the genome has been identified. To contrast viral fluorescence intensities and demonstrate probe specificity, two

SCN populations were selected which have differing viral titers. From previous work, the MM21 population is known to possess lower titers (undetectable via qRT-PCR) of SbCNV-1 and SCN NLV (Ruark *et al*., 2017; Ruark *et al*., 2018). SCN BLV was detectable within MM21 but at a lower level than LY1. Contrastingly, LY1 tested positive for the three viruses as determined via qRT-PCR.

ATTO-565 conjugated probes that hybridized to viral RNAs were colocalized with ATTO-647N conjugated probes hybridized to SCN GAPDH mRNA in the same nematode specimen. Figure 4.4 demonstrates SbCNV-1 localized alongside SCN GAPDH within the higher-titer population, LY1 (panels A-C), and the lower titer population, MM21 (panels D-F). The same experiments were repeated for SCN NLV (Figure 4.5) and SCN BLV (Figure 4.6). Similar patterns are visible within LY1 for the three viruses in which it appears viral RNAs are present throughout the J2s with the exception of the intestinal tract. Differences are visible in the viral fluorescence intensities between LY1 and MM21 samples with more viral probes binding within LY1. Additionally, viral RNA locations appear to correspond with GAPDH mRNA, with the highest fluorescence intensities in the gland cells that are likely the most metabolically active. Colocalization of viral RNA probes with the subventral glands secretory ubiquitin protein mRNA (4G06) are shown in Supplemental Figure 4.1.

A non-binding probe was designed to verify the results of viral RNA localization. This probe was designed to the RNA-dependent RNA polymerase (RdRP) region of FHV which is not known to naturally infect SCN. Similarly, FHV was not detectable in SCN via PCR. However, the FHV probe does bind within the nematode (Supplemental Figure 4.2) and could potentially be binding to a host RdRP or that of another virus.

Viral replication within eggs and J2s

In addition to localization within the J2, replication is demonstrated within the LY1 population for the single-stranded RNA viruses SbCNV-1, SCN BLV, and SCN NLV. Total RNA was extracted from either eggs or J2s of SCN, cDNA synthesized with strand-specific viral primers (Table 4.2), and then detected via qRT-PCR (Table 4.3). For the three viruses tested, the anti-genomic strand is detectable demonstrating active viral replication within both eggs and J2s of SCN (Figure 4.7). qRT-PCR cycle threshold (Ct) values are displayed in Supplemental Table 4.1. qRT-PCR data will be regenerated for the MM21 population to compare against previous results (Ruark *et al*., 2017; Ruark *et al*., 2018) and determine viral replication if detectable.

DISCUSSION

The presented work describes an efficient methodology for whole-mount FISH within SCN. Moreover, a novel protocol was devised for probe introduction into nematodes via square-wave electroporation. Both host mRNA and genomic RNA from three viral species (SbCNV-1, SCN NLV, and SCN BLV) were localized within juvenile nematodes. A SCN secretory ubiquitin protein mRNA was specifically located within the two subventral esophageal gland cells, and transcripts of SCN GAPDH were localized throughout the J2 body with fluorescence intensity highest in the gland cells followed by cells within the tip of the tail. Two SCN populations with varying viral titers were compared against one another to confirm the specificity of the viral FISH probes. The higher titer population of SCN, LY1, had visibly more fluorescence intensity for the viral probes than the MM21 population of SCN consistent with previous qRT-PCR results (Ruark *et al*., 2017; Ruark *et al*., 2018). In

J2s of the LY1 population, the RNA distribution of the three viruses showed similarity to GAPDH mRNA expression with brighter labeling within the gland cells, and viral probes were visible throughout the J2 except for the intestinal tract. Additionally, replication of the three negative-sense RNA viruses was confirmed in SCN LY1 eggs and J2s via strand-specific cDNA synthesis followed by qRT-PCR detection of the anti-genomic strands.

In past ISH experiments, nematodes were diced into multiple segments since probes were unable to easily permeate past the cuticle (de Boer *et al*., 1998). To overcome this issue, small DNA oligo probes were combined with improved whole-mount permeabilization protocols for efficient one-step probe entry and hybridization within SCN J2s. The probes are 20-nt long with ATTO fluorophores attached to the 5' end, amounting to a total size of approximately 6.8 kDa per oligo probe. By merely incubating nematodes with the probes in hybridization buffer (without prior permeabilization steps), the subventral glands of J2s were successfully labelled (data not shown); although, fluorescence was not nearly as intense in comparison to either of two developed permeabilization protocols. The two different probe entry protocols involve either subjecting the nematode sample to a series of chemical washes or electroporating the probes into the nematode. Both permeabilization protocols have their advantages and disadvantages. The chemical permeabilization option adapted from Brown *et al*. (2015) is preferable if a square-wave electroporator is not available. Although the electropermeabilization method requires more equipment, it does reduce active protocol time by roughly two hours and reduces sample loss with less required aspiration steps. Both methodologies were effective at RNA hybridization within SCN with electropermeabilization arguably generating greater hybridization efficiency (Figure 4.1).

Autofluorescence observed in SCN J2s was overcome by using probes with absorbance wavelengths of 565 and 647 nm (fluorescence values are nearly identical to absorbance values for both ATTO-565 and ATTO-647N). These probes can be utilized together, allowing co-localization studies within a single specimen. Attempts were made to label probes within eggs, but it was discovered that eggshells autofluoresced at both 565 nm and 647 nm in addition to the lower wavelengths seen in juveniles (Figure 4.2). Additional steps of dissolving the vitelline membrane and chitinous layer of eggshells were conducted in an effort to allow probes to permeate and be visible above background noise at higher wavelengths. Thus, eggs were washed with sodium hypochlorite followed by chitinase (isolated from *Streptomyces griseus*). Increasing the sodium hypochlorite concentration and wash times dissolved eggshells but resulted in more severe damage to cells and increased autofluorescence at 565 nm above that of untreated samples. Additionally, chitinase treatment had no visible effect without the addition of sodium hypochlorite (tested up to 1.5 hours), likely because either the vitelline layer must first be dissolved or this particular type of chitinase from *Streptomyces griseus* was not as effective against SCN chitin compared to *C. elegans* (Tabara *et al*., 1996). Elucidating the correct combination of solvents and incubation times to dissolve multiple layers of the eggshell without damaging nucleic acids will be required for successful probe permeation and hybridization with eggs of SCN.

Using the developed FISH assay, both host mRNA and RNA from three viral species were localized. The probe developed for the 4G06 SCN secretory ubiquitin protein mRNA was selected to test protocol efficacy as it was expected to localize only to the single large dorsal esophageal gland cell in SCN (Gao *et al*., 2003). After testing the probe, it became apparent that mRNA of 4G06 was instead specifically expressed within the two subventral

gland cells during the J2 life stage (Figure 4.3A). Fortunately, this result did not affect the outcome of this FISH assay since the 4G06 gene was expressed within a clearly defined cell type. The second control probe targeted host mRNA of GAPDH, and it was selected because, like viruses, it should be expressed most abundantly in cells which are metabolically active. GAPDH did follow this pattern and expressed most abundantly in gland cells and was also visible within the anterior half of the J2, cells in the tip of the tail, longitudinal muscle cells, and occasionally within the genital primordia (Figures 4.3B and 4.4B). Moreover, viral genomic RNAs demonstrated a similar distribution as GAPDH mRNA within the J2. This similar patterning is demonstrated for SbCNV-1 (Figure 4.4A-C), SCN NLV (Figure 4.5A-C), and SCN BLV (Figure 4.6).

The viral RNAs appear to be present in cells throughout the J2 (including the genital primordium) but absent within the intestinal tract. These results are possible evidence for vertical transmission of the three viruses, in which case, the intestine would be a poor location for survival. Nodaviruses infecting *Caenorhabditis spp.* were found to infect only intestinal cells and are not transmitted vertically (Franz *et al*., 2014). Offering additional support for vertical transmission, SCN viruses are detectable within eggs and J2s via qRT-PCR (Figure 4.7; Supplemental Table 4.1). Furthermore, these viruses are actively replicating within both life stages as the anti-genomic strands are present for the three viruses examined within this study. These data are in agreement with previous research from the authors (Ruark *et al*., 2017) that showed replication of other SCN RNA viruses (including SbCNV-1, formally called ScNV) within eggs, J2, and pooled J3 and J4s. Moreover, from previous work, we know the three SCN viruses to be prevalent within SCN populations, and thus far, appear specific to SCN and clover cyst nematodes (*Heterodera trifolii*) (Ruark *et al*.,

2017; Ruark *et al*., 2018). According to Skantar *et al*. (2012), clover cyst nematodes are most closely related to SCN, and so these viruses may have evolved alongside these two cyst nematode species over a long period of time.

Additionally, viral fluorescence levels were compared between two SCN populations to test probe specificity. These SCN populations were previously tested for viruses and selected due to variance in their viral loads as measured by qRT-PCR (Ruark *et al*., 2017; Ruark *et al*., 2018). The population with higher viral titers, LY1, tested positive for the three viruses examined in this study; whereas, the MM21 population previously tested positive for SCN BLV, with SbCNV-1 and SCN NLV below the detectable limits of qRT-PCR. Unlike LY1 in which fluorescence mirrors a pattern similar to GAPDH mRNA, SbCNV-1 and SCN NLV probes are dispersed evenly and faintly throughout the MM21 J2 (Figures 4.4 and 4.5). SCN BLV within MM21 shows patterning more distinct with GAPDH mRNA; however, the fluorescence intensity is weaker when compared against LY1 (Figure 4.6). The presence of visible probes in MM21 for viruses which were non-detectable via qRT-PCR suggests two possible explanations: 1) the population may be infected with a very low viral titer, and the ATTO conjugates are more sensitive for RNA detection than qRT-PCR, or 2) trace amounts of non-bound probe are still present in the sample after wash buffer treatments. GAPDH mRNA hybridizations were similar between populations regardless of their viral titers. This demonstrates that if the viruses are indeed present in MM21, there should be adequate metabolic activity to support viral replication and titer may be suppressed by other factors.

To limit the possibility of non-specific binding, probe sequences were compared against nucleotide sequences in GenBank to limit similarities to other viruses and the *Heteroderidae* family. Additionally, no dimerization was calculated between colocalized host

and viral probe sequences. The intended non-binding control probe for FHV, unfortunately, bound within the nematode. This is likely a result of unknown specificity to a RdRP of the nematode or another unknown virus. Unfortunately, the complete SCN genome is not yet available, and so a truly non-binding probe cannot be designed with confidence. Future experiments will include additional probes specific to other regions of the viral genomes for additional confirmation of viral RNA locations. A probe specific to another SCN gene will also be implemented to ideally represent a host mRNA target that does not bind to the esophageal gland cells.

With this research, the authors hope to demonstrate visual evidence for viruses within SCN as well as provide useful FISH methodology to localize other endosymbionts or expressed genes of interest in whole-mount PPN. Future work on localizing the expression of nematode genes as well as elucidating the significance of viruses within SCN may be instrumental in understanding the biology of viral infection of nematodes and its potential exploitation for nematode management.

ACKNOWLEDGEMENTS

The authors would like to acknowledge the Cellular and Molecular Imaging Facility at NC State University for training and use of the Zeiss LSM 880 microscope. Thank you to Amanda M.V. Brown at Texas Tech University for guidance and providing her FISH protocol. CLR-S was supported by NSF grant DGE-1252376.

LITERATURE CITED

1. Bekal, S., Domier, L.L., Niblack, T.L., Lambert, K.N. Discovery and initial analysis of novel viral genomes in the soybean cyst nematode. *J. Gen. Virol*. 92 (8): 1870-1879 (2011).

2. Bekal, S., Domier, L.L., Gonfa, B., McCoppin, N.K., Lambert, K.N., Bhalerao, K. A novel flavivirus in the soybean cyst nematode. *J. Gen. Virol*. 95 (6): 1272-1280 (2014).

3. Brown, A.M.V., Howe, D.K., Wasala, S.K., Peetz, A.B., Zasada, I.A., and Denver, D.R. Comparative genomics of a plant-parasitic nematode endosymbiont suggest a role in nutritional symbiosis. *Genome Biol. Evol.* 7 (9): 2727-2746 (2015).

4. Brown, A.M.V., Wasala, S.K., Howe, D.K., Peetz, A.B., Zasada, I.A., and Denver, D.R. Genome evidence for plant-parasitic nematodes as the earliest *Wolbachia* hosts. *Sci. Rep.* 6: 34955 (2016).

5. Brown, D.J., Robertson, W.M., Trudgill, D.L. Transmission of viruses by plant nematodes. *Annu. Rev. Phytopathol*. 33: 223–249 (1995).

6. Colgrove, A.L., Niblack, T.L. Correlation of female indices from virulence assays on inbred lines and field populations of *Heterodera glycines*. *J. Nematol.* 40 (1): 39-45 (2008).

7. de Boer, J.M., Yan, Y., Smant, G., Davis, E.L., and Baum, T.J. *In-situ* hybridization to messenger RNA in *Heterodera glycines. J. Nematol*. 30 (3): 309-312 (1998).

8. Felix, M.A., Ashe, A., Piffaretti, J., Wu, G., Nuez, I., Belicard, T., Jian, Y., Franz, C.J., Goldstein, L.D., Sanroman, M., Miska, E.A., and Wang, D. Natural and experimental infection of *Caenorhabditis* nematodes by novel viruses related to nodaviruses. *PLOS Biol*. 9 (1): e1000586 (2011).

9. Franz, C.J., Zhao, G., Félix, M.A., Wang, D. Complete genome sequence of Le Blanc virus, a third *Caenorhabditis* nematode-infecting virus. *J Virol*. 86 (21): 11940 (2012).

10. Franz, C.J., Renshaw, H., Frezal, L., Jiang, Y., Felix, M.A., and Wang, D. Orsay, Santeuil and Le Blanc viruses primarily infect intestinal cells in *Caenorhabditis* nematodes. *Virol.* 448: 255-264 (2014).

11. Gao, B., Allen, R., Maier, T., Davis, E.L., Baum, T.J., and Hussey, R.S. The parasitome of the phytonematode *Heterodera glycines*. *Mol. Plant Mic. Int.* 16 (8): 720-726 (2003).

12. Ithal, N., Recknor, J., Nettleton, D., Hearne, L., Maier, T., Baum, T.J., Mitchum, M.G. Parallel genome-wide expression profiling of host and pathogen during soybean cyst nematode infection of soybean. *Mol. Plant Mic. Int*. 20 (3): 293-305 (2007).

13. Jones, J.T., Haegeman, A., Danchin, E.G., Gaur, H.S., Helder, J., Jones, M.G., Kikuchi, T., Manzanilla-Lopez, R., Palomares-Ruis, J.E., Wesemael, W.M., and Perry, R.N. Top 10 plant parasitic nematodes in molecular plant pathology. *Mol Plant Pathol*. 14 (9): 946-961 (2013).

14. Kines, K.J., Rinaldi, G., Okatcha, T.I., Morales, M.E., Mann, V.H., Tort, J.F., and Brindley, P.J. Electroporation facilitates introduction of reporter transgenes and virions into schistosome eggs. *PLOS Negl. Trop. Dis*. 4 (2): e593 (2010).

15. Lu, R., Maduro, M., Li, H.W., Broitman-Maduro, G., Li, W.X., Ding, S.W. Animal virus replication and RNAi-mediated antiviral silencing in *Caenorhabditis elegans*. *Nature*. 436 (7053): 1040-1043 (2005).

16. Ruark, C.L., Koenning, S.R., Davis, E.L., Opperman, C.H., Lommel, S.A., Mitchum, M.G., Sit, T.L. Soybean cyst nematode culture collections and field populations from North Carolina and Missouri reveal high incidences of infection by viruses. *PLOS ONE*. 12 (1): e0171514 (2017).

17. Ruark, C.L., Gardner, M., Mitchum, M.G., Davis, E.L., Sit, T.L. Novel RNA viruses within plant parasitic cyst nematodes. *PLOS ONE*. 13 (3): e0193881 (2018).

18. Skantar, A.M., Handoo, Z.A., Zanakis, G.N., Tzortzakakis, E.A. Molecular and morphological characterization of the corn cyst nematode, *Heterodera zeae*, from Greece. *J Nematol*. 44 (1): 58-66 (2012).

19. Tabara, H., Motohashi, T., and Kohara, Y. A multi-well version of *in situ* hybridization on whole mount embryos of *Caenorhabditis elegans*. *Nuc. Acids Res.* 24 (11): 2119-2124 (1996).

20. Townshend, J.L. A modification and evaluation of the apparatus for the Oostenbrink direct cotton wool filter extraction method. *Nematologica.* 9 (1): 106-110 (1963).

21. Wrather JA, Koenning SR. Estimates of disease effects on soybean yields in the United States 2003 to 2005. *J Nematol.* 2006; 38: 173-180.

TABLES

Table 4.1. Fluorescent DNA probes used for fluorescence *in situ* hybridization (FISH). Abbreviations: SCN (soybean cyst nematode), SvG (subventral glands), GAPDH (glyceraldehyde 3-phosphate dehydrogenase), RdRP (RNA dependent RNA polymerase).

Organism	Target	Sequence [5' to 3']	Accession #
SCN	SvG 4G06[a]	ATTO647N/CTTCTGTATGTTGTAGTCGG	AF469060
SCN	GAPDH	ATTO647N/TATTTCTCTTTTCCTGGTCC	CA939315
SCN Socyvirus-1	RdRP	ATTO565/CCGGAAACTTGGGATTTTGG	HM849038
SCN Nyami-like virus	Nucleocapsid[b]	ATTO565/TATGGGGGCACTTGACAACG	MG550265
SCN Nyami-like virus	RdRP	ATTO565/GAACTTTATTTGGCTCCTGA	MG550265
SCN Bunya-like virus	RdRP	ATTO565/ACTGTATCTCCATCTTACTC	MG550269
Flock house virus[c]	RdRP	ATTO565/TTTTGGGCGATGTTTCTTTG	X77156

[a] 4G06 is a cloned sequence of a secretory ubiquitin protein with specificity to the subventral glands of J2s.
[b] Probe results are not yet available.
[c] *Flock house virus* probe was used as a non-binding control.

Table 4.2. Primers used to generate strand-specific cDNA templates. Abbreviations: SbCNV-1 (SCN Socyvirus-1), SCN (soybean cyst nematode), NLV (nyami-like virus), BLV (bunya-like virus).

Primer	**Sequence [5' to 3']**
SbCNV-1 anti-genomic strand[a]	TTAAACTCATCCGCTGCTCGT
SbCNV-1 genomic strand[b]	ACATAGTCAGTGGCCGATTC
SCN NLV anti-genomic strand	CGGAGTACACTGTCGAGACG
SCN NLV genomic strand	TGAATCGTGGTTTGAGGGCA
SCN BLV anti-genomic strand	TCCTCTAACAACAGTAGTCGT
SCN BLV genomic strand	TGACTCTGATTCTTTGTGCAA

[a] Anti-genomic strand primers were used for synthesis of the anti-genomic, positive strand.
[b] Genomic strand primers were used for synthesis of the genomic, negative strand.

Table 4.3. Primers used to detect viral sequences and *Heterodera glycines* internal control (GAPDH) via qRT-PCR. Abbreviations: SbCNV-1 (SCN Socyvirus-1), SCN (soybean cyst nematode), NLV (nyami-like virus), BLV (bunya-like virus), GAPDH (glyceraldehyde 3-phosphate dehydrogenase).

Primer	**Sequence [5' to 3']**
SbCNV-1 QF	GGTCCTGCTTAGCTTGTGA
SbCNV-1 QR	CATCTGTGGTGATTGGAC
SCN NLV QF	GTTGACGGCACTTGAACACC
SCN NLV QR	GGGATTCAACTCAAGCCGGA
SCN BLV QF	GCCAGCCAGCATTTACAAGG
SCN BLV QR	CCAGGGGACATGAGAATCACC
GAPDH QF	TCCAAGGCATAGAAAGACGACG
GAPDH QR	AACAAGTCATTGGACGGCATCA

FIGURES

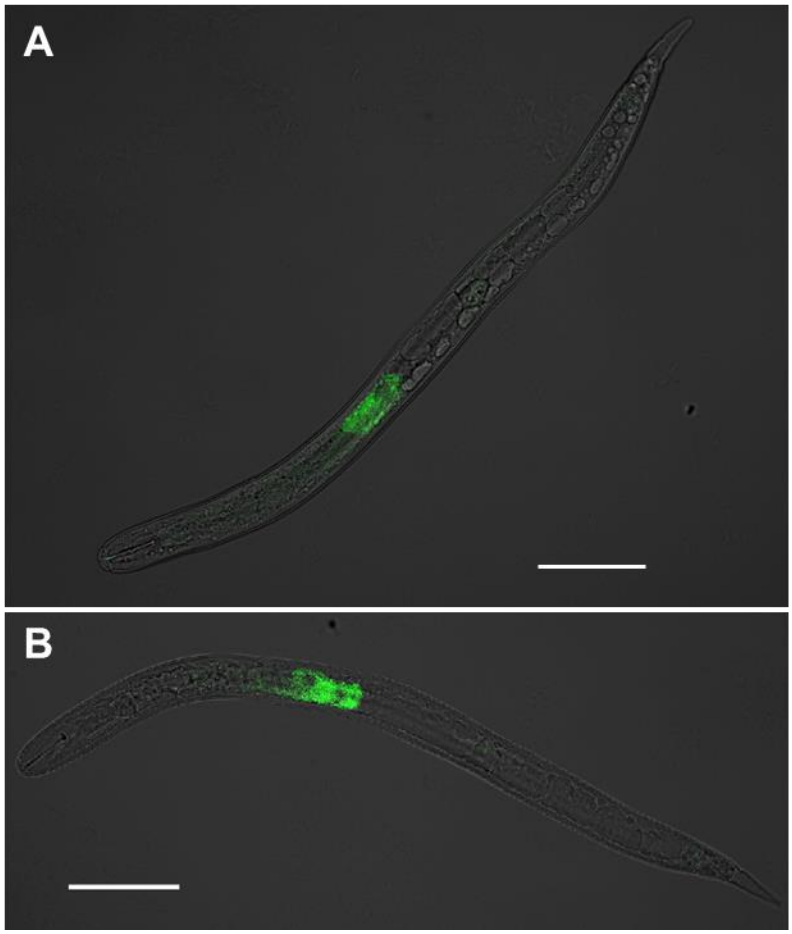

Figure 4.1. Comparison of FISH methodologies for fluorescent probe entry into whole nematodes. Two preparation methodologies of SCN J2 for mRNA hybridization with fluorescent DNA probes are displayed in the LY1 population of SCN. **A** Results via the chemical permeabilization protocol option; **B** Results via the electropermeabilization protocol option. Both nematodes were treated with the same ATTO-647N conjugated probe complementary to mRNA of a ubiquitin protein (4G06) that localizes to the two subventral esophageal gland cells in SCN. The brightfield channel is muted but retained in images for better structure clarity. Scale bar represents 50 µm (Zeiss LSM 880).

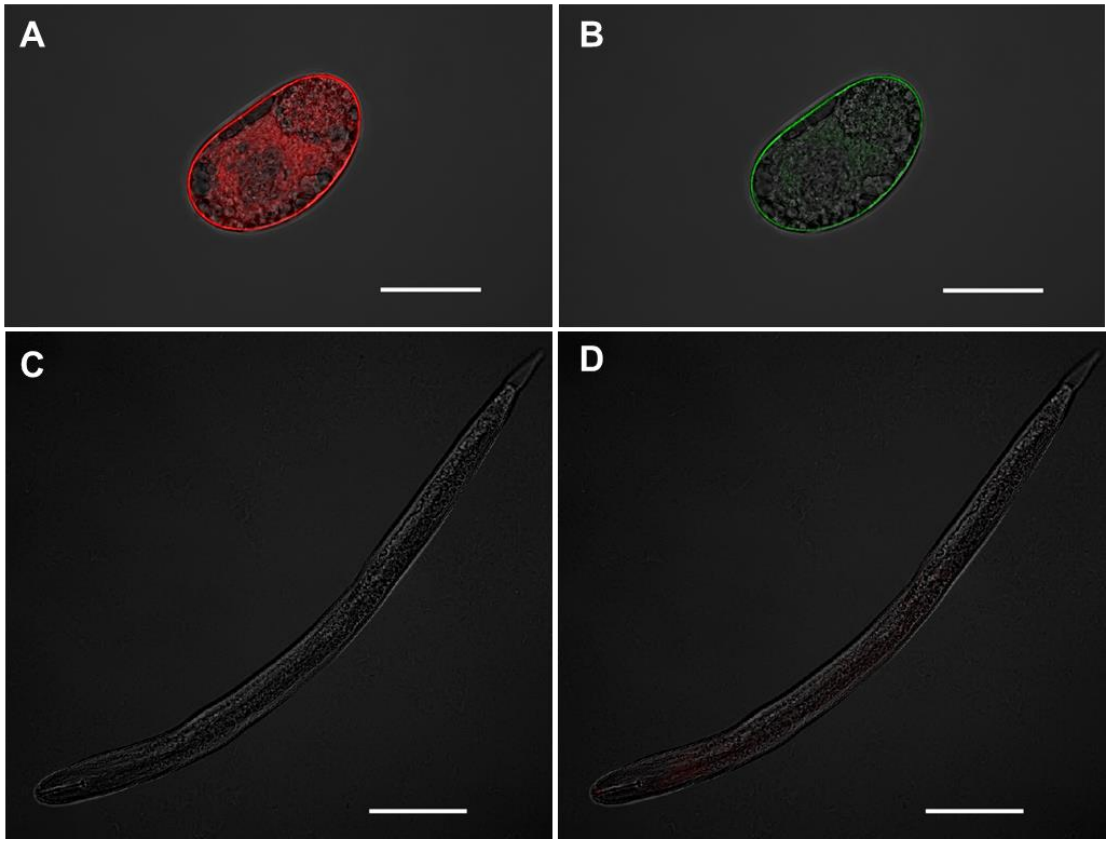

Figure 4.2. Autofluorescence of SCN eggs and J2s with 565 and 633 nm laser lines. SCN LY1 eggs and J2s without probes were viewed for autofluorescence with the settings used for ATTO-565 and ATTO-647N dyes. **A, B** untreated egg viewed with 565 and 633 nm laser, respectively. **C, D** untreated J2 viewed with 565 and 633 nm laser, respectively. The brightfield channel is muted but retained in images for better structure clarity. Scale bar represents 50 µm (Zeiss LSM 880).

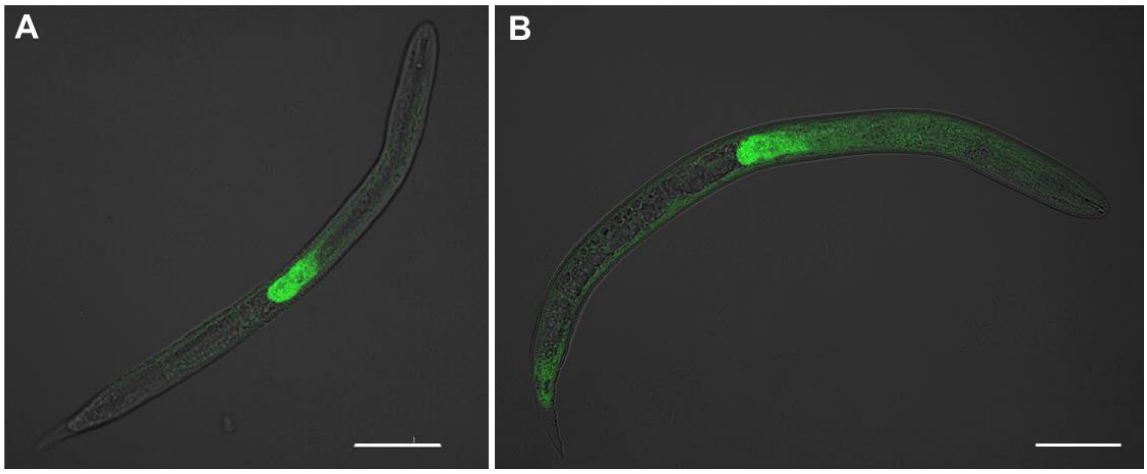

Figure 4.3. Localization of SCN mRNA. RNA within SCN LY1 J2s was hybridized with fluorescent DNA probes via fluorescence *in situ* hybridization (FISH). Hybridization to host mRNA is visualized with a conjugated ATTO-647N fluorophore. **A** Localization of the transcript encoding the 4G06 ubiquitin protein within the two subventral esophageal gland cells of SCN **B** The probe to nematode GAPDH hybridizes in cells throughout the nematode body. The brightfield channel is muted but retained in images for better structure clarity. Scale bar represents 50 µm (Zeiss LSM 880).

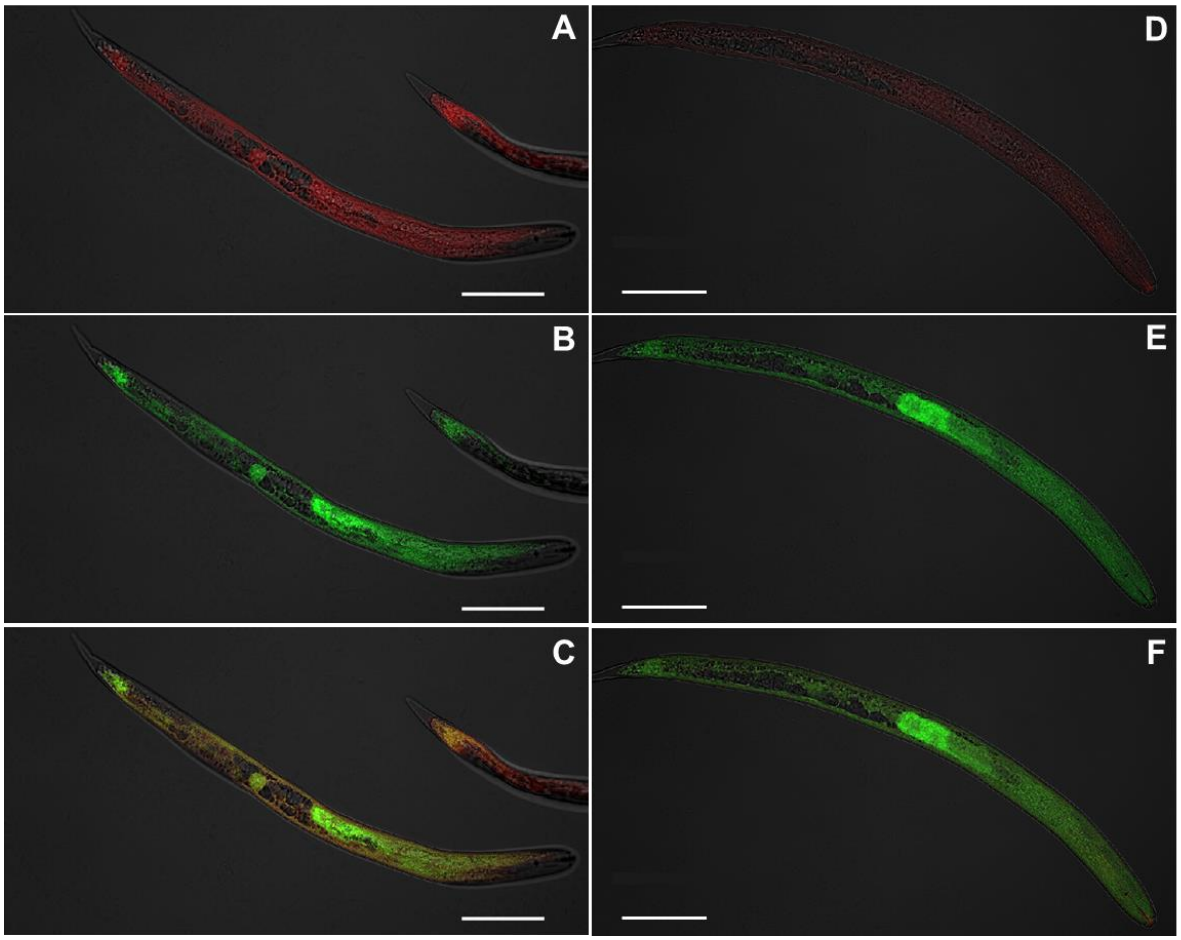

Figure 4.4. Colocalization of SCN Socyvirus (SbCNV-1) with host GAPDH. RNA within SCN J2s was labelled with fluorescent DNA probes via fluorescence *in situ* hybridization (FISH). Host mRNA is labelled with ATTO-647N dye and SbCNV-1 with ATTO-565. **A-C** SCN population LY1 (A: SbCNV-1 single channel [red], B: GAPDH single channel [green], and C: overlay). **D-F** SCN population MM21 (D: SbCNV-1 single channel [red], E: GAPDH single channel [green], and F: overlay). The brightfield channel is muted but retained in images for better structure clarity. Scale bar represents 50 µm (Zeiss LSM 880).

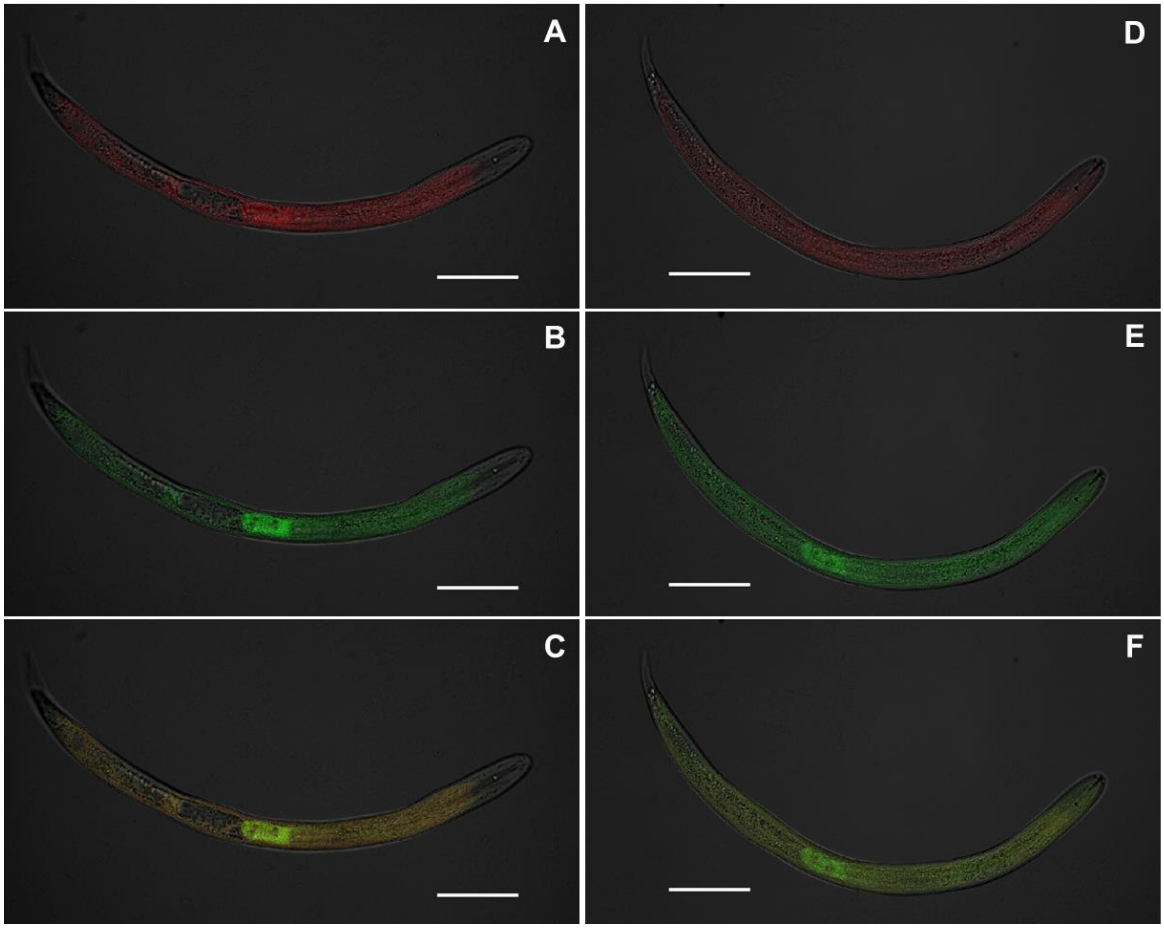

Figure 4.5. Colocalization of SCN Nyami-like virus (NLV) with host GAPDH. RNA within SCN J2s was labelled with fluorescent DNA probes via fluorescence *in situ* hybridization (FISH). Host mRNA is labelled with ATTO-647N dye and SCN NLV with ATTO-565. **A-C** SCN population LY1 (A: SCN NLV single channel [red], B: GAPDH single channel [green], and C: overlay). **D-F** SCN population MM21 (D: SCN NLV single channel [red], E: GAPDH single channel [green], and F: overlay). The brightfield channel is muted but retained in images for better structure clarity. Scale bar represents 50 µm (Zeiss LSM 880).

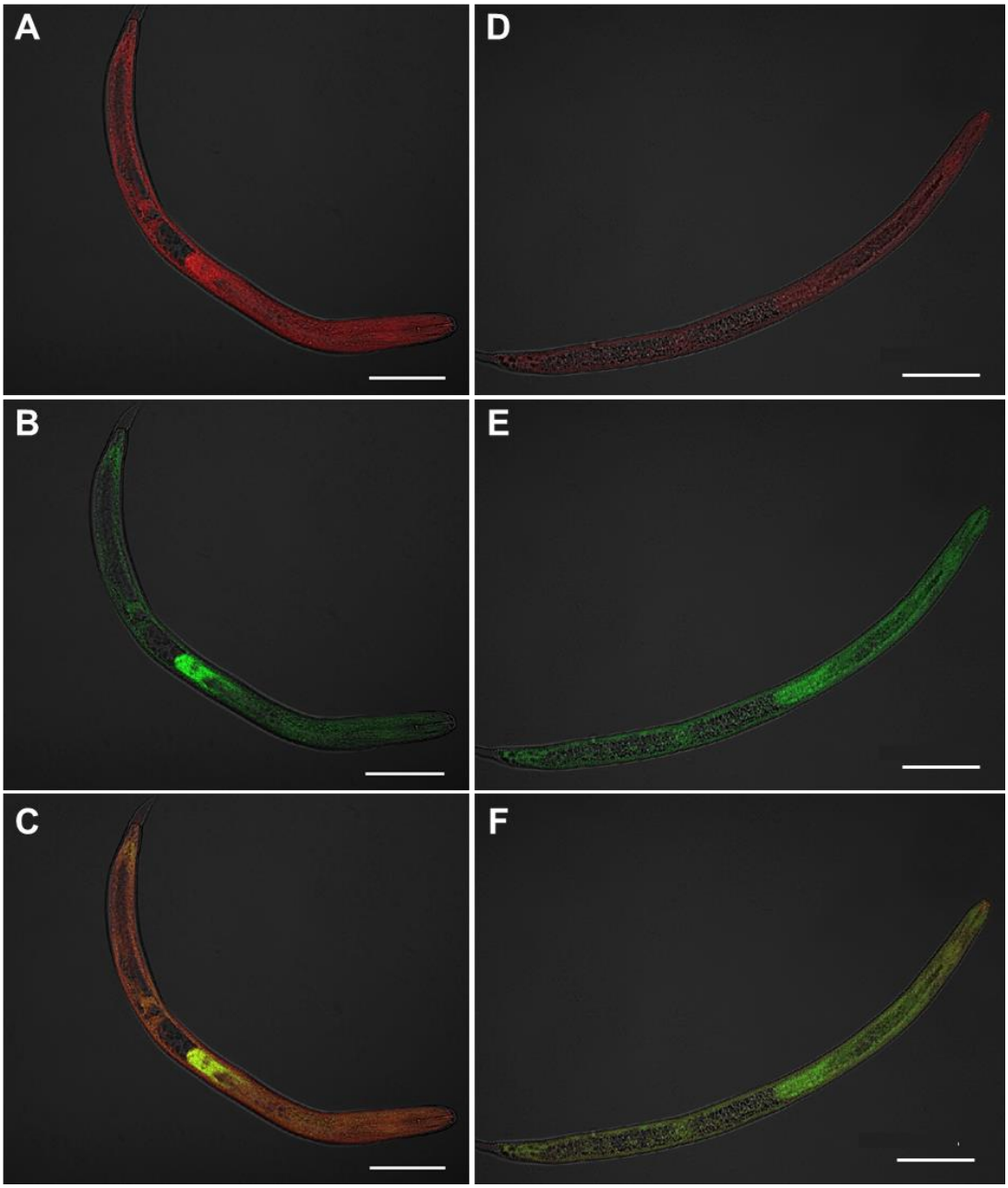

Figure 4.6. Colocalization of SCN Bunya-like virus (BLV) with host GAPDH. RNA within SCN J2s was labelled with fluorescent DNA probes via fluorescence *in situ* hybridization (FISH). Host mRNA is labelled with ATTO-647N dye and SCN BLV with ATTO-565. **A-C** SCN population LY1 (A: SCN BLV single channel [red], B: GAPDH single channel [green], and C: overlay). **D-F** SCN population MM21 (D: SCN BLV single channel [red], E: GAPDH single channel [green], and F: overlay). The brightfield channel is muted but retained in images for better structure clarity. Scale bar represents 50 µm (Zeiss LSM 880).

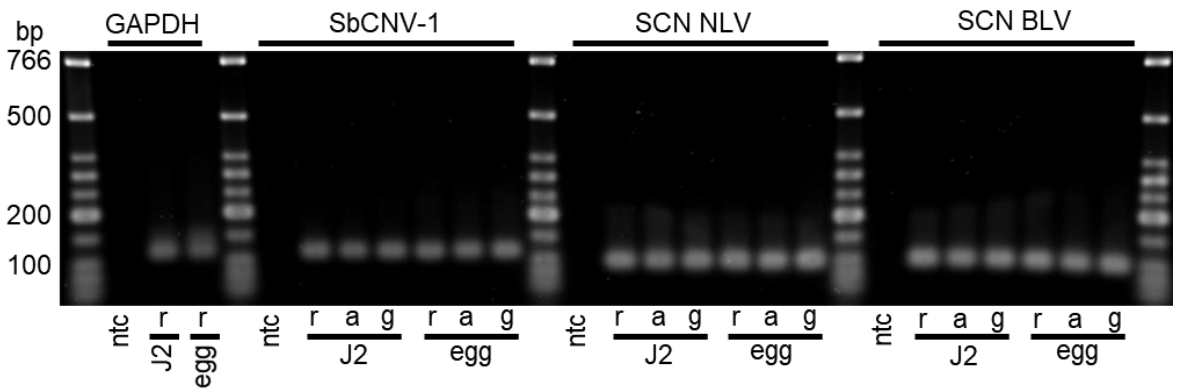

Figure 4.7. Strand-specific amplification of viruses within SCN J2s and eggs. SCN population LY1 cDNA was synthesized with strand specific (a or g) or random (r) primers and detected with qRT-PCR. Pooled technical triplicates were run on a 2% agarose gel with low molecular weight ladder (New England BioLabs). Abbreviations: SCN (soybean cyst nematode), GAPDH (glyceraldehyde 3-phosphate dehydrogenase) internal control, SbCNV-1 (SCN socyvirus-1), NLV (nyami-like virus), BLV (bunya-like virus), ntc (no template control), J2 (second-stage juvenile), **r** (random primer), **a** (anti-genomic strand), **g** (genomic strand).

APPENDICES

APPENDIX A

Chapter 2 Supporting Information

S2.1 Table. Sequence primers of approximately 500 bp regions of viral RdRPs via Sanger sequencing.

Primer	Sequence [5' to 3']
ScNVSEQ	TCACGACTATGCTCTACACC
ScNV(-)SEQ	GCCTCGTCCTCCACATCAAG
ScPVSEQ	GACGCGCAAGATGGAAGACC
ScPV(-)SEQ	TTTCTTATGACCGACTGACC
ScRVSEQ	CAATGTGAAGTGCTACATC
ScRV(-)SEQ	ACGAGCCTCAAACCCGCAC
ScTVSEQ	CATGCCGGCCTCCACTCCGC
ScTV(-)SEQ	CCGGTGTAGCAGGGAGATCAGG
SbCNV-5SEQ	GCCCACCTATTTTACGAGC
SbCNV-5(-)SEQ	CTCAAGAGGTCAAACCGCG

S2.2 Table. Average Ct values for detectable viruses in SCN (OP50) life stages egg, J2, and mixed J3/J4 stages. The Ct value of each virus was normalized against the SCN internal control gene GAPDH.

	Egg				J2				J3/J4			
	[a]Avg Ct rep 1	[b]Avg NAR rep 1	Avg Ct rep 2	Avg NAR rep 2	Avg Ct rep 1	Avg NAR rep 1	Avg Ct rep 2	Avg NAR rep 2	Avg Ct rep 1	Avg NAR rep 1	Avg Ct rep 2	Avg NAR rep 2
ScNV	29.13	0.044	30.84	0.21	33.33	0.12	26.71	0.043	31.09	0.034	31.10	0.011
ScPV	28.29	0.066	34.94	0.013	34.33	0.050	28.30	0.013	30.60	0.040	30.59	0.013
GAPDH	21.62	-	25.31	-	26.68	-	19.43	-	23.01	-	21.47	-

[a] average cycle threshold (Ct; technical replicates repeated in triplicate)
[b] average normalized abundance ratio (NAR)

S2.3 Table. Average Ct values for detectable viruses in SCN (PA3) life stages egg, J2, and J3/J4 stages. The Ct value of each virus was normalized against the SCN internal control gene GAPDH.

	Egg				J2				J3/J4			
	[a]Avg Ct rep 1	[b]Avg NAR rep 1	Avg. Ct rep 2	Avg. NAR rep 2	Avg. Ct rep 1	Avg. NAR rep 1	Avg. Ct rep 2	Avg. NAR rep 2	Avg. Ct rep 1	Avg. NAR rep 1	Avg. Ct rep 2	Avg. NAR rep 2
ScNV	21.00	5.58	21.29	8.00	29.57	16.57	21.63	4.19	27.65	2.05	25.14	25.09
ScPV	20.02	9.46	20.01	16.45	29.04	20.14	19.91	11.50	24.05	18.50	24.91	25.60
ScRV	23.18	1.96	23.25	3.26	32.17	5.13	23.14	2.27	29.47	1.00	27.34	9.33
ScTV	20.83	7.77	21.20	10.59	29.59	22.44	21.13	7.24	25.03	14.48	25.57	24.86
GAPDH	21.04	-	21.79	-	30.16	-	21.21	-	25.58	-	26.79	-

[a] average cycle threshold (Ct; technical replicates repeated in triplicate)
[b] average normalized abundance ratio (NAR)

S2.4 Table. Mean qRT-PCR Ct value for SCN (OP50) egg, J2 and J3/J4 stages used to determine viral replication in SCN. Data presented are the means of technical triplicates. Genomic and anti-genomic RNA was detected by initiating first strand cDNA synthesis with primers specific to each strand. Random primers were also used for cDNA synthesis as a control for both genomic and anti-genomic RNA.

	Egg			J2			J3/J4		
	Genomic	Anti-genomic	Random	Genomic	Anti-genomic	Random	Genomic	Anti-genomic	Random
ScNV	22.23	25.16	22.94	27.40	29.28	26.60	23.63	25.51	22.78
ScPV	24.59	31.04	25.30	31.40	33.70	31.09	25.49	31.51	25.34
GAPDH	-	-	23.34	-	-	28.50	-	-	23.92
18*S*	-	-	9.04	-	-	12.85	-	-	10.63

S2.5 Table. Mean qRT-PCR Ct value for SCN (PA3) egg, J2, and J3/J4 stages used to determine viral replication in SCN. Data presented are the means of technical triplicates. Genomic and anti-genomic RNA was detected by initiating first strand cDNA synthesis with primers specific to each strand. Random primers were also used for cDNA synthesis as a control for both genomic and anti-genomic RNA.

	Egg			J2			J3/J4		
	Genomic	Anti-genomic	Random	Genomic	Anti-genomic	Random	Genomic	Anti-genomic	Random
ScNV	22.38	23.94	21.59	22.47	23.81	21.93	26.81	28.42	26.16
ScPV	18.43	22.01	18.30	18.72	21.47	18.60	23.35	27.17	23.19
ScRV	27.11	30.16	25.60	26.32	29.66	25.36	31.54	36.09	30.19
ScTV	21.52	23.04	20.62	21.34	22.89	20.87	25.99	28.55	25.25
GAPDH	-	-	21.79	-	-	21.21	-	-	26.79
18*S*	-	-	8.93	-	-	8.15	-	-	11.57

S2.6 Table. Mean of qRT-PCR Ct values of SCN greenhouse populations. Data presented are the means of technical triplicates. SCN internal controls for relative quantification are HgFAR1 and GAPDH.

	Internal Controls		SCN Viruses				
SCN Population	HgFAR1	GAPDH	ScNV	ScPV	ScRV	ScTV	SbCNV-5
LY1	26.19	26.88	25.68	28.09	30.74	27.09	22.35
LY2	24.33	24.75	26.14	27.19	29.13	29.82	24.55
MM1	26.42	26.56	28.35	29.20	33.03	28.78	ND[b]
MM2	20.74	20.65	22.35	22.24	27.45	23.53	32.79
MM3	21.32	22.41	23.58	22.91	26.87	24.13	ND
MM4	26.24	26.57	27.27	28.40	29.94	27.71	ND
MM7	18.03	19.06	17.07	18.91	21.70	31.22	ND
MM7/Williams82	26.41	26.23	26.47	28.07	31.54	ND	ND
MM8	18.95	20.32	21.99	21.73	24.30	22.32	ND
MM8/Williams82	20.46	21.22	22.68	22.97	27.57	23.36	ND
MM8/Peking	19.86	20.52	21.00	22.09	24.44	22.23	ND
MM10	19.75	22.51	20.15	21.85	24.02	21.33	ND
MM10/Williams82	18.45	21.76	18.58	20.28	22.29	20.21	ND
MM16	18.37	18.88	ND	ND	32.37	ND	ND
MM18	21.09	21.62	31.00	29.94	ND	ND	ND
MM19	20.44	21.12	28.56	ND	33.58	30.81	ND
MM21	24.19	24.44	ND	ND	ND	ND	ND
MM23	27.25	27.60	ND	ND	ND	ND	ND
MM24	29.23	29.06	ND	ND	ND	ND	ND
OP20	21.88	22.26	23.21	ND	ND	ND	ND
OP20[a]	19.91	–	29.02	ND	ND	ND	ND
OP25	22.03	27.54	31.25	28.61	ND	ND	26.35
OP25[a]	23.21	–	32.08	32.59	ND	ND	ND
OP50	24.57	24.78	23.06	ND	ND	ND	ND
OP50[a]	21.25	–	31.99	31.79	ND	ND	ND
PA3	24.69	26.25	26.45	27.76	30.88	26.72	ND
TN1	26.66	26.97	26.64	ND	29.82	28.59	23.72
TN2/soybean	24.36	25.17	25.81	ND	ND	34.15	ND
TN2/tomato	19.81	20.17	20.18	ND	25.57	ND	34.99
TN6	25.18	26.29	34.39	ND	ND	ND	32.69
TN7 (a)	17.99	19.00	19.24	19.69	23.07	19.56	16.75
TN7 (b)	22.09	22.69	23.42	24.74	24.80	23.60	20.03
TN8 (a)	22.37	22.07	31.69	ND	20.70	ND	22.90
TN8 (b)	23.21	24.60	ND	ND	34.57	ND	21.98
TN12	26.79	27.94	27.18	30.58	31.51	28.48	ND
TN13	21.33	22.13	21.17	ND	24.66	22.51	20.18
TN14	26.66	27.26	27.04	ND	32.47	ND	ND
TN15	26.82	26.23	26.87	ND	31.52	28.01	ND
TN19	26.01	27.86	27.64	33.22	31.72	28.93	ND
TN20	26.01	26.26	ND	ND	34.32	ND	30.89
TN21	18.61	19.60	18.87	21.00	23.18	21.09	ND
TN22	18.38	18.53	18.07	19.63	27.45	19.76	30.93
VL1	23.98	25.04	34.69	ND	30.37	25.42	ND

[a] Samples are maintained in NCSU greenhouses; all other samples are from MU greenhouses; [b] virus not detected (ND)

S2.7 Table. Mean of qRT-PCR Ct values of field populations of SCN. Data presented are the means of technical triplicates. The SCN internal control HgFAR1 is used for relative quantification of virus abundance.

	Internal Controls		SCN Viruses				
SCN Population	HgFAR1	GAPDH	ScNV	ScPV	ScRV	ScTV	SbCNV-5
Beaufort	23.86	25.05	34.96	34.39	ND[b]	ND	ND
Bertie	25.75	26.99	ND	33.88	ND	ND	ND
Bladen	25.83	27.50	30.32	ND	ND	ND	ND
Columbus	18.78	–	23.76	27.54	ND	ND	34.47
Craven	28.61	27.78	30.78	ND	ND	ND	ND
Duplin	19.38	–	27.62	ND	30.19	ND	ND
Edgecombe	29.47	–	ND	33.95	ND	ND	29.52
Gates	20.74	–	25.72	ND	ND	ND	ND
Greene	24.12	25.51	32.42	33.69	ND	ND	ND
Guilford	22.99	23.50	28.93	31.42	34.50	ND	ND
Hertford	20.96	–	25.53	32.24	ND	ND	ND
Jones	22.57	–	25.76	ND	ND	ND	ND
Lee	23.48	–	ND	ND	ND	ND	ND
Onslow	24.53	21.06	28.13	32.40	ND	ND	ND
Pamlico	21.52	–	23.49	28.25	ND	ND	34.23
Person	20.76	–	30.10	29.76	ND	ND	ND
Robeson	24.18	25.31	25.75	33.80	31.79	ND	ND
Tyrell	23.01	24.96	ND	32.93	ND	ND	ND
Wake	25.18	25.61	30.72	34.07	ND	ND	ND
Washington	26.92	–	32.51	ND	ND	ND	ND
Barton[a]	20.22	17.51	31.75	ND	ND	ND	ND
Dunklin 1[a]	21.60	22.53	ND	ND	ND	ND	ND
Dunklin 2[a]	24.35	25.19	ND	ND	ND	ND	ND
Scott 1[a]	24.99	25.66	ND	ND	ND	ND	ND
Scott 2[a]	24.03	24.62	ND	ND	ND	ND	ND

[a] Samples were collected from infested fields in Missouri; all other samples are from North Carolina fields
[b] virus not detected (ND)

APPENDIX B

Chapter 3 Supporting Information

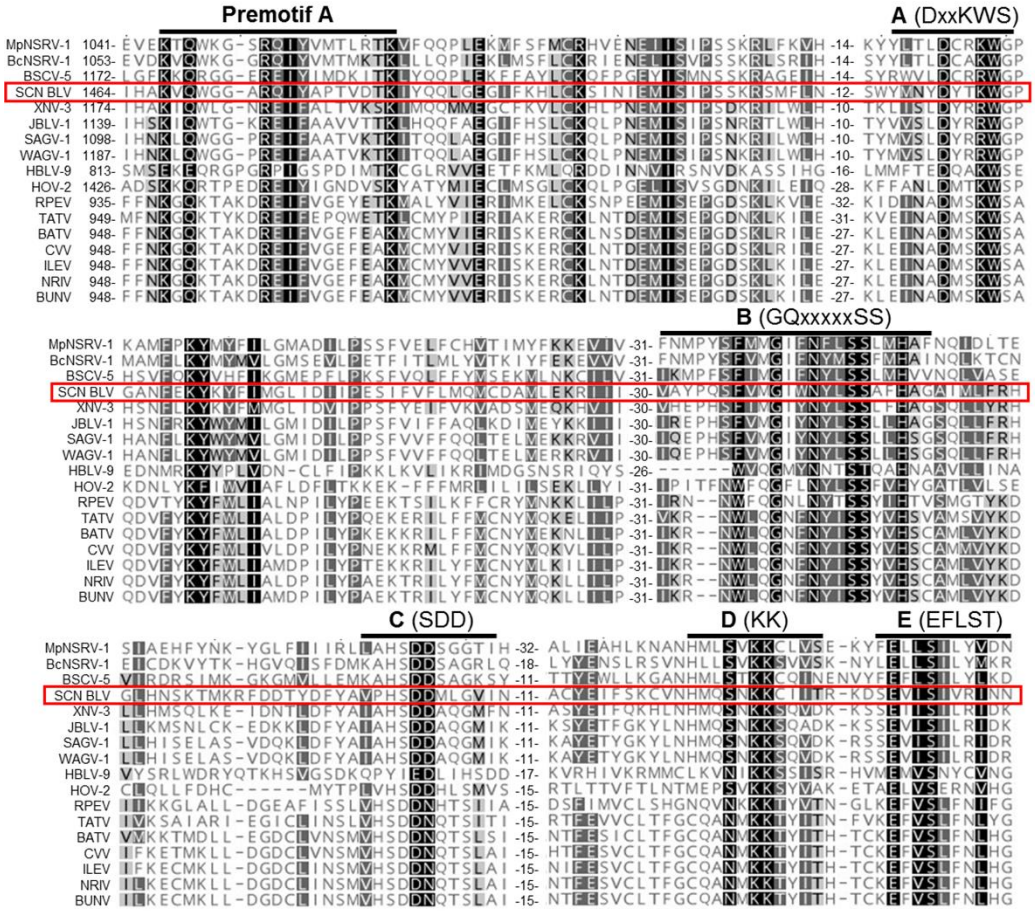

S3.1 Fig. Conserved protein motifs of soybean cyst nematode (SCN) bunya-like virus (BLV). Most closely related RNA-dependent RNA polymerase (RdRP) sequences were identified with NCBI PSI-BLAST and aligned with ClustalW protein alignment. Conserved protein motifs identified by [31] are shown above the alignments.

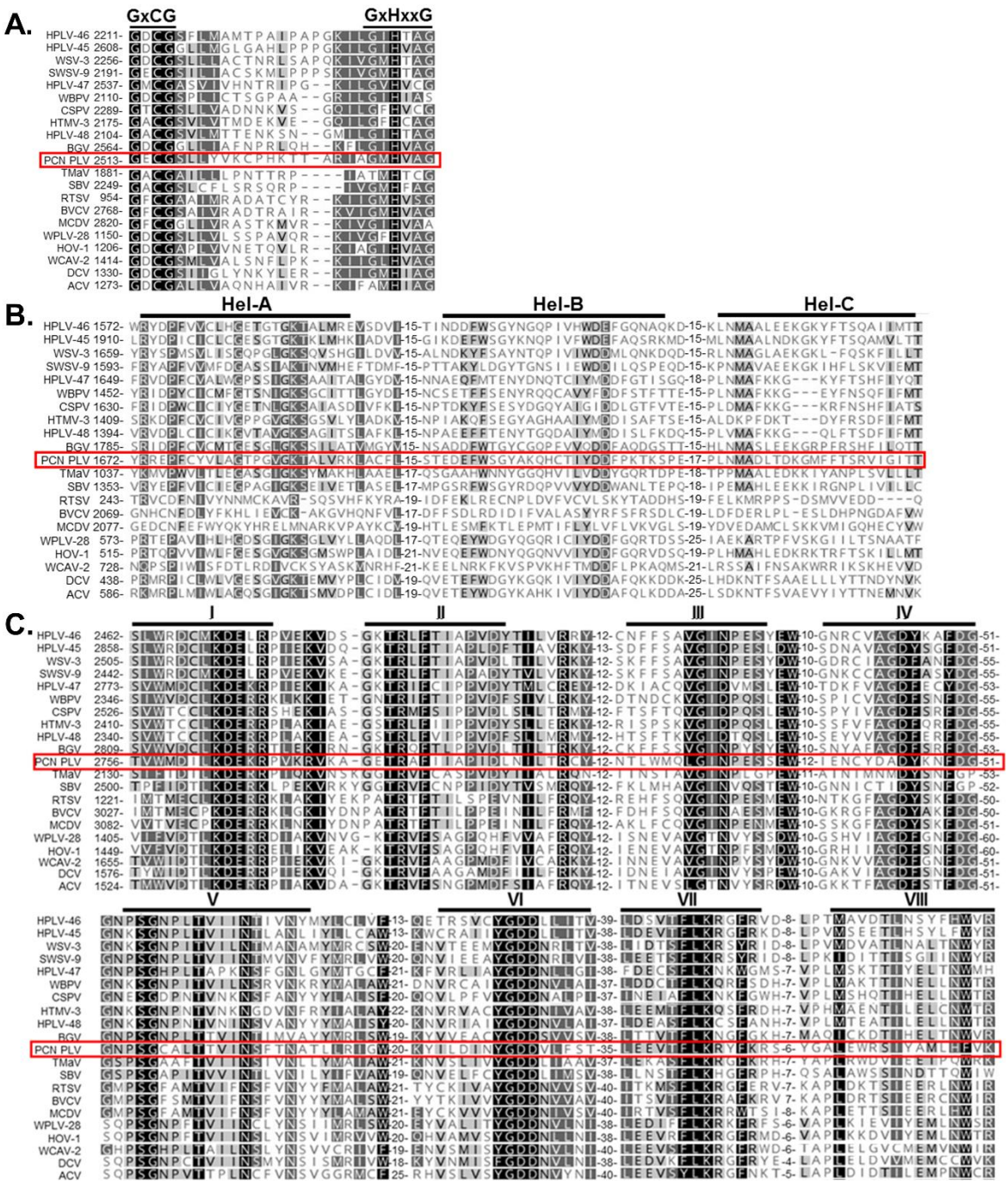

S3.2 Fig. Conserved protein motifs of potato cyst nematode (PCN) picorna-like virus (PLV). Most closely related viruses were identified via NCBI PSI-BLAST. Proteins were aligned with ClustalW. Conserved picorna-like virus motifs were described in [37,38] and are shown above the sequence alignments. Motifs are identified within (**A**) protease, (**B**) helicase, and (**C**) RNA-dependent RNA polymerase (RdRP).

.

S3.3 Fig. Amplification of viral products and alignments of translated soybean cyst nematode (SCN) nyami-like virus (NLV) and SCN bunya-like virus (BLV) RNA-dependent RNA polymerases (RdRPs) via Sanger sequencing. (**A**) PCR products of SCN NLV ORFs isolated from SCN population MM8. Fragments sizes are 405 bp (ORF I), 327 bp (ORF II), 181 bp (ORF III), 448 bp (ORF IV), and 838 bp (ORF V). Viral products were amplified from total RNA of SCN MM8 and electrophoresed on a 2% gel with 100 bp molecular ladder (New England BioLabs). (**B**) Amino acid alignment of SCN NLV RdRP fragments. Nucleotides were translated from Sanger sequencing results and aligned via Geneious software (Biomatters) using ClustalW (Blosum62, threshold of 4 is represented). The sequence from SCN population OP50 was obtained via Next Gen sequencing and acts as a reference for comparison. (**C**) Amino acid alignment of SCN BLV RdRP fragments. Nucleotides were translated from Sanger sequencing results and aligned via Geneious software using ClustalW (Blosum62, threshold of 4 is represented). The sequence from SCN OP50 was obtained via Next Gen sequencing and acts as a reference for comparison

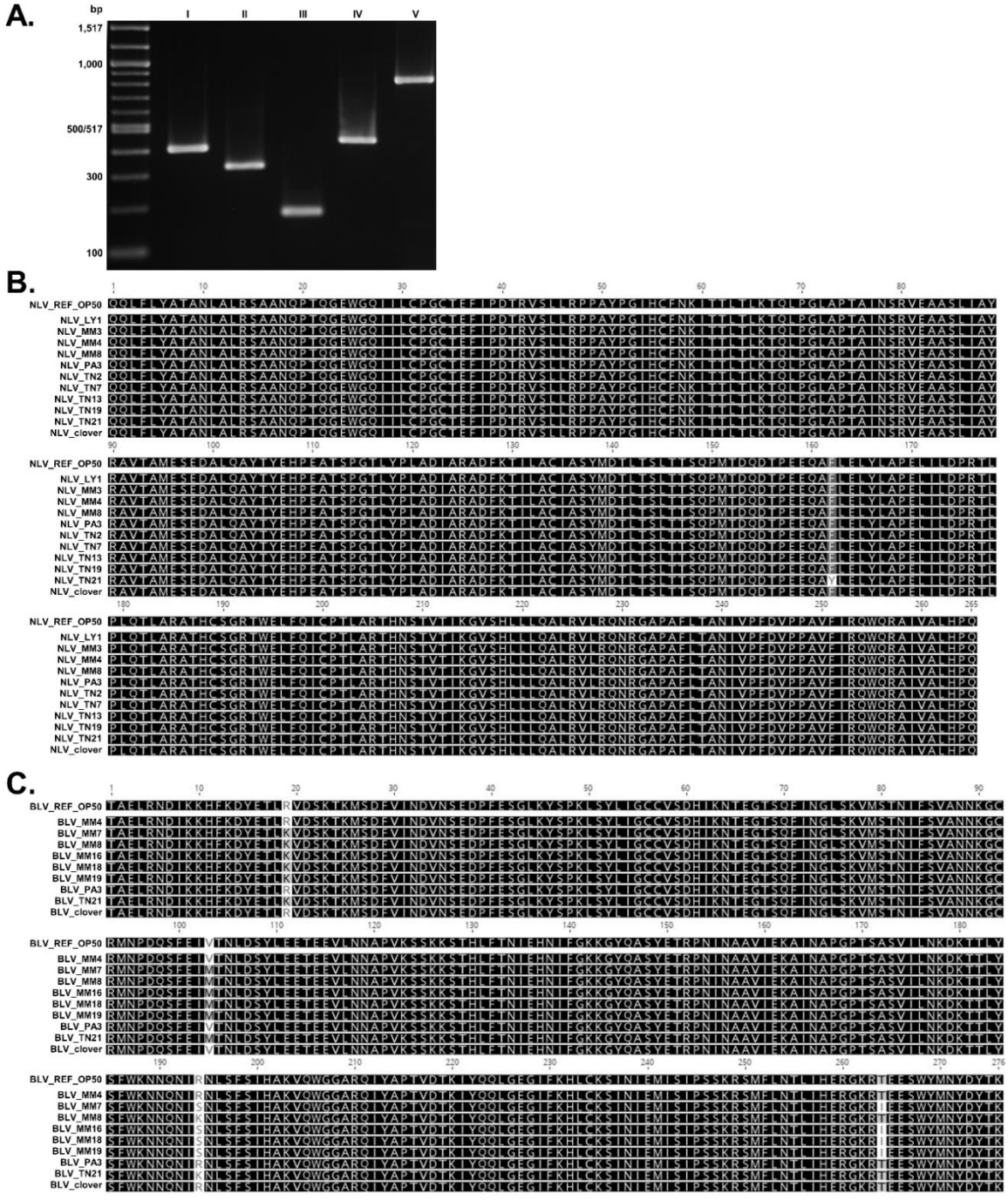
A.
bp
I
II
III
IV
V
1,517
1,000
500/517
300
100
B.
NLV_REF_OP50
NLV_LY1
NLV_MM3
NLV_MM4
NLV_MM8
NLV_PA3
NLV_TN2
NLV_TN7
NLV_TN13
NLV_TN19
NLV_TN21
NLV_clover
C.
BLV_REF_OP50
BLV_MM4
BLV_MM7
BLV_MM8
BLV_MM16
BLV_MM18
BLV_MM19
BLV_PA3
BLV_TN21
BLV_clover

APPENDIX C

Chapter 4 Supporting Information

Supplemental Table 4.1. qRT-PCR cycle threshold values for viral replication detection of SCN LY1. Strand-specific cDNA amplification for the viruses was conducted followed by detection via qRT-PCR. Random primers were used as a control to detect both genomic and anti-genomic strands. Abbreviations: Ct (cycle threshold), SD (standard deviation), SbCNV-1 (SCN Socyvirus-1), SCN (soybean cyst nematode), NLV (nyami-like virus), BLV (bunya-like virus), NTC (no template control), ND (not detected).

Life Stage	Strand	Target	Ct Mean	Ct SD
Egg	Genomic	SbCNV-1	18.33	0.207
Egg	Anti-Genomic	SbCNV-1	19.40	0.307
Egg	Both	SbCNV-1	18.33	0.040
J2	Genomic	SbCNV-1	19.34	0.046
J2	Anti-Genomic	SbCNV-1	22.29	0.259
J2	Both	SbCNV-1	19.39	0.176
-	NTC	SbCNV-1	ND	-
Egg	Genomic	SCN NLV	18.79	0.045
Egg	Anti-Genomic	SCN NLV	20.24	0.145
Egg	Both	SCN NLV	19.79	0.036
J2	Genomic	SCN NLV	20.13	0.035
J2	Anti-Genomic	SCN NLV	21.78	0.050
J2	Both	SCN NLV	20.45	0.075
-	NTC	SCN NLV	ND	-
Egg	Genomic	SCN BLV	17.27	0.055
Egg	Anti-Genomic	SCN BLV	19.09	0.128
Egg	Both	SCN BLV	18.20	0.055
J2	Genomic	SCN BLV	19.71	0.055
J2	Anti-Genomic	SCN BLV	21.80	0.057
J2	Both	SCN BLV	19.68	0.062
-	NTC	SCN BLV	ND	-
Egg	Both	GAPDH	19.34	0.081
J2	Both	GAPDH	21.52	0.053
-	NTC	GAPDH	ND	-

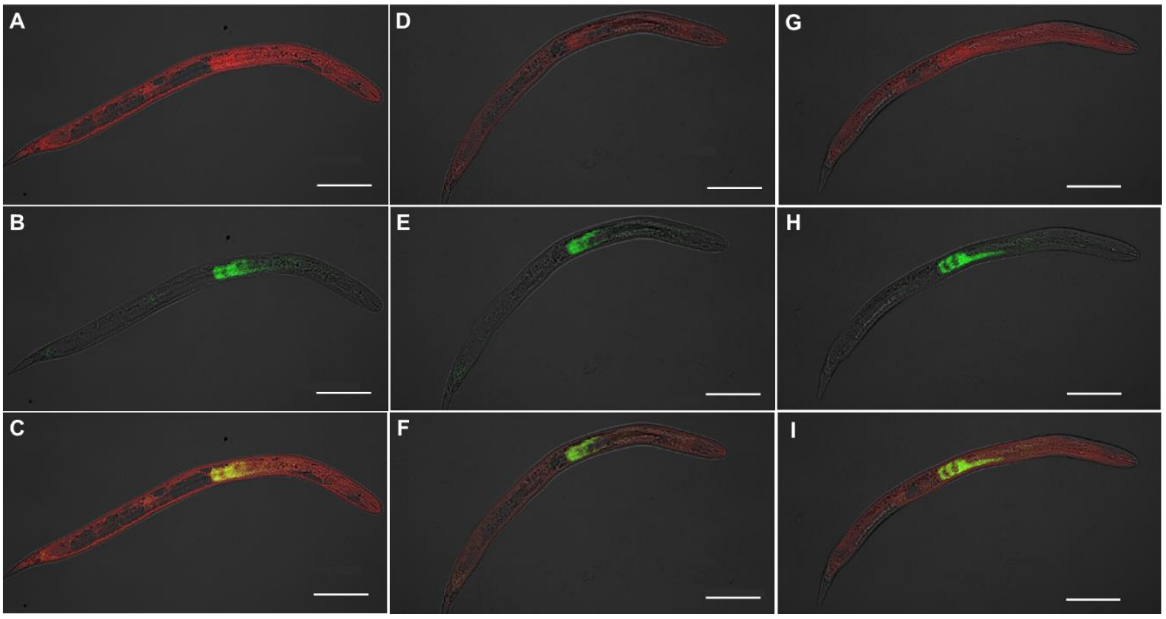

Supplemental Figure 4.1. Colocalization of SCN viruses with host subventral gland (SvG) secretory ubiquitin protein (4G06). RNA within SCN LY1 J2s was labelled with fluorescent DNA probes via fluorescence *in situ* hybridization (FISH). Host mRNA is labelled with ATTO-647N dye and SCN viruses with ATTO-565. **A-C** Colocalization of SbCNV-1 with SvG protein (A: SbCNV-1 single channel [red], B: SvG single channel [green], C: overlay). **D-F** Colocalization of SCN NLV with SvG protein (D: SCN NLV single channel [red], E: SvG single channel [green], F: overlay). **G-I** Colocalization of SCN BLV with SvG protein (G: SCN BLV single channel [red], H: SvG single channel [green], I: overlay). The brightfield channel is muted but retained in images for better structure clarity. Scale bar represents 50 µm (Zeiss LSM 880).

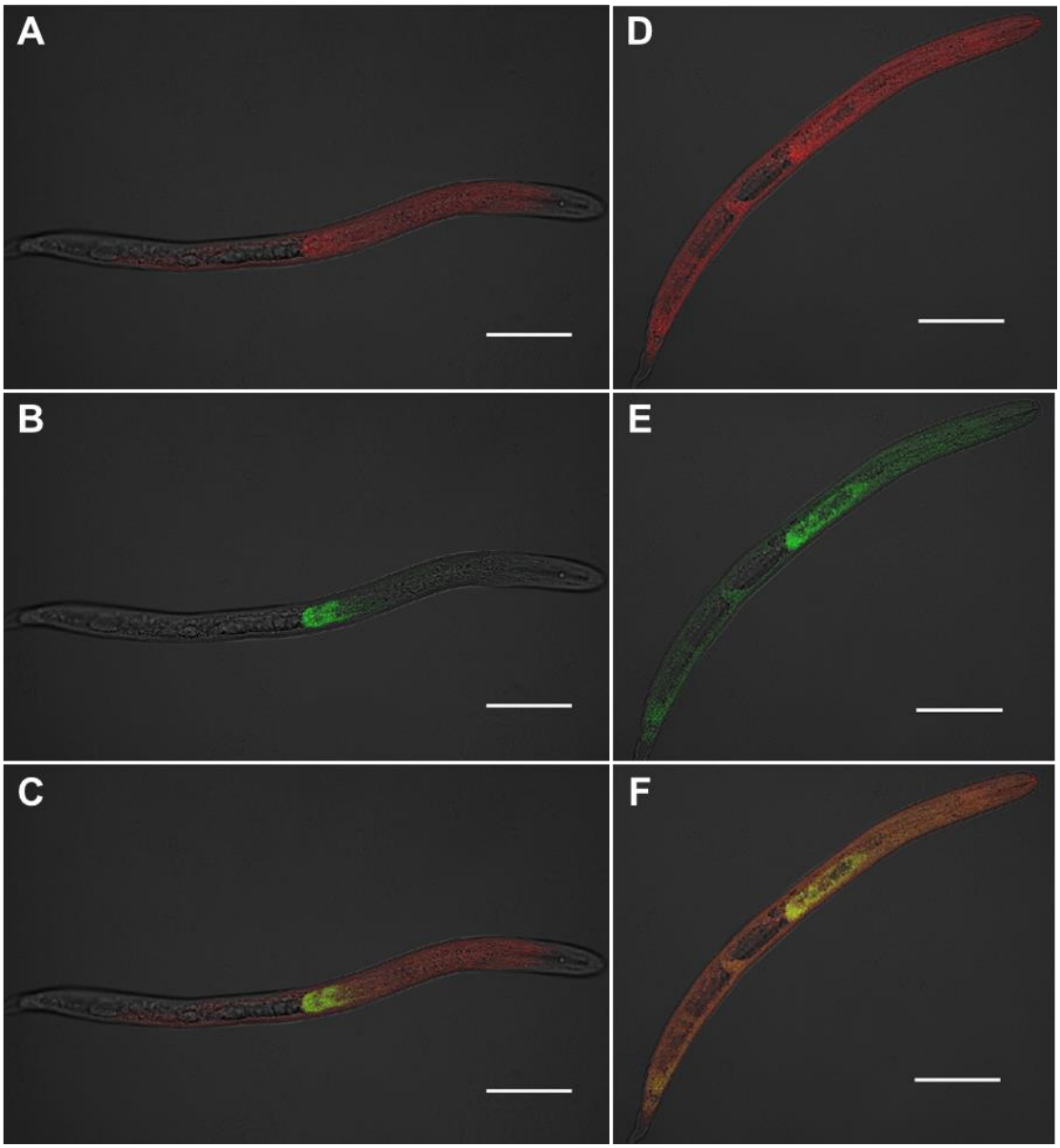

Supplemental Figure 4.2. Colocalization of Flock house virus (FHV) with host mRNA. RNA within SCN LY1 J2s was labelled with fluorescent DNA probes via fluorescence *in situ* hybridization (FISH). Host mRNA is labelled with ATTO-647N dye and FHV with ATTO-565. **A-C** FHV colocalized with SCN subventral gland ubiquitin protein. (A: FHV single channel [red], B: SvG single channel [green], and C: overlay). **D-F** FHV colocalized with SCN GAPDH probe (D: FHV single channel [red], E: SvG single channel [green], and F: overlay). The brightfield channel is muted but retained in images for better structure clarity. Scale bar represents 50 µm (Zeiss LSM 880).